CALIFORNIA INSTITUTE OF TECHNOLOGY

DYNAMICS LABORATORY

STUDIES IN THE STATICS AND DYNAMICS OF SIMPLE CABLE SYSTEMS

by

H. Max Irvine

DYNL-108

A report on research conducted under a grant from the National Science Foundation

Pasadena, California
January, 1974

STUDIES IN THE STATICS AND DYNAMICS OF SIMPLE CABLE SYSTEMS

Thesis by

H. Max Irvine

In Partial Fulfillment of the Requirements
for the Degree of
Civil Engineer

California Institute of Technology
Pasadena, California
1974

(Submitted January 18, 1974)

ACKNOWLEDGMENTS

The author is indebted to his two supervisors, Professors P. C. Jennings and T. K. Caughey, for their assistance and guidance during the course of this research. He has also to thank many other faculty members and students who, by way of course work and discussions, contributed to the stimulating atmosphere which is a feature of the California Institute of Technology.

The author appreciates the assistance given by: Mrs. Inge Stork, who typed the manuscript; the Graphic Arts Facility, for final preparation of the diagrams; Mr. Don Laird of the Mechanical Engineering Workshop, for construction of the model equipment; and Dr. Robert Koh for advice on the photographic work.

Thanks are extended to the following for permission to reproduce photographs: Mr. M. F. Parsons of Freeman, Fox and Partners, London; Dr. Lev Zetlin of Lev Zetlin Associates, New York; and Mr. W. C. Mosteller of Southern California Gas Company.

The financial assistance of the California Institute of Technology and the National Science Foundation is gratefully acknowledged.

ABSTRACT

An investigation is made of the static and dynamic response of simple cable systems to applied load. Both the single, suspended cable and the counterstressed double cable system (the cable truss) are treated. More complicated systems, such as cable nets, are not treated. The geometry of the simple cable systems is such that the cable slopes are, and remain, small. For example, the ratio of sag to span of the suspended cable must be about 1:8, or less.

Closed form solutions are given to a variety of cable problems which have important applications in practice. The work is divided into two chapters.

In the first chapter solutions are given for the response of a single, suspended cable to static loading, and a comprehensive theory is presented for the free, linear vibrations of the suspended cable. Where necessary, in the static analyses, the solutions are given accurate to the second order of small quantities. The results of simple experiments are reported.

The second chapter deals with the cable truss and, again, static analyses are given and a theory is presented for the free, linear vibrations of the cable truss. The possible lateral instability of the cable truss under applied load is investigated.

An attempt is made to give static solutions which are of general significance. In the past this has rarely been done. It is shown that a parameter which involves cable elasticity and geometry has a very important bearing on several of the theories presented. The param-

eter does not appear to have been given before and, for this reason, most previous works are of limited applicability and in some cases they are wrong. For example, the linear in-plane vibrations of these simple cable systems can be analyzed correctly only if this parameter is included. The lateral instability of the cable truss is important, not only because previously it appears that it has been ignored, but also because it opens up a new field of buckling problems which are unlike any others.

TABLE OF CONTENTS

GENERAL INTRODUCTION

The thesis is divided into two chapters and each chapter is further divided into several sections and sub-sections. Each chapter, and many of the sections, have their own introductions where a brief account is given of the historical development of the particular subject under investigation. The historical information has been collected from many sources; in some cases the original works have been referred to, in others, where source material is difficult to obtain, the reader is directed to treatises which list the references.

The first chapter contains analyses of the single, suspended cable which are valid provided that the ratio of sag to span is about 1:8, or less. The use of such cable systems is widespread, transmission lines of various sorts and suspension bridges being two cases in point. In the first section topics which receive attention are the free-hanging, inextensible parabolic cable, the elastic parabola and the response of a parabolic cable to various forms of applied static loading. The second section contains a detailed treatment of the linear theory of free vibrations of a suspended cable. Both the in-plane and out-of-plane modes are investigated. In each section examples are given, both numerical and theoretical, which illustrate and augment the theories, and the results of simple experiments, conducted on model cables, are presented.

The second chapter is concerned with analyses of the cable truss. The cable truss is a counterstressed system consisting of two pretensioned cables, anchored off between rigid supports, which

form the chords of the truss and between which numerous spacers are placed to provide the web members. Cable trusses have been used in arrays to support the roofs of large-span buildings. In the first section static analyses are given for those types of loadings which will be commonly encountered in practice. The second section contains a brief discussion of the dynamic analysis of the cable truss and, in the third section, a detailed presentation is made of the lateral instability which may be exhibited by the truss in resisting applied loading. Once again, several examples are given.

Chapter I

THE PARABOLIC CABLE

The Bosporus bridge, Istanbul (main span 1074m)
opened 30 October 1973.

An investigation is made of the response of a suspended parabolic cable to various types of static and dynamic loadings. The study is primarily theoretical, although the results of some simple experiments are reported and illustrative examples are presented.

The cable is assumed to be of uniform cross section and is made from a material of uniform density which obeys Hooke's Law. Expansions and contractions of the cross section, associated with changes in the length of the cable and the effects of Poisson's Ratio, are considered negligible. The flexural rigidity of the cable is ignored (see Appendix I). It is assumed that the cable is perfectly flexible and, consequently, resists applied load by developing direct stresses only. It follows, therefore, that at any cross section the resultant cable force is tangential to the cable profile at that point, and it acts through the centroid of the cross section. For simplicity, each end of the cable is assumed to be anchored on rigid supports which are at the same level.

The assumption of a parabolic profile for a free-hanging, uniform cable, rather than the exact solution of the catenary, requires that the ratio of the sag to span be kept relatively small. The analyses to be presented are valid provided that the ratio of sag to span is 1:8, or less. Usually, uniform cables whose geometry does not satisfy the above requirement are inaccurately described by parabolic profiles. However, such cables are rarely used as structural members supporting transverse loading.

A. RESPONSE TO TRANSVERSE STATIC LOADING

1. Parabolic Cable Hanging Under Its Own Weight

Following a brief historical note, and in order to lay a foundation from which later work is developed, two fundamental results are given for the free-hanging, parabolic cable.

a. Historical background

It appears that Galileo[15], in the early seventeenth century, was the first to investigate the form of the curve adopted by a uniform, inextensible cable or chain*, which is fixed at each end and hangs under its own weight. Apparently, he went no further than to notice the similarity between this curve and the parabola.

It is now known, of course, that the curve adopted by such a cable is the catenary. The solution was first published in 1691 by an eminent group of geometers consisting of James Bernoulli, his brother John, Leibnitz and Huygens[15]. Later, in 1697, David Gregory[15] obtained a solution. Several other "catenary" problems were pursued by James Bernoulli (including the first attempt to allow for the effects of cable stretch). Subsequently, the investigations were taken up by others. Perhaps the most interesting of these other investigations is the catenary of uniform strength, in which the area of the cable is varied to allow the stress to remain constant along the

---

*Hereinafter, "cable" will be used in lieu of "chain", although it was not until the mid-nineteenth century that metal cables (i. e., iron and, later, steel) became common.

cable. The solution was obtained by Gilbert[15], in 1826, in connection with Telford's design of the Menai Straits suspension bridge.

In spite of Galileo's early musings on the subject, it is surprising that more than one hundred years elapsed after the discovery of the catenary before the simpler, parabolic cable was discovered. In 1794, again in connection with the design of a proposed suspension bridge, this time in Leningrad, the engineer Fuss[15] (Euler's son-in-law) found that, if the cable's weight was assumed to be uniformly distributed along the span rather than along the cable, the cable hung in a parabolic profile. The parabolic cable has since received considerable attention, not only because of its simplicity, but also because in many situations (such as suspension bridges), a substantial part of the load is uniformly distributed along the span.

However, in all work prior to the mid-nineteenth century, apart from that mentioned in connection with James Bernoulli's researches, no allowance was made for the finite, but usually small, extensibility which such cable systems possess. As a result, the concept of cable elasticity received little recognition until 1858 when Rankine[10] gave an approximate solution for the increase in sag obtained when an inextensible, free-hanging parabolic cable is allowed to stretch. This was followed in 1891 by Routh's[15] solution of the more difficult elastic catenary.

b. The inextensible parabola

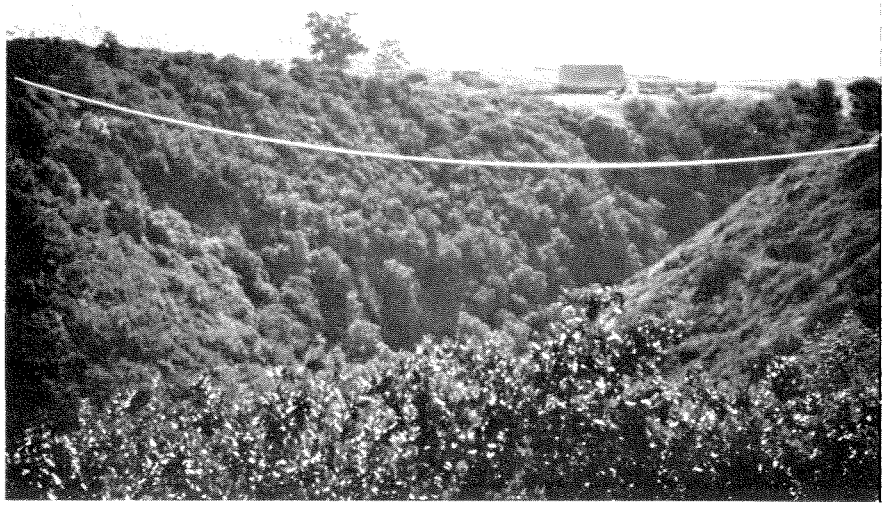

High pressure gas line Ventura County, California (span 135m, pipe diameter 40cm).

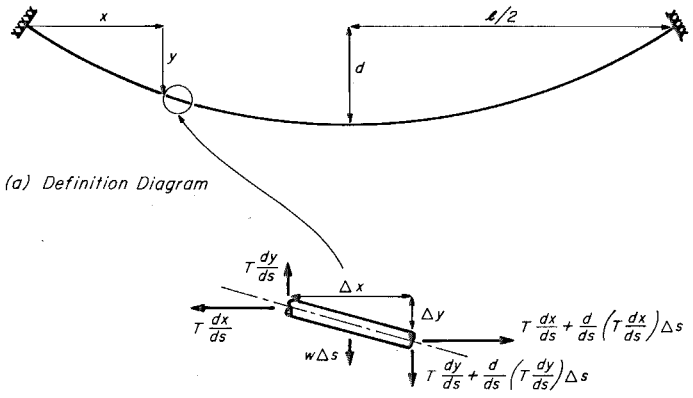

Figure 1

The first result given concerns the profile adopted by, and associated properties of, a uniform inextensible cable hanging under its own weight. Because the ratio of sag to span is 1:8, or less, the load may be assumed uniformly distributed along the span.

Vertical equilibrium of an element of the cable, shown in Fig. 1, requires that

$$\frac{d}{ds}\left(T\,\frac{dy}{ds}\right) = -w \tag{1.1}$$

where T is the tension in the cable, w is the weight of the cable per unit length and $\frac{dy}{ds}$ is the sine of the angle of inclination.

The horizontal component of cable tension, H, is constant since no longitudinal components of load are acting.

$$H = T\,\frac{dx}{ds} = \text{Constant} \tag{1.2}$$

where $\frac{dx}{ds}$ is the cosine of the angle of inclination. Consequently, Eq. 1.1 is reduced to

$$\left.\begin{aligned} H\,\frac{d^2y}{dx^2} &= -w\,\frac{ds}{dx} \\ \text{or} \\ H\,\frac{d^2y}{dx^2} &= -w\left\{1 + \left(\frac{dy}{dx}\right)^2\right\}^{\frac{1}{2}} \end{aligned}\right\} \tag{1.3}$$

When w is constant the solution of Eq. 1.3 gives the catenary. When $w\,\frac{ds}{dx}$ is constant the profile of the cable is a parabola (which is the essence of the discovery made by Fuss).

However, for flat-sag cables of constant weight per unit length, the slope of the cable profile is everywhere small and, therefore

$$ds \simeq dx$$

The equilibrium of an element of such a cable is then accurately specified by

$$H \frac{d^2y}{dx^2} = -w \tag{1.4}$$

The solution of this differential equation, for the coordinate system shown in Fig. 1, is the parabola

$$y = \frac{w\ell^2}{2H}\left\{\frac{x}{\ell} - \left(\frac{x}{\ell}\right)^2\right\} \tag{1.5}$$

The cable deflection at mid-span $(x = \frac{\ell}{2})$ is the sag, d, and the horizontal component of cable tension is

$$H = \frac{w\ell^2}{8d} \tag{1.6}$$

The tension at any point in the cable is

$$T = H\left\{1 + \left(\frac{dy}{dx}\right)^2\right\}^{\frac{1}{2}} \tag{1.7}$$

which is little different from H. With the aid of Eq. 1.6, Eq. 1.5 is more conveniently written as

$$y = 4d\left\{\frac{x}{\ell} - \left(\frac{x}{\ell}\right)^2\right\} \tag{1.8}$$

But the solution is not yet complete. For example, if only w and ℓ are known, H cannot be determined until d is known. In such a situation the length of the cable, L, must be known a priori, and then the sag may be found. In calculating the sag it is imperative to include the quadratic term, $\left(\frac{dy}{dx}\right)^2$, otherwise the sag is zero.

Now

$$L = \int_0^{\ell} \left\{1 + \left(\frac{dy}{dx}\right)^2\right\}^{\frac{1}{2}} dx$$

and because

$$\frac{dy}{dx} = \frac{4d}{\ell}\left\{1 - 2\left(\frac{x}{\ell}\right)\right\}$$

it follows that

$$L = \int_0^{\ell} \left[1 + \left\{\frac{4d}{\ell}\left(1 - 2\left(\frac{x}{\ell}\right)\right)\right\}^2\right]^{\frac{1}{2}} dx \qquad (1.9)$$

The above integral may be evaluated exactly[7]. However, it is convenient, and sufficiently accurate, to expand the integrand of Eq. 1.9 in a binomial series and then to carry out the integration term by term. If this is done it is found that

$$L = \ell\left\{1 + \frac{8}{3}\left(\frac{d}{\ell}\right)^2 - \frac{32}{5}\left(\frac{d}{\ell}\right)^4 + \ldots\right\} \qquad (1.10)$$

From the first three terms of the series

$$\left(\frac{d}{\ell}\right)^2 \cong \frac{5}{24}\left\{\left(1 + \frac{18}{5}\left(\frac{L-\ell}{\ell}\right)\right)^{\frac{1}{2}} - 1\right\} \qquad (1.11)$$

Therefore, in general, if w and ℓ are known it is necessary to specify only one of the three remaining variables (H, d, L) in order to obtain a complete solution.

c. The elastic parabola

In many situations the increase in sag owing to the stretching of the cable in its free-hanging position is of little importance. Indeed, for steel cables spanning distances of 100 m, the increase in sag may be safely ignored and the classical, inextensible theory of the previous section may be used with confidence.

For long-span cables, with spans of the order of 1000 m, the situation is different. While the fractional increase in the sag, owing to cable stretch, may be much the same as in shorter spans, the absolute increase in sag is many times greater. Sag increases of 1 m or more are possible for long-span steel cables, such as occur in construction of suspension bridges when the cables are in their free-hanging positions. In such situations it is imperative to be able to calculate the sag accurately.

Rankine's work represented the first serious attempt to solve this problem and this was followed by Routh's exact solution. However, Rankine's solution contains unnecessary approximations and, unfortunately, Routh's solution is inconvenient on account of the coordinate system used. The following is an attempt to bridge the gap between these two previous approaches.

For a given inextensible sag d, an unstressed length of cable L is laid out (see Eq. 1.10). When this cable is hung

between the two supports, a distance ℓ (< L) apart, stretching occurs; the sag increases to $(d + \Delta d)$ and the horizontal component of tension reduces from its inextensible value (see Eq. 1.6) to $(H - \Delta H)$.

It can be seen from Fig. 2 that an element at point P in the inextensible profile, with coordinates (x, y), moves to a new position at P′ in the stretched profile, with coordinates $(x + u, y + v)$. The quantities u and v are the longitudinal and vertical movements of the cable element respectively.

Provided that these movements are small, vertical equilibrium of the element in the stretched configuration is given by

$$(H - \Delta H)\frac{d^2}{dx^2}(y+v) = -w \tag{1.12}$$

which can be integrated directly to give the parabola

$$y + v = \frac{1}{(1 - H_*)} \frac{w\ell^2}{2H} \left\{\frac{x}{\ell} - \left(\frac{x}{\ell}\right)^2\right\} \tag{1.13}$$

where $H_* = \frac{\Delta H}{H}$. *After Eq. 1.5 is substituted into Eq. 1.13, the* parabola for the additional deflection is found to be

$$v = \frac{H_*}{(1 - H_*)} \frac{w\ell^2}{2H} \left\{\frac{x}{\ell} - \left(\frac{x}{\ell}\right)^2\right\} \tag{1.14}$$

Hence, the fractional increase in sag owing to cable stretch is

$$d_* = \frac{H_*}{(1 - H_*)} \tag{1.15}$$

where $d_* = \frac{\Delta d}{d}$.

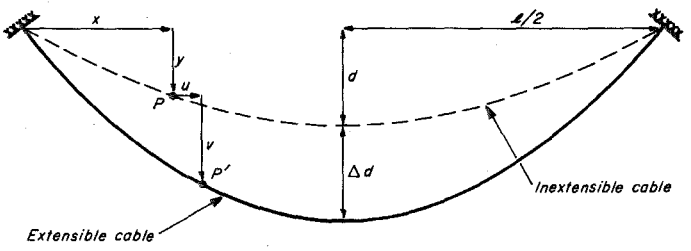

Figure 2 Definition diagram for elastic parabola.

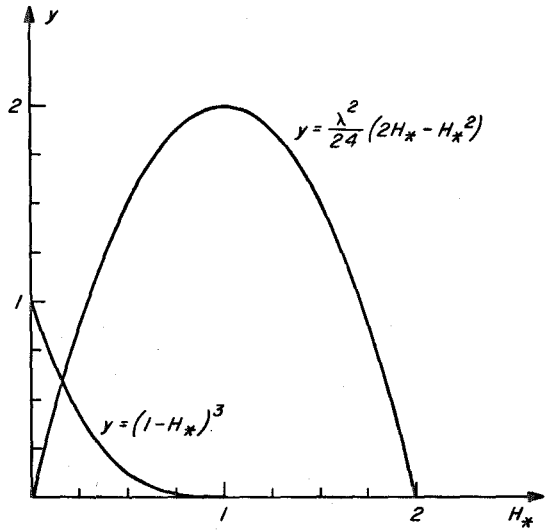

Figure 3 Graphical solution of H_* for elastic parabola.

In order to evaluate H_*, recourse must be made to the cable equation which relates the stretching of the cable element to the geometric displacements which it undergoes. In the present context the equation reads

$$\frac{(H - \Delta H)\left(\frac{ds}{dx}\right)^3}{E_c A_c} = \frac{du}{dx} + \frac{dy}{dx}\frac{dv}{dx} + \frac{1}{2}\left(\frac{dv}{dx}\right)^2 \qquad (1.16)$$

where E_c is Young's modulus and A_c is the area of the cable. This equation is of fundamental importance and is accurate to the second order of small quantities. A derivation of the general cable equation can be found in Appendix II.

The displacements u and v are zero at each end of the cable, $\frac{dy}{dx}$ and $\frac{dv}{dx}$ are continuous along the span, and so integration by parts of Eq. 1.16 yields

$$\frac{(H - \Delta H)L_e}{E_c A_c} = -\left(\frac{d^2y}{dx^2} + \frac{1}{2}\frac{d^2v}{dx^2}\right)\int_0^{\ell} v\, dx \qquad (1.17)$$

where L_e is a virtual length of the cable defined by

$$L_e = \int_0^{\ell}\left(\frac{ds}{dx}\right)^3 dx \simeq \ell\left\{1 + 8\left(\frac{d}{\ell}\right)^2\right\}$$

After substitution, integration and rearrangement the following cubic is obtained from Eq. 1.17

$$(1 - H_*)^3 = \frac{\lambda^2}{24}(2H_* - H_*^2) \qquad (1.18)$$

where

$$\lambda^2 = \left(\frac{w\ell}{H}\right)^2 \frac{\ell}{\left(\frac{HL_e}{E_cA_c}\right)}$$

The dimensionless variable, λ^2, is the fundamental parameter of the extensible cable. It takes account of the effects of initial cable geometry and cable elasticity and will arise repeatedly throughout this thesis.

Equation 1.18 can be solved in standard ways, but a graphical solution is convenient here. Figure 3 shows that H_* must lie between

$$0 < H_* < 1$$

an intuitively obvious result. Consider now the two limits for λ^2:

(i) λ^2 large (i.e. $\lambda^2 > 100$)

This covers most freely hanging cables which have small, although appreciable, sag to span ratios. To sufficient accuracy Eq. 1.18 then becomes

$$1 - 3H_* \simeq \frac{\lambda^2}{12} H_*$$

from which

$$\left.\begin{aligned} H_* &\simeq \frac{1}{\left(3 + \frac{\lambda^2}{12}\right)} \\ d_* &\simeq \frac{1}{\left(2 + \frac{\lambda^2}{12}\right)} \end{aligned}\right\} \qquad (1.19)$$

The corresponding result from Rankine's approximate theory (as reported by Pugsley[10]), may be rearranged to

$$d_* \simeq \frac{1}{\frac{\lambda^2}{12}\left\{1 - \frac{32}{15}\left(\frac{d}{\ell}\right)^2\right\}}$$

which is somewhat larger.

Consider the following example which could apply to a free-hanging cable of a long-span suspension bridge.

Example 1

Cable properties: ℓ = 915 m (3000 ft); w = 4.4 kN/m (300 lb/ft); $E_c = 180 \times 10^6$ kN/m^2 (26×10^6 psi); A_c = 0.161 m^2 (250 in^2); sag ratio (initial geometry) = 1:12.

Hence

$$\lambda^2 = 2 \times 10^3 >> 100$$

and consequently

$$H_* \simeq \frac{1}{170}$$

$$d_* \simeq \frac{1}{169}$$

from which

$$\Delta d \simeq 0.455 \text{ m } (1.49 \text{ ft})$$

Rankine's theory gives

$$d_* \simeq \frac{1}{164}$$

In a more realistic example attention would have to be paid to the possible influence of the towers and side-spans.

(ii) λ^2 small (i.e. $\lambda^2 << 1$)

Cables for which λ^2 is small may be flat (in which case $\frac{w\ell}{H}$ is small) and/or they may be very extensible (in which case E_c is small). Some care has to be exercised in taking the limits of Eqs. 1.13 (or 1.14) and 1.18 as λ^2 approaches zero. In such cases

$$\left.\begin{aligned} H_* &\simeq 1 - \left(\frac{\lambda^2}{24}\right)^{\frac{1}{3}} \\ \frac{(d + \Delta d)}{\ell} &\simeq \frac{\sqrt[3]{3}}{4}\left\{\left(\frac{w\ell}{H}\right)\left(\frac{H}{E_c A_c}\right)\left(\frac{L_e}{\ell}\right)\right\}^{\frac{1}{3}} \end{aligned}\right\} \qquad (1.20)$$

Three separate situations may be isolated, in each of which λ^2 is small. When $\left(\frac{w\ell}{H}\right)$ is small and E_c is large, as in a taut, flat steel cable, it is seen that $\Delta d \to 0$, as expected. If, for some cable, both $\left(\frac{w\ell}{H}\right)$ and E_c are small, then Δd is finite. Alternatively, if $\left(\frac{w\ell}{H}\right)$ is of order unity and E_c is small, $\Delta d \to \infty$.

The last two situations are of little practical importance. Indeed, the third case can be correct only in a qualitative sense since the assumption of small additional deflections, on which the analysis is based, is clearly violated.

It is noticed from Eq. 1.20 that a substantial change in tension occurs when λ^2 is very small. This could be important in a practical situation involving taut, flat steel cables if a procedure was followed whereby the cable was cut and then hung in position.

However, this procedure is usually impracticable since the unstressed length of such a cable is only a minute fraction longer than the span and problems of accurate measurement and construction would certainly arise. Normally, the construction of such a cable would be effected by placing it in jacks, prestressing the cable to a given pretension, and then anchoring it off. Since the weight and span of the cable are known, the sag in the free-hanging position is found directly from the inextensible theory, Eq. 1.6.

It may be concluded that the theory of the elastic parabola will find an application primarily in the construction of the cables of suspension bridges and possibly in the construction of large, overhead electric power lines. The approximate results given by Eq. 1.19 may be used with confidence for such problems. In most other practical situations, the stretching of the cable in its free-hanging position may be ignored.

2. Parabolic Cable Under Applied Loads

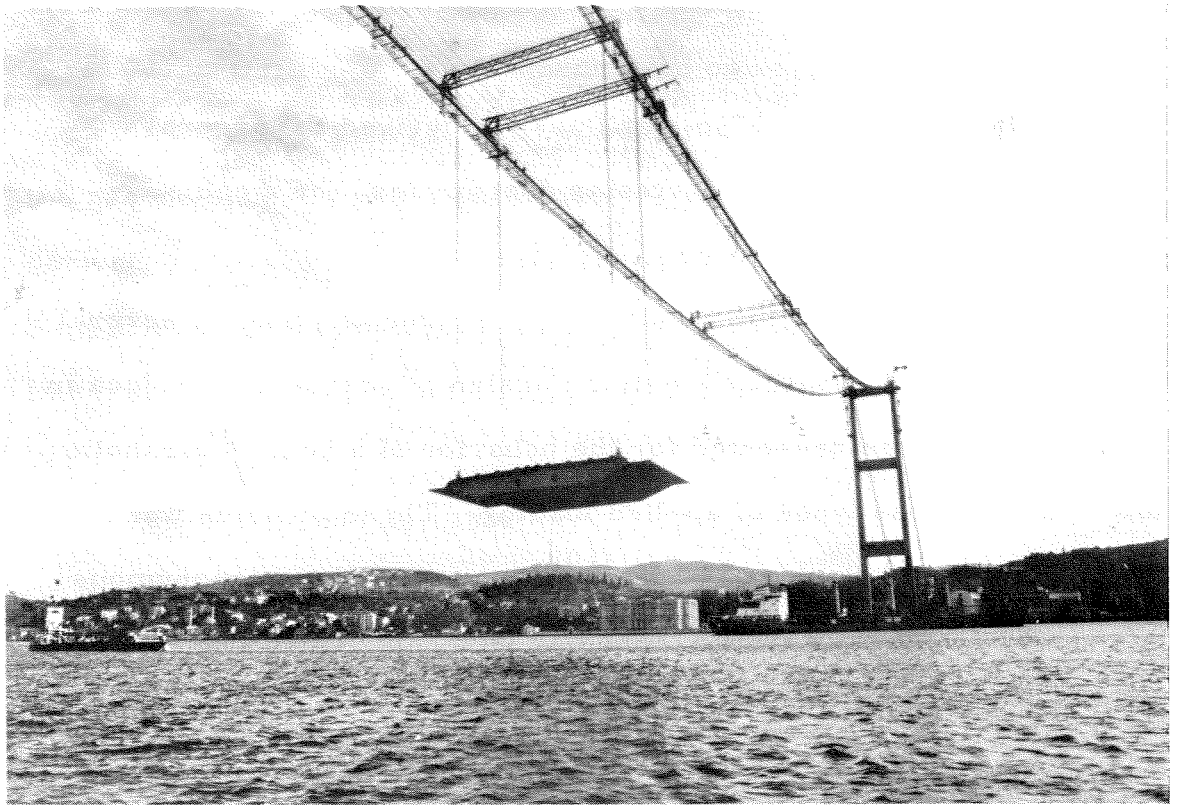

Erection of first segment of deck of the Bosporus bridge.

After the discovery of the catenary, the first work which considered the behavior of a free-hanging cable under the action of an applied load was that of James Bernoulli[15] at the end of the seventeenth century. Using geometrical principles, as was common at that time, he investigated the response of a catenary to a central force.

It was not until 1796 that Fuss[15] derived the general equations of equilibrium, in Cartesian coordinates, for a cable element under any type of force.

Later, around the middle of the nineteenth century, several papers appeared in connection with the design of suspension bridges in which analyses were presented for the behavior of a heavy, parabolic cable under various types of applied loading. These theories were developed partly by Rankine in 1858[10], but mainly by an anonymous writer in 1860 and 1862[10]. It was realized at this time that the response of the cable was non-linear. Successive equal increments of load were seen to cause successive increments in the corresponding deflection, each smaller than the last. This non-linear stiffening effect was later discussed in some detail by Pugsley[10]. These later theories have been presented in book form by Pugsley[10].

More recently, with the advent of the digital computer, numerical solutions have been presented. For example, O'Brien[9] has shown how numerical techniques may be employed to obtain general solutions to suspended cable problems. Buchanan[1] has presented a brief analysis of two-dimensional cable systems using

perturbation methods. The digital computer is sometimes an essential tool in analyzing complicated problems, however, its use is not required to solve the problem at hand.

In the analyses to be presented here, the equations of equilibrium are solved in a straightforward and physically meaningful manner. Compatibility of displacements will be satisfied by a cable equation which, in general, will allow for terms up to and including the second order of small quantities. Thus, general results are derived which are accurate to the second order of small quantities. Simplifications are then made to the general theory; the solutions are linearized and they are also adapted to apply to cables which are initially taut and flat.

a. Point load on cable

To begin with, it is assumed that the shape of the cable, in its free-hanging position, is given by the parabola

$$y = \frac{w\ell^2}{2H}\left\{\frac{x}{\ell} - \left(\frac{x}{\ell}\right)^2\right\}$$

where any initial effects, owing to cable elasticity, have been accounted for.

Consider a point load P acting at a distance x_1 from the left-hand support (see Fig. 4). Provided that the additional movements of the cable are small, so that the slope of the cable remains small, vertical equilibrium at a cross section of the cable requires that

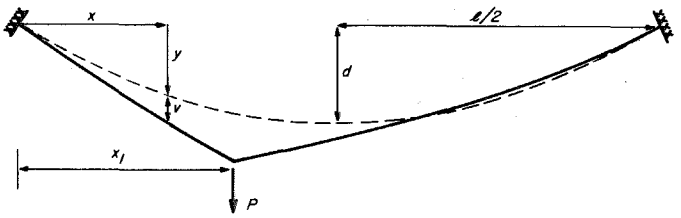

Figure 4 Definition diagram for point load on cable.

(i) for $0 \leq \frac{x}{\ell} < \frac{x_1}{\ell}$,

$$(H + h)\frac{d}{dx}(y + v) = P\left(1 - \frac{x_1}{\ell}\right) + \frac{w\ell}{2}\left(1 - \frac{2x}{\ell}\right)$$

where v is the additional vertical cable deflection and h is the increment in the horizontal component of cable tension owing to the point load. The right-hand side of the above equation is analogous to the shear force in a simply supported beam of uniform weight under the action of a point load. Hence,

$$(H + h)\frac{dv}{dx} = P\left(1 - \frac{x_1}{\ell}\right) - h\frac{dy}{dx} \qquad (1.21)$$

Similarly it is found that

(ii) for $\frac{x_1}{\ell} < \frac{x}{\ell} \leq 1$,

$$(H + h)\frac{dv}{dx} = -\frac{Px_1}{\ell} - h\frac{dy}{dx} \qquad (1.22)$$

Equations 1.21 and 1.22 are then integrated and, after the boundary conditions have been satisfied, the dimensionless equations for the additional vertical cable deflection are found to be:

(i) for $0 \leq \frac{x}{\ell} \leq \frac{x_1}{\ell}$,

$$v_* = \frac{1}{(1 + h_*)}\left\{\left(1 - \frac{x_1}{\ell}\right)\frac{x}{\ell} - \frac{h_*}{P_*}\left(\frac{1}{2}\left(\frac{x}{\ell}\right) - \frac{1}{2}\left(\frac{x}{\ell}\right)^2\right)\right\} \qquad (1.23)$$

(ii) for $\frac{x_1}{\ell} \leq \frac{x}{\ell} \leq 1$,

$$v_* = \frac{1}{(1 + h_*)}\left\{\frac{x_1}{\ell}\left(1 - \frac{x}{\ell}\right) - \frac{h_*}{P_*}\left(\frac{1}{2}\left(\frac{x}{\ell}\right) - \frac{1}{2}\left(\frac{x}{\ell}\right)^2\right)\right\} \qquad (1.24)$$

where

$$v_* = \frac{v}{\left(\frac{P\ell}{H}\right)} \quad , \quad h_* = \frac{h}{H} \quad , \quad P_* = \frac{P}{w\ell} \ .$$

The non-linear nature of the response of the cable to the applied loading is apparent from these two equations.

In order to complete the solution, h_* must now be evaluated. Use is made of the cable equation, where terms up to and including the second order of small quantities have been retained (see Appendix II).

$$\frac{hL_e}{E_cA_c} = \int_0^{\ell} du + \int_0^{\ell} \frac{dy}{dx}\frac{dv}{dx}\,dx + \frac{1}{2}\int_0^{\ell}\left(\frac{dv}{dx}\right)^2 dx$$

Since $\frac{dy}{dx}$ is continuous along the span and u and v are zero at each support, this equation reduces to

$$\frac{hL_e}{E_cA_c} = \frac{w}{H}\int_0^{\ell} v\,dx + \frac{1}{2}\int_0^{\ell}\left(\frac{dv}{dx}\right)^2 dx \qquad (1.25)$$

Under point loading $\left(\frac{dv}{dx}\right)$ is discontinuous at the position of load application and the last integral above, when integrated by parts, gives

$$\frac{1}{2}\int_0^{\ell}\left(\frac{dv}{dx}\right)^2 dx = -\frac{1}{2}\left\{\frac{dv}{dx}\,v\Big|_{x_1^-}^{x_1^+} + \frac{d^2v}{dx^2}\int_0^{x_1} v\,dx + \frac{d^2v}{dx^2}\int_{x_1}^{\ell} v\,dx\right\}$$

This result may now be substituted into Eq. 1.25. After Eqs. 1.23 and 1.24 have been substituted into Eq. 1.25 and the integration has been performed, the following dimensionless cubic equation for h_* is derived

$$2h_*(1 + h_*)^2 = \lambda^2 \left\{ \left(\left(\frac{x_1}{\ell}\right) - \left(\frac{x_1}{\ell}\right)^2 \right) (P_* + P_*^2) - \frac{h_*}{12}(2 + h_*) \right\}$$

This equation may be rearranged to the standard form for a cubic

$$h_*^3 + \left(2 + \frac{\lambda^2}{24}\right) h_*^2 + \left(1 + \frac{\lambda^2}{12}\right) h_* - \frac{\lambda^2}{2} \left(\left(\frac{x_1}{\ell}\right) - \left(\frac{x_1}{\ell}\right)^2 \right) P_*(1 + P_*) = 0 \tag{1.26}$$

This cubic is of the form

$$z^3 + az^2 + bz - c = 0$$

where a, b, c are positive, real quantities. Accordingly, from Descartes' "rule of signs", there is just one, positive real root of Eq. 1.26. This root is the required value of h_*.

The cubic can be solved exactly using the requisite forms of Cardan's equations (see, for example, Uspensky[20]).

For a given problem it is clear that h_* depends not only on P_* and $\frac{x_1}{\ell}$, but also on λ^2 — the parameter which allows for cable geometry and elasticity. Also, it may easily be shown that, for given values of P_* and λ^2, h_* is a maximum when $x_1 = \frac{\ell}{2}$. The variables P_* and λ^2 may take on any value, large or small, provided that the slope of the cable remains small.

A knowledge of the small, longitudinal cable movement induced by the loading, may be important in some applications. These movements may be calculated from the cable equation and in dimensionless form they read:

(i) for $0 \le \frac{x}{\ell} \le \frac{x_1}{\ell}$,

$$u_* = \frac{h_* \frac{L_x}{L_e}}{\lambda^2 P_*} - \left\{ \frac{2 + h_*}{(1 + h_*)} \left(\frac{1}{2} - \frac{x}{\ell} \right) + \frac{P_*}{(1 + h_*)} \left(1 - \frac{x_1}{\ell} \right) \right\} \frac{v_*}{2}$$

$$- \frac{2 + h_*}{(1 + h_*)} \int_0^{\frac{x}{\ell}} \frac{v_*}{2} \, d\left(\frac{x}{\ell}\right) \qquad (1.27)$$

(ii) for $\frac{x_1}{\ell} \le \frac{x}{\ell} \le 1$,

$$u_* = \frac{h_* \frac{L_x}{L_e}}{\lambda^2 P_*} - \left\{ \frac{2 + h_*}{(1 + h_*)} \left(\frac{1}{2} - \frac{x}{\ell} \right) - \frac{P_*}{(1 + h_*)} \left(\frac{x_1}{\ell} \right) \right\} \frac{v_*}{2}$$

$$- \frac{2 + h_*}{(1 + h_*)} \int_0^{\frac{x}{\ell}} \frac{v_*}{2} \, d\left(\frac{x}{\ell}\right) - \frac{P_*}{(1 + h_*)} \frac{v_{*1}}{2} \qquad (1.28)$$

where v_{*1} is the value of v_* at x_1,

$$u_* = \frac{u}{\left(\frac{P\ell}{H}\right)\left(\frac{w\ell}{H}\right)}$$

and

$$L_x = \ell \left[\left(\frac{x}{\ell} \right) + 24 \left(\frac{d}{\ell} \right)^2 \left\{ \left(\frac{x}{\ell} \right) - 2 \left(\frac{x}{\ell} \right)^2 + \frac{4}{3} \left(\frac{x}{\ell} \right)^3 \right\} \right]$$

The above results are general and will provide accurate solutions for practical problems in which the effects of a point load on a parabolic cable have to be assessed.

Two useful simplifications are possible for the general theory. In the first the solutions are linearized, in the second the solutions are simplified to provide results for cables which are initially straight (as in the taut string).

(1) Linearized theory

The problem is linearized by neglecting all second order terms which appear in the differential equations of equilibrium and in the cable equation. This requires that the term $h\frac{dv}{dx}$ be left out of Eqs. 1.21 and 1.22. The term $\frac{1}{2}\int_0^{\ell}\left(\frac{dv}{dx}\right)^2 dx$ must also be removed from Eq. 1.25. As a consequence, the equations for v_* read:

(i) for $0 \leq \frac{x}{\ell} \leq \frac{x_1}{\ell}$,

$$v_* = \left\{\left(1 - \frac{x_1}{\ell}\right)\frac{x}{\ell} - \frac{h_*}{P_*}\left(\frac{1}{2}\left(\frac{x}{\ell}\right) - \frac{1}{2}\left(\frac{x}{\ell}\right)^2\right)\right\} \qquad (1.29)$$

(ii) for $\frac{x_1}{\ell} \leq \frac{x}{\ell} \leq 1$,

$$v_* = \left\{\frac{x_1}{\ell}\left(1 - \frac{x}{\ell}\right) - \frac{h_*}{P_*}\left(\frac{1}{2}\left(\frac{x}{\ell}\right) - \frac{1}{2}\left(\frac{x}{\ell}\right)^2\right)\right\} \qquad (1.30)$$

The cable equation is reduced to

$$\frac{hL_e}{E_c A_c} = \frac{w}{H}\int_0^{\ell} v\, dx \qquad (1.31)$$

and after substitution, integration and rearrangement the following linearized expression is obtained for h_*

$$h_* = \frac{1}{\left(1 + \frac{12}{\lambda^2}\right)}\, 6P_* \left\{\left(\frac{x_1}{\ell}\right) - \left(\frac{x_1}{\ell}\right)^2\right\} \qquad (1.32)$$

Usually these linearized solutions will be accurate only as long as P_* remains small. In fact, when λ^2 is large P_* should not be greater than about 10^{-1} if the equations are to be accurate to within 10%. However, when λ^2 is small, larger values of P_* are admissible. In practice, steel cables are invariably used for structural purposes. Thus, changes in λ^2 are brought about mainly by changes in the cable geometry. Small values of λ^2 correspond to very flat-sag cables, while large values of λ^2, reflecting the relatively inextensible nature of the steel material, correspond to more appreciable sag ratios ($\leq 1:8$).

For taut, flat cables $\lambda^2 << 1$, and it can be seen from Eq. 1.32 that $h_* \to 0$. Hence Eqs. 1.29 and 1.30 reduce to those of the classical linear theory of the taut string.

For cables, such as those of the suspension bridge, where the sag ratio is of the order of 1:10, $\lambda^2 >> 1$ and

$$h_* \to 6P_* \left\{ \left(\frac{x_1}{\ell}\right) - \left(\frac{x_1}{\ell}\right)^2 \right\}$$

This result is reported by Pugsley[10].

One final point, which is of interest for the linear cable, concerns the overall maximum additional deflection under a point load. For a given value of $\frac{x_1}{\ell}$ the maximum additional deflection occurs at x_1. Since $\frac{x_1}{\ell}$ may take on any value between 0 and 1, the overall maximum depends on position. To locate this overall maximum, x is set equal to x_1 and Eq. 1.32 is substituted

in either Eq. 1.29 or Eq. 1.30 to give

$$v_* = \left(\left(\frac{x_1}{\ell}\right) - \left(\frac{x_1}{\ell}\right)^2\right)\left\{1 - \frac{3}{\left(1 + \frac{12}{\lambda^2}\right)}\left(\left(\frac{x_1}{\ell}\right) - \left(\frac{x_1}{\ell}\right)^2\right)\right\} \qquad (1.33)$$

Setting the derivative, with respect to $\frac{x_1}{\ell}$, of this equation equal to zero indicates that possible turning points exist at

(i) $\frac{x_1}{\ell} = \frac{1}{2}$

(ii) $\frac{x_1}{\ell} = \frac{1}{2}\left\{1 \mp \left(1 - \frac{2}{3}\left(1 + \frac{12}{\lambda^2}\right)\right)^{\frac{1}{2}}\right\}$

For real roots (which are equally spaced about mid-span), it is necessary that

$$\lambda^2 \geq 24$$

This is an important criterion and leads to the following observations:

(i) If $\lambda^2 \geq 24$,

then v_* has an overall maximum when

$$\frac{x_1}{\ell} = \frac{1}{2}\left\{1 \mp \left(1 - \frac{2}{3}\left(1 + \frac{12}{\lambda^2}\right)\right)^{\frac{1}{2}}\right\} \qquad (1.34)$$

When $\lambda^2 >> 24$ (i.e. the cable is "inextensible")

$$\frac{x_1}{\ell} \rightarrow \frac{1}{2}\left(1 \mp \frac{1}{\sqrt{3}}\right) = 0.211,\ 0.789$$

This latter result is reported by Pugsley[10]. The overall maximum value of v_* is

$$v_* = \frac{1}{12}\left(1 + \frac{12}{\lambda^2}\right) \tag{1.35}$$

and when $\lambda^2 >> 24$

$$v_* \to \frac{1}{12}$$

(ii) If $\lambda^2 \leq 24$,

then v_* has an overall maximum when

$$\frac{x_1}{\ell} = \frac{1}{2} \tag{1.36}$$

and this overall maximum value of v_* is

$$v_* = \frac{1}{4}\left\{1 - \frac{3}{4\left(1 + \frac{12}{\lambda^2}\right)}\right\} \tag{1.37}$$

When $\lambda^2 << 24$ (i.e. a taut string)

$$v_* \to \frac{1}{4}$$

Therefore, for the linear parabolic cable, the overall maximum value of v_*, owing to a point load, occurs at the point of loading and lies between

$$\frac{1}{12} < v_* < \frac{1}{4}$$

The location of the maximum occurs at

$$\frac{1}{2}\left(1 - \frac{1}{\sqrt{3}}\right) < \frac{x_1}{\ell} \leq \frac{1}{2}$$

It may be concluded for the linear cable that both the overall maximum value of v_*, and the associated value of $\frac{x_1}{\ell}$, depend on the value of λ^2. It is emphasized that these results refer only to a linear cable. It is difficult to solve the more useful non-linear problem since the solutions will depend on P_* as well as λ^2.

The linearized solutions presented here will be accurate provided that $P_* \sim 10^{-1}$. If P_* is larger, as it will often be, then second order effects must usually be considered. There is some difference of opinion on what second order terms must be retained. In the general theory of this thesis, all second order terms are retained. However, Pugsley[10] allows for second order terms in the equations for cable deflection, but both second order effects and the effects of cable elasticity are removed from the cable equation. While this appears a reasonable assumption for such problems as the response of a suspension bridge cable to a point load (see Example 2), it is somewhat inconsistent and will lead to inaccuracies in other situations (see Example 3). Incidentally, if the cable is assumed inextensible from the outset (as Pugsley has done), there is no way that the linear theory can give the correct result as the initial cable profile approaches that of the classical taut string.

(2) Taut, flat cable

Since in this situation the cable is initially flat (or, in reality, nearly so), $y \equiv 0$. Therefore, the equations for the vertical cable deflection are:

(i) for $0 \leq \frac{x}{\ell} \leq \frac{x_1}{\ell}$,

$$v_* = \frac{1}{(1 + h_*)} \left\{ \left(1 - \frac{x_1}{\ell}\right) \frac{x}{\ell} \right\} \tag{1.38}$$

(ii) for $\frac{x_1}{\ell} \leq \frac{x}{\ell} \leq 1$,

$$v_* = \frac{1}{(1 + h_*)} \left\{ \frac{x_1}{\ell} \left(1 - \frac{x}{\ell}\right) \right\} \tag{1.39}$$

The cable equation becomes

$$\frac{h\ell}{E_c A_c} = \frac{1}{2} \int_0^{\ell} \left(\frac{dv}{dx}\right)^2 dx \tag{1.40}$$

Since $\frac{d^2v}{dx^2} = 0$, the cable equation may be reduced, after integration by parts, to

$$\frac{h\ell}{E_c A_c} = \frac{1}{2} \, v \, \frac{dv}{dx} \Bigg|_{x_1^+}^{\bar{x_1}} \tag{1.41}$$

and differentiation and substitution of Eqs. 1.38 and 1.39 in Eq. 1.41 and rearrangement gives

$$h_*(1 + h_*)^2 = \frac{\lambda^2}{2} \left\{ \left(\frac{x_1}{\ell}\right) - \left(\frac{x_1}{\ell}\right)^2 \right\} P_*^2 \tag{1.42}$$

In this situation λ^2 is always very small since $\left(\frac{w\ell}{H}\right)^2$ is very small for a flat cable. However, P_* is usually large so that the product $\lambda^2 P_*^2$ is not necessarily small. If P_* is small, then $h_* \to 0$, and the classical results for the linear taut string are obtained.

Equation 1.42 has an exact solution of the form

$$h_* = \frac{1}{\sqrt[3]{A}} \left\{ \sqrt[3]{A} - \frac{1}{3} \right\}^2 \tag{1.43}$$

where

$$A = -\frac{q}{2} + \sqrt{\frac{q^2}{4} + \frac{p^3}{27}}$$

and

$$p = -\frac{1}{3} \quad , \quad q = -\frac{2}{27} - \frac{\lambda^2}{2} \left\{ \left(\frac{x_1}{\ell}\right) - \left(\frac{x_1}{\ell}\right)^2 \right\} P_*^2$$

As expected, it can be shown that $\sqrt[3]{A} \geq \frac{1}{3}$, and $\sqrt[3]{A} = \frac{1}{3}$ only when $P_* = 0$, or $\frac{x_1}{\ell} = 0, 1$.

The results given by Eqs. 1.38, 1.39 and 1.42 may be rearranged to give a standard, classical form. If the value of v at $x = x_1$ is written as δ, then it is found that

$$h_* = \frac{1}{2} \left(\frac{E_c A_c}{H} \right) \frac{1}{\left\{ \left(\frac{x_1}{\ell}\right) - \left(\frac{x_1}{\ell}\right)^2 \right\}} \left(\frac{\delta}{\ell}\right)^2 \tag{1.44}$$

and

$$\frac{1}{2}\left(\frac{E_c A_c}{H}\right)\frac{1}{\left\{\left(\frac{x_1}{\ell}\right)-\left(\frac{x_1}{\ell}\right)^2\right\}}\left(\frac{\delta}{\ell}\right)^3+\frac{\delta}{\ell}=\left\{\left(\frac{x_1}{\ell}\right)-\left(\frac{x_1}{\ell}\right)^2\right\}\frac{P}{H} \tag{1.45}$$

When $x_1 = \frac{\ell}{2}$, Eqs. 1.44 and 1.45 are those reported by Inglis[3].

These two latter solutions are particularly useful if δ, rather than P, is the independent variable; otherwise, the previous formulation is of most use. The classical formulation, as given by Inglis, is obtained by considering equilibrium at the position of load application and then applying a binomial series expansion to Pythagoras' theorem in order to estimate the relationship between the deflection and the stretching which the inclined cable components undergo. This method of solution is straightforward only when a point load is applied to a flat cable. By comparison, the other approach outlined here is a particular adaptation of the general theory which can be used readily in other situations where the classical formulation would be extremely difficult to apply.

b. Examples

As a means of illustrating the theories derived so far, consider the following examples.

Example 2

The first segment of the deck of a long-span suspension bridge is to be lifted into place at mid-span (for example, see the photograph on p. 19). It is required to find the additional deflection at mid-span and the increment in the horizontal component of cable tension. The following properties refer to the cables in their free-

hanging position.

ℓ = 915 m (3000 ft); w = 4.4 kN/m (300 lb/ft); $E_c = 180 \times 10^6$ kN/m^2 (26×10^6 psi); A_c = 0.161 m^2 (250 in^2); sag ratio (in free-hanging position) = 1:12

The weight of the segment, per cable, is

$$P = 890 \text{ kN} \quad (200,000 \text{ lbs})$$

Hence, $\lambda^2 = 2 \times 10^3$, $\frac{x_1}{\ell} = 0.5$, $P_* = 0.221$. The cubic to be solved becomes (Eq. 1.26)

$$h_*^3 + 85.5\, h_*^2 + 168\, h_* - 67.5 = 0$$

and the solution is found to be

$$h_* = 0.343$$

This may be compared with the linear theory (Eq. 1.32) which gives

$$h_* = 0.33$$

Although this is little different from the more exact theory, the close agreement is misleading. For this problem the relationship between additional cable tension and applied loads appears essentially linear, but the relationship between additional deflection and applied load is not linear.

The additional deflection at mid-span is, (Eq. 1.23)

$$v_* = 0.0415$$

from which

$$v = 5.6 \text{ m } (18.4 \text{ ft})$$

In a more realistic example the possible influence of the towers and sidespans would have to be assessed.

Example 3

A "flying fox" is used to transport materials across a ravine. In its free-hanging position the cable spans 91.5 m (300 ft) with a ratio of sag to span of 1:50. It is required to find the additional horizontal component of cable tension and the additional cable deflection when a point load of 17.8 kN (4000 lbs) is carried at mid-span. Properties of the cable are: $w = 38.8$ N/m (2.66 lb/ft); $E_c = 104 \times 10^6$ kN/m^2 (15×10^6 psi); $A_c = 5.06 \times 10^{-4}$ m^2 (0.785 in^2). Hence, $\lambda^2 = 60.2$, $\frac{x_1}{\ell} = 0.5$, $P_* = 5.0$.

From the general theory (Eq. 1.26) the cubic for h_* becomes

$$h_*^3 + 4.5\, h_*^2 + 6\, h_* - 226 = 0$$

and the solution is

$$h_* = 4.65$$

If the theory of the taut, flat cable is applied, the cubic for h_* becomes (Eq. 1.42)

$$h_*(1 + h_*)^2 = 189$$

from which

$$h_* = 5.1$$

On the other hand, the linear theory (Eq. 1.32) gives

$$h_* = 6.25$$

In this problem the general theory is indispensible if the correct solution is to be obtained.

The additional cable deflection at mid-span is

(Eq. 1.23)

$$v_* = 0.0237$$

from which

$$v = 1.73 \text{ m } (5.68 \text{ ft})$$

Under this loading the sag of the cable has almost doubled but, since the cable slope is still small, the result is reliable.

(c) Experiments on a taut cable

In order to check the accuracy of the theories presented for the response of a cable to a point load, it was decided to carry out a short experimental program. A flat, taut cable was chosen since it is the easiest to experiment on. Also, it was felt that, since the theory for the taut cable is closely related to the general theory, good agreement here between the theory and experiment could reasonably be construed as verification for the general theory.

Consequently, a small rigid test rig was constructed which had a clear span of 91.5 cm (3 ft). See Fig. 5. The cable was anchored at one end and passed over two rigid uprights before being anchored in a nut and bolt device at the other end. The initial cable tension was adjusted by this device.

Two types of cables were tested. One consisted of multiple twisted strands, the other was a piano wire.

In each case the experimental procedure employed was as follows. The cable was placed in the rig and pretensioned to some value H. This initial pretension was calculated by measuring the deflection caused by hanging a small weight from the mid-span point. The linear theory was then applied to determine H. Successively larger weights were then hung from the mid-span point and the corresponding deflections were measured.

The equation governing load and deflection at mid-span is (see Eq. 1.38)

$$v = \frac{1}{(1 + h_*)} \cdot \frac{P\ell}{4H}$$

where h_* is determined from Eq. 1.43. When P is small, $h_* \simeq 0$, and the initial pretension can be found from

$$H = \frac{P\ell}{4v}$$

The results have been tabulated and also presented in graphical form to facilitate comparison with the linear theory and the second order, non-linear theory.

(i) Multistrand cable

The cable used was a Bethlehem steel aircraft cord of diameter 0.12 cm (3/64 in) and properties: $E_c = 104 \times 10^6$ kN/m^2 (15×10^6 psi); w = 0.0553 N/m (0.0038 lb/ft). Because the cable comprised numerous twisted strands it did not kink at the uprights and was able to move freely over them. Consequently, the virtual cable length, L_e, was greater than 91.5 cm being

approximately

$$L_e \simeq 91.5 + 2 \times 15.25 \times \sec^3 45^\circ$$

$$\simeq 177 \text{ cm } (69.9 \text{ in})$$

The initial pretension was

$$H = 182 \text{ N } (41 \text{ lbs})$$

Hence

$$\lambda^2 = 2.51 \times 10^{-5}$$

and the cubic from which h is found becomes

$$h_*(1 + h_*)^2 = \frac{\lambda^2}{8} P_*^2 = 3.14 \times 10^{-6} P_*^2$$

Increments in load of 4.45 N (1 lb) were applied from 4.45 N (1 lb) up to 40.05 N (9 lb) and the corresponding deflections were measured. At higher loads the modulus of elasticity of a twisted strand cable is load dependent and, therefore, the cable stress was kept well below the elastic limit to avoid any unnecessary complications.

Table 1 lists the experimental results and the results from the linear and non-linear theories. Figure 6 shows dimensional plots of the experimental results and the theories.

It is clear that there exists excellent agreement between the experimental results and the non-linear theory. Agreement between the linear theory and the experimental results is poor at all but the smallest loads. The linear theory does not allow for additional cable tension and therefore predicts deflections which are too high. It

Table 1

Comparison of theory and experiment
for the twisted strand cable

Experiment			Non-linear theory		Linear theory	
P (N)	v (cm)	H+h = $\frac{P\ell}{4v}$ (N)	v (cm)	H+h (N)	v (cm)	H (N)
0	0	182	0	182	0	182
4.45	0.56	182	0.56	182	0.56	182
8.90	1.03	197	1.03	197	1.12	182
13.35	1.43	214	1.44	212	1.68	182
17.80	1.78	229	1.79	227	2.24	182
22.25	2.06	247	2.07	244	2.80	182
26.70	2.34	261	2.35	260	3.36	182
40.05	2.65	345	2.97	308	5.04	182

Table 2

Comparison of theory and experiment
for the piano wire

Experiment			Non-linear theory		Linear theory	
P (N)	v (cm)	H+h = $\frac{P\ell}{4v}$ (N)	v (cm)	H+h (N)	v (cm)	H (N)
0	0	116	0	116	0	116
4.45	0.88	116	0.88	116	0.88	116
8.90	1.59	127	1.61	126	1.76	116
13.35	2.19	140	2.19	139	2.64	116
17.80	2.66	153	2.70	152	3.52	116
22.25	3.10	164	3.10	164	4.40	116

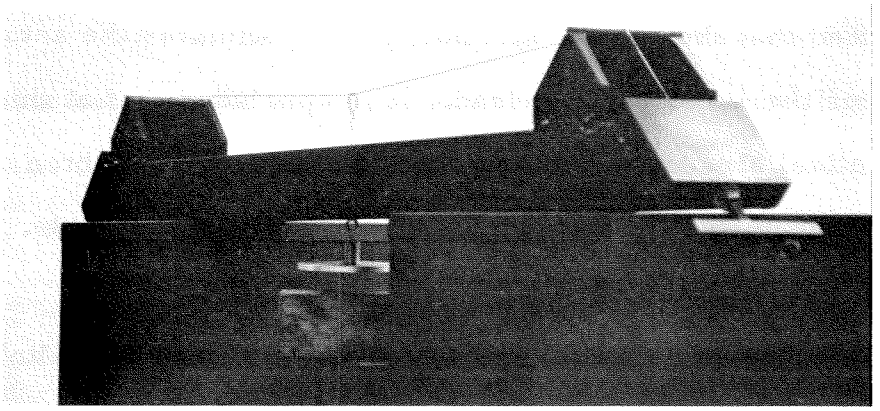

Figure 5 Test rig.

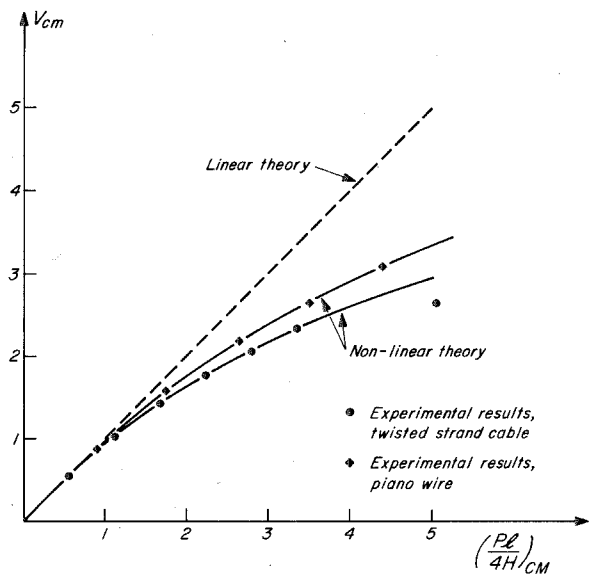

Figure 6 Comparison of theories and experiments.

will be noticed that the non-linear theory overestimates the actual deflection for the 40.05 N (9 lb) load. It is concluded that at this load, the helical strands of the cable are starting to straighten out, with a consequent rise in the modulus of elasticity of the cable.

(ii) Piano wire

The cable used here was a single strand of Malin's Musical Wire (#5) of diameter 0.0355 cm (0.012 in) and properties: $E_c = 207 \times 10^6$ kN/m^2 (30×10^6 psi); $w = 7.63 \times 10^{-3}$ N/m (5.22×10^{-4} lb/ft). It was noticed that this piano wire formed kinks where it passed over each upright. Under load there was no cable movement past the uprights and consequently the virtual cable length L_e was taken to be just the clear span

$$L_e = 91.5 \text{ cm } (3 \text{ ft})$$

The initial pretension was 116 N (26.2 lbs). Hence

$$\lambda^2 = 6.33 \times 10^{-9}$$

and the cubic from which h is found becomes

$$h_*(1 + h_*)^2 = \frac{\lambda^2}{8} P_*^2 = 7.92 \times 10^{-10} P_*^2$$

Increments in load of 4.45 N (1 lb) were applied from 4.45 N up to 22.25 N (5 lb), and the corresponding deflections were measured. The cable stress was always well below the elastic limit.

Table 2 lists the experimental results and the results from the linear and non-linear theories. Figure 6 shows dimensional plots of the experimental results and the theories.

As in the previous experiment, there exists excellent agreement between the experimental results and the non-linear theory. Again, the linear theory, which does not allow for additional cable tension, predicts deflections which are too high.

Conclusions

Excellent agreement was obtained between the non-linear theory and the experimental results. The experimental results confirm the theory as applied to the case of the initially taut, flat cable and lend credence to the applicability and accuracy of the general theory.

d. Uniformly distributed load on part of cable

Consider a uniformly distributed load of intensity p per unit length applied along the span from $x = x_2$ to $x = x_3$. (see Fig. 7.)

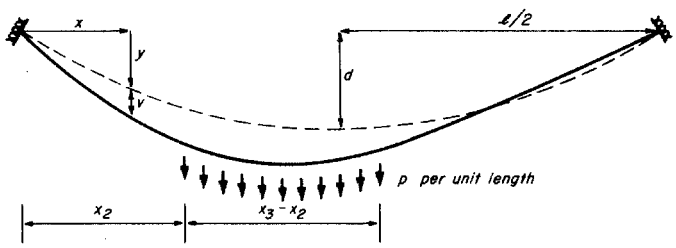

Figure 7 Definition diagram for uniformly distributed load on cable.

By again exploiting the analogy which exists with the simply supported beam, vertical equilibrium at a cross section requires that:

(i) for $0 \le \frac{x}{\ell} \le \frac{x_2}{\ell}$,

$$(H + h)\frac{dv}{dx} = p\ell\left\{\left(\frac{x_3}{\ell} - \frac{x_2}{\ell}\right) - \frac{1}{2}\left(\left(\frac{x_3}{\ell}\right)^2 - \left(\frac{x_2}{\ell}\right)^2\right)\right\} - h\frac{dy}{dx} \qquad (1.46)$$

(ii) for $\frac{x_2}{\ell} \le \frac{x}{\ell} \le \frac{x_3}{\ell}$,

$$(H + h)\frac{dv}{dx} = p\ell\left\{\left(\frac{x_3}{\ell} - \frac{x}{\ell}\right) - \frac{1}{2}\left(\left(\frac{x_3}{\ell}\right)^2 - \left(\frac{x_2}{\ell}\right)^2\right)\right\} - h\frac{dy}{dx} \qquad (1.47)$$

(iii) for $\frac{x_3}{\ell} \le \frac{x}{\ell} \le 1$,

$$(H + h)\frac{dv}{dx} = p\ell\left\{-\frac{1}{2}\left(\left(\frac{x_3}{\ell}\right)^2 - \left(\frac{x_2}{\ell}\right)^2\right)\right\} - h\frac{dy}{dx} \qquad (1.48)$$

After integration and adjustment for the requisite boundary conditions, the following dimensionless equations are obtained for the additional vertical cable deflection:

(i) for $0 \le \frac{x}{\ell} \le \frac{x_2}{\ell}$,

$$v_* = \frac{1}{(1 + h_*)}\left[\left\{\left(\frac{x_3}{\ell} - \frac{x_2}{\ell}\right) - \frac{1}{2}\left(\left(\frac{x_3}{\ell}\right)^2 - \left(\frac{x_2}{\ell}\right)^2\right)\right\}\left(\frac{x}{\ell}\right) - \frac{h_*}{p_*}\left(\frac{1}{2}\left(\frac{x}{\ell}\right) - \frac{1}{2}\left(\frac{x}{\ell}\right)^2\right)\right] \qquad (1.49)$$

(ii) for $\frac{x_2}{\ell} \le \frac{x}{\ell} \le \frac{x_3}{\ell}$,

$$v_* = \frac{1}{(1 + h_*)} \left[\left\{ -\frac{1}{2}\left(\frac{x_2}{\ell}\right)^2 + \left(\frac{x_3}{\ell}\right)\left(\frac{x}{\ell}\right) - \frac{1}{2}\left(\frac{x}{\ell}\right)^2 - \frac{1}{2}\left(\left(\frac{x_3}{\ell}\right)^2 - \left(\frac{x_2}{\ell}\right)^2\right)\left(\frac{x}{\ell}\right) \right\} - \frac{h_*}{p_*}\left(\frac{1}{2}\left(\frac{x}{\ell}\right) - \frac{1}{2}\left(\frac{x}{\ell}\right)^2\right) \right] \qquad (1.50)$$

(iii) for $\frac{x_3}{\ell} \le \frac{x}{\ell} \le 1$,

$$v_* = \frac{1}{(1 + h_*)} \left[\frac{1}{2}\left\{\left(\frac{x_3}{\ell}\right)^2 - \left(\frac{x_2}{\ell}\right)^2\right\}\left(1 - \frac{x}{\ell}\right) - \frac{h_*}{p_*}\left(\frac{1}{2}\left(\frac{x}{\ell}\right) - \frac{1}{2}\left(\frac{x}{\ell}\right)^2\right) \right] \qquad (1.51)$$

where $v_* = \frac{v}{\left(\frac{p\ell^2}{H}\right)}$, $h_* = \frac{h}{H}$, $p_* = \frac{p}{w}$.

The increment in the horizontal component of cable tension, h, is found from the cable equation (see Appendix II) which, since both $\frac{dy}{dx}$ and $\frac{dv}{dx}$ are continuous along the span, is of the form

$$\frac{hL_e}{E_c A_c} = -\int_0^{\ell} \left(\frac{d^2y}{dx^2} + \frac{1}{2}\frac{d^2v}{dx^2}\right) v \, dx \qquad (1.52)$$

After substitution of Eqs. 1.49, 1.50, 1.51 into Eq. 1.52, integration and rearrangement, the following dimensionless cubic for h_* is obtained

$$h_*^3 + \left(2 + \frac{\lambda^2}{24}\right) h_*^2 + \left(1 + \frac{\lambda^2}{12}\right) h_* - \frac{\lambda^2}{2}\left\{\frac{1}{2}\left(\left(\frac{x_3}{\ell}\right)^2 - \left(\frac{x_2}{\ell}\right)^2\right) - \frac{1}{3}\left(\left(\frac{x_3}{\ell}\right)^3 - \left(\frac{x_2}{\ell}\right)^3\right)\right\} p_* - \frac{\lambda^2}{2}\left\{\frac{1}{3}\left(\left(\frac{x_3}{\ell}\right)^3 + 2\left(\frac{x_2}{\ell}\right)^3\right) - \left(\frac{x_3}{\ell}\right)\left(\frac{x_2}{\ell}\right)^2 - \frac{1}{4}\left(\left(\frac{x_3}{\ell}\right)^2 - \left(\frac{x_2}{\ell}\right)^2\right)^2\right\} p_*^2 = 0 \qquad (1.53)$$

This general cubic is of the form

$$z^3 + az^2 + bz - c = 0$$

where a, b, c are positive real quantities. From Descartes' "rule of signs" there is just one, positive root to the above equation. This root is the required value of h_*.

As before, the general solution for h_* can be obtained using the requisite form of Cardan's equations.

It will be noted that there is a symmetry in the coefficient of the cubic involving x_2 and x_3. As is to be expected, the solution of the cubic is the same if $x_3 = 1.0\,\ell$, $x_2 = 0.9\,\ell$ as if $x_3 = 0.1\,\ell$, $x_2 = 0$, etc.

If the loaded length $(x_3 - x_2)$ is allowed to become very small, while $p(x_3 - x_2)$ remains finite, it is easily shown that Eq. 1.53 reduces to Eq. 1.26, the result previously obtained for a point load on the cable.

It can also be shown that when p_* and λ^2 are given, h_* is a maximum when the loading is placed symmetrically about mid-span.

Equations from which the longitudinal cable movements can be found will not be given here. These small movements can be calculated from the cable equation by employing the same procedure as was used to obtain Eqs. 1.27, 1.28.

The above solutions are accurate to the second order of small quantities. They will find particular application in the calculations involved in the construction of suspension bridges, when the

deck is being hung in position. Here, use of the general non-linear theory is essential since the deck load is usually many times greater than the weight of the cables and λ^2 is large. At this stage the stiffness of the deck is negligible since, in order to eliminate flexural stresses owing to dead load, continuity of rotations is rarely provided between adjacent segments of the deck until near the end of the construction of the deck.

In certain situations the theory can be simplified and these are now briefly considered.

(1) Linearized theory

In keeping with the approach given in the section on the point load on a cable, all second order terms are dropped from the cable equation and the deflection equations. Consequently, the equations for additional, vertical cable deflection are:

(i) for $0 \le \frac{x}{\ell} \le \frac{x_2}{\ell}$,

$$v_* = \left[\left\{ \left(\frac{x_3}{\ell} - \frac{x_2}{\ell} \right) - \frac{1}{2} \left(\left(\frac{x_3}{\ell} \right)^2 - \left(\frac{x_2}{\ell} \right)^2 \right) \right\} \left(\frac{x}{\ell} \right) - \frac{h_*}{p_*} \left(\frac{1}{2} \left(\frac{x}{\ell} \right) - \frac{1}{2} \left(\frac{x}{\ell} \right)^2 \right) \right] \tag{1.54}$$

(ii) for $\frac{x_2}{\ell} \le \frac{x}{\ell} \le \frac{x_3}{\ell}$,

$$v_* = \left[\left\{ - \frac{1}{2} \left(\frac{x_2}{\ell} \right)^2 + \left(\frac{x_3}{\ell} \right) \left(\frac{x}{\ell} \right) - \frac{1}{2} \left(\frac{x}{\ell} \right)^2 - \frac{1}{2} \left(\left(\frac{x_3}{\ell} \right)^2 - \left(\frac{x_2}{\ell} \right)^2 \right) \left(\frac{x}{\ell} \right) \right\} - \frac{h_*}{p_*} \left(\frac{1}{2} \left(\frac{x}{\ell} \right) - \frac{1}{2} \left(\frac{x}{\ell} \right)^2 \right) \right] \tag{1.55}$$

(iii) for $\frac{x_3}{\ell} \le \frac{x}{\ell} \le 1$,

$$v_* = \left[\left\{ \frac{1}{2} \left(\left(\frac{x_3}{\ell} \right)^2 - \left(\frac{x_2}{\ell} \right)^2 \right) \left(1 - \frac{x}{\ell} \right) \right\} - \frac{h_*}{p_*} \left(\frac{1}{2} \left(\frac{x}{\ell} \right) - \frac{1}{2} \left(\frac{x}{\ell} \right)^2 \right) \right] \qquad (1.56)$$

The cable equation is reduced to

$$\frac{hL_e}{E_c A_c} = \frac{w}{H} \int_0^{\ell} v \, dx \qquad (1.57)$$

and after substitution, integration and rearrangement the following linearized, dimensionless expression is obtained for h_*

$$h_* = \frac{1}{\left(1 + \frac{12}{\lambda^2} \right)} 6 p_* \left\{ \frac{1}{2} \left(\left(\frac{x_3}{\ell} \right)^2 - \left(\frac{x_2}{\ell} \right)^2 \right) - \frac{1}{3} \left(\left(\frac{x_3}{\ell} \right)^3 - \left(\frac{x_2}{\ell} \right)^3 \right) \right\} \qquad (1.58)$$

Because of the linearity of the problem, this result could also have been obtained by integrating Eq. 1.32 directly.

These solutions will be accurate for all λ^2 provided p_* is small, near 10^{-1}.

Again, if $\lambda^2 << 1$, as in taut, flat cables, $h_* \to 0$ and the classical results of the linear, taut string are obtained.

For cables, such as those of the suspension bridge, where the ratio of sag to span is of order 1:10, $\lambda^2 >> 1$ and

$$h_* \to 6 p_* \left\{ \frac{1}{2} \left(\left(\frac{x_3}{\ell} \right)^2 - \left(\frac{x_2}{\ell} \right)^2 \right) - \frac{1}{3} \left(\left(\frac{x_3}{\ell} \right)^3 - \left(\frac{x_2}{\ell} \right)^3 \right) \right\}$$

which is the result obtained if the cable is assumed inextensible, and second order effects are neglected.

(2) Taut, flat cable

A considerable simplification results here since $y \equiv 0$. The deflection equations become:

(i) for $0 \le \frac{x}{\ell} \le \frac{x_2}{\ell}$,

$$v_* = \frac{1}{(1 + h_*)} \left[\left\{ \left(\frac{x_3}{\ell} - \frac{x_2}{\ell} \right) - \frac{1}{2} \left(\left(\frac{x_3}{\ell} \right)^2 - \left(\frac{x_2}{\ell} \right)^2 \right) \right\} \left(\frac{x}{\ell} \right) \right] \tag{1.59}$$

(ii) for $\frac{x_2}{\ell} \le \frac{x}{\ell} \le \frac{x_3}{\ell}$,

$$v_* = \frac{1}{(1 + h_*)} \left[- \frac{1}{2} \left(\frac{x_2}{\ell} \right)^2 + \left(\frac{x_3}{\ell} \right) \left(\frac{x}{\ell} \right) - \frac{1}{2} \left(\frac{x}{\ell} \right)^2 - \frac{1}{2} \left(\left(\frac{x_3}{\ell} \right)^2 - \left(\frac{x_2}{\ell} \right)^2 \right) \left(\frac{x}{\ell} \right) \right] \tag{1.60}$$

(iii) for $\frac{x_3}{\ell} \le \frac{x}{\ell} \le 1$,

$$v_* = \frac{1}{(1 + h_*)} \left[\frac{1}{2} \left(\left(\frac{x_3}{\ell} \right)^2 - \left(\frac{x_2}{\ell} \right)^2 \right) \left(1 - \frac{x}{\ell} \right) \right] \tag{1.61}$$

The cable equation may here be reduced to

$$\frac{h\ell}{E_c A_c} = \frac{p}{2(H + h)} \int_{x_2}^{x_3} v \, dx \tag{1.62}$$

and substitution, integration and rearrangement gives

$$h_* \left(1 + h_* \right)^2 = \frac{\lambda^2}{2} \left\{ \frac{1}{3} \left(\left(\frac{x_3}{\ell} \right)^3 + 2 \left(\frac{x_2}{\ell} \right)^3 \right) - \left(\frac{x_3}{\ell} \right) \left(\frac{x_2}{\ell} \right)^2 - \frac{1}{4} \left(\left(\frac{x_3}{\ell} \right)^2 - \left(\frac{x_2}{\ell} \right)^2 \right)^2 \right\} p_*^2 \tag{1.63}$$

where here

$$\lambda^2 = \left(\frac{w\ell}{H}\right)^2 \left(\frac{E_c A_c}{H}\right)$$

This is a cubic of the same form as Eq. 1.42. The parameter λ^2 is always very small since $\left(\frac{w\ell}{H}\right)^2$ is very small for a flat cable. However, p_* is usually large so that the product $p_*^2 \lambda^2$ is not necessarily small. If p_* is small then $h_* \to 0$, and the classical results for the linear, taut string are obtained.

This cubic has an exact solution of the form

$$h_* = \frac{1}{\sqrt[3]{B}} \left(\sqrt[3]{B} - \frac{1}{3}\right)^2 \tag{1.64}$$

where

$$B = -\frac{s}{2} + \sqrt{\frac{s^2}{4} + \frac{r^3}{27}}$$

and

$$r = -\frac{1}{3}\ , \quad s = -\frac{2}{27} - \frac{\lambda^2}{2}\left\{\frac{1}{3}\left(\left(\frac{x_3}{\ell}\right)^3 + 2\left(\frac{x_2}{\ell}\right)^3\right) - \left(\frac{x_3}{\ell}\right)\left(\frac{x_2}{\ell}\right)^2 - \frac{1}{4}\left(\left(\frac{x_3}{\ell}\right)^2 - \left(\frac{x_2}{\ell}\right)^2\right)^2\right\} p_*^2$$

It can also be shown that $\sqrt[3]{B} \geq \frac{1}{3}$; and $\sqrt[3]{B} = \frac{1}{3}$ only when $p_* = 0$ or $\frac{x_1}{\ell} = 0, 1$.

This theory will find an application in the analysis and design of cable roof structures which are rectangular in plan. If one side is much larger than the other side then it is practicable to use cables which span only the short side. If these

cables are initially taut and flat (as will often be the case), it is a simple matter to calculate the additional deflections and tensions developed after the (usually) light and flexible roof is hung from, or made continuous with, the cable system.

e. Examples

Consider the following examples which illustrate the results obtained for the response of cables to distributed loads.

Example 4

It is required to calculate the additional tensions and deflections induced in the cables of the long-span suspension bridge of Example 2 (p. 34) as construction of the deck proceeds. In particular, the additional horizontal component of cable tension and the additional vertical cable deflection at mid-span are to be evaluated for:

(i) deck in place over the central half of the span,

(ii) deck in place over all the span.

The distributed weight of the deck is

$$p = 5.84 \times 10^4 \text{ N/m (4000 lb/ft), per cable}$$

and it is assumed that during construction the deck has no flexural stiffness. Other properties are as given in Example 2.

(i) deck in place over central half of the span

Here

$$\lambda^2 = 2 \times 10^3 , \quad \frac{x_2}{\ell} = 0.25 , \quad \frac{x_3}{\ell} = 0.75 , \quad p_* = 13.3$$

The cubic from which h_* is found (Eq. 1.53) becomes

$$h_*^3 + 85.5\, h_*^2 + 168\, h_* - 8,950 = 0$$

from which

$$h_* = 8.9$$

The additional deflection at mid-span is (Eq. 1.50)

$$v_* = 0.00102$$

$$v = 8.3 \text{ m } (27.2 \text{ ft})$$

If the cables were assumed inextensible, and the second order term was left out of the cable equation, then h_* would have a value given by (see p. 48)

$$h_* = 9.17$$

which is quite close to the value given by the general theory.

However, the cables are not inextensible. In fact, under this loading, the cable length has increased by an amount

$$\Delta L \simeq h_* \frac{H\ell}{E_c A_c} \left(1 + \frac{16}{3} \left(\frac{d}{\ell}\right)^2\right) = 1.75 \text{ m } (5.75 \text{ ft})$$

which is far from negligible. The "inextensible" theory gives a good result because two terms in the cable equation, namely

$$\frac{hL_e}{E_c A_c} \quad \text{and} \quad \frac{1}{2}\int_0^\ell \left(\frac{dv}{dx}\right)^2 dx$$

are approximately equal in this case. Consequently, the value of h_* found from the equation

$$\int_0^\ell \frac{dy}{dx}\frac{dv}{dx}\, dx = 0$$

is close to the value given by the general theory.

(ii) deck in place over all the span

Here

$$\lambda^2 = 2 \times 10^3 \ , \ \frac{x_2}{\ell} = 0 \ , \ \frac{x_3}{\ell} = 1.0 \ , \ p_* = 13.3$$

The cubic to be solved is

$$h_*^3 + 85.5\, h_*^2 + 168\, h_* - 17,000 = 0$$

from which

$$h_* = 12.35$$

This may be compared with the result from the "inextensible" theory, namely

$$h_* = p_* = 13.3$$

The additional deflection at mid-span is

$$v_* = 0.000670$$

from which

$$v = 5.43 \text{ m } (17.8 \text{ ft})$$

Therefore, in placing the deck on the mainspan, the cable sag has increased from 76.2 m (250 ft) to 81.7 m (267.8 ft). Each cable has increased in length (from its length in the free-hanging position) an amount

$$\Delta L \simeq 2.42 \text{ m } (7.95 \text{ ft})$$

The fractional increase in cable length is

$$\frac{\Delta L}{L} = 0.0026$$

which is much smaller than the fractional increase in sag of

$$\frac{\Delta d}{d} = 0.071 .$$

Example 5

A factory, the roof of which has plan dimensions of 91.5 m x 30.5 m (300 ft x 100 ft), is to have its roof supported by, and made continuous with, a parallel network of cables which span the shorter side at a spacing of 6.1 m (20 ft). The cables are anchored into rigid supporting frames as shown in Fig. 8.

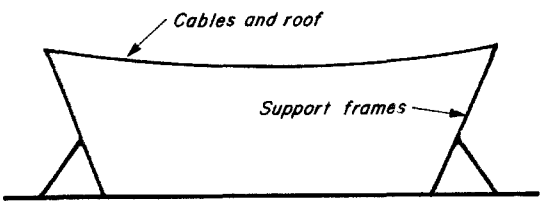

Figure 8

As a part of the preliminary design of the roof structure, consider the following possible structural solution:

Steel cables, 3.8 cm (1.5 in) in diameter, are connected to the supporting frames and pretensioned to 111 kN

(25, 000 lb). Using formwork to support its weight, the roof is then built around the cable network. The roof material has a total weight (excluding cables) of 470 N/m^2 (10 lb/ft^2). The formwork is then removed and it is required to find the additional cable tension and the sag of the roof in the new position of equilibrium. Cable properties are: $w = 87.5$ N/m (6.0 lb/ft), $E_c = 104 \times 10^6$ kN/m^2 (15×10^6 psi); $A_c = 1.14 \times 10^{-3}$ m^2 (1.77 in^2).

To a good first approximation, the pretensioned cables may be considered flat initially. The theory of the taut, flat cable under distributed loading may be applied.

For this problem $\lambda^2 = 0.61$, $\frac{x_2}{\ell} = 0$, $\frac{x_3}{\ell} = 1$, $p_* = 33.3$. The additional cable tension is found from (Eq. 1.63)

$$h_* (1 + h_*)^2 = 28.1$$

from which

$$h_* = 2.41$$

Consequently, the new horizontal component of cable tension is

$$H = 380 \text{ kN } (85, 200 \text{ lbs})$$

and the deflection at mid-span is

$$v_* = 0.0367$$

$$v = 0.89 \text{ m } (2.92 \text{ ft})$$

A more refined analysis using the general theory, which allows for the small initial sag of 0.091 m which the pretensioned cables possess before the roof is hung, shows that in the new equilibrium position the total sag is

$$d = 0.905 \text{ m } (2.97 \text{ ft})$$

and the horizontal component of the cable tension is

$$H = 386 \text{ kN } (86,700 \text{ lbs}) .$$

B. THE LINEAR THEORY OF FREE VIBRATIONS OF A PARABOLIC CABLE

The theory of the vibrations of suspended cables, which are supported at one or at both ends, has been increasingly refined during its development. There is, however, an inadequacy in part of the theory which has apparently gone unnoticed or unsolved until now.

Stated briefly, the inadequacy has arisen because practically all previous theories which are valid for cables with ratios of sag to span of about 1:8 (and one of which tends to the theory for the vibrations of a vertical cable as the ratio of sag to span becomes very great), cannot be reconciled with the theory of the vibrations of a taut string when the ratio of sag to span becomes very small.

When cables, which are fixed at each end, are used to support transverse loads, structural efficiency requires that the profiles of the cables be relatively flat. It appears that a correct linear theory of vibration is missing for cables of this sort, where the ratio of sag to span is about 1:8, or less.

Consequently, attention is confined in this section to uniform cables, supported at each end, for which the sags are sufficiently small for parabolic profiles to describe accurately their static geometry. The theories to be presented, for which experimental confirmation has been obtained, are of considerable practical importance.

1. Historical Background

During the first half of the eighteenth century elements of the theory of vibration of a taut string, which was fixed at each end, were presented by Brook Taylor, D'Alembert, Euler and Daniel Bernoulli[23]. In 1732 Daniel Bernoulli[22] investigated the transverse oscillations of a uniform cable, supported at one end and hanging under gravity. The same problem was also discussed by Euler[22], nearly fifty years later, in 1781. Both Bernoulli and Euler gave the solution for the frequencies of vibration in the form of an infinite series. This series is now represented by a zero order Bessel function of the first kind, and so their work on this mechanical problem was a forerunner of the theory of Bessel functions.

At this time, however, the theory of partial differential equations was still in its infancy and considerable work had centered around the analysis of discrete, rather than continuous, systems. For example, by 1788 Lagrange[16], and others before him, had obtained solutions of varying degrees of completeness for the vibrations of an inextensible, massless string, fixed at each end, from which numerous weights were hung. The general equations of motion of discrete systems were first given by Lagrange in 1760 and appeared later in Mécanique Analytique in 1788[23].

The most important contribution to the theory of cable vibrations came in 1820 when Poisson[16] published a paper which gave the general Cartesian partial differential equations of the motion of a cable element under the action of a general force system. These

equations were the dynamic analogue of the static equations given by Fuss[15] in 1796. Poisson used these equations to improve the solutions previously obtained for the vertical cable and the taut string.

Thus by 1820 correct solutions had been given for the linear, free vibrations of uniform cables the geometries of which were the limiting forms of the catenary. Apart from Lagrange's work on the equivalent discrete system, no results had been given for the free vibrations of cables where the sag to span ratio was not either zero or infinite.

In 1851 Rohrs[14], in collaboration with Stokes, obtained an approximate solution for the symmetric vertical vibrations of a uniform suspended cable where the sag to span ratio was small, although appreciable. He arrived at his solution using a form of Poisson's general equations, correct to the first order and, in addition, used another equation which he termed, "the equation of continuity of the chain." He assumed the chain to be inextensible so this continuity equation related only to geometric compatibility.

In 1868 Routh[16] gave an exact solution for the symmetric vertical vibrations (and associated longitudinal motion) of a heterogeneous cable which hung in a cycloid. Like Rohrs, he also assumed that the cable was inextensible. He showed that the result for the cycloidal cable reduced to Rohrs' solution for the uniform cable when the ratio of sag to span was small. Routh also obtained an exact solution for the antisymmetric, vertical vibrations (and associated longitudinal motion) of the cycloidal cable.

At this point the subject appears to have been laid to rest until 1941 when Rannie and von Kármán[12, 13] independently derived results for both the symmetric and antisymmetric vertical vibrations of an inextensible, three-span cable. In work done in 1945, Vincent[24] extended Rannie and von Kármán's analysis to allow for the effects of cable elasticity in the calculation of the symmetric vertical motion of the three-span cable. However, he did not explore the nature of the solution so obtained and, therefore, he appears to have been unaware of the substantial effect which the inclusion of cable elasticity can have on the analysis. These works were prompted by the aerodynamic failure of the Tacoma Narrows suspension bridge.

A semi-empirical theory for the natural frequencies of the first three in-plane modes of a uniform suspended cable was put forward by Pugsley[11] in 1949. He demonstrated the applicability of the results by conducting experiments on cables in which the ratio of sag to span ranged from 1:10 up to approximately 1:4.

By assuming again that the uniform cable was inextensible, Saxon and Cahn[17] made a major contribution to the theory of the in-plane vibrations in 1953. They obtained solutions which effectively reduced to the previously known results for inextensible cables of small sag to span ratios, and for which asymptotic solutions gave extremely good results for large ratios of sag to span. The accuracy of their theory was demonstrated by comparing it with the experiments of Rudnick, Leonard and Saxon; Cahn and Saxon; and Pugsley. In all these experiments the ratio of sag to span was 1:10, or greater.

One of the most interesting aspects of the latter development of the theory of symmetric, vertical vibrations of a suspended cable is that there have been neither theories nor experiments which have sought to explain a discrepancy that arises as the ratio of sag to span reduces to zero. For small sag to span ratios previous theories, which have been derived assuming the cable to be inextensible, show that the first symmetric in-plane mode, primarily involving vertical motion, occurs at a frequency which is contained in the first non-zero root of (as will be shown)

$$\tan\left(\frac{\beta\ell}{2}\right) = \left(\frac{\beta\ell}{2}\right)$$

namely

$$(\beta\ell)_1 \simeq 2.86\ \pi$$

where $\beta = \left(\frac{m\omega^2}{H}\right)^{\frac{1}{2}}$, and m is the mass per unit length of the cable, H is the horizontal component of cable tension (static), ω is the natural circular frequency of vibration and ℓ is the span of the cable.

However, it has long been known that the frequency of the first symmetric mode of the transverse vibration of a taut string is contained in the first root of

$$\cos\left(\frac{\beta\ell}{2}\right) = 0$$

namely

$$(\beta\ell)_1 = \pi$$

This discrepancy, which amounts to almost 300%, cannot be resolved by the previous analyses of inextensible cables.

Inextensibility is a concept which needs to be used with great care. No real cables or chains are ever inextensible. Clearly, a taut string must stretch when vibrating in a symmetric mode, although standard analyses often overlook this point. Likewise, a cable which has a very small sag to span ratio must stretch when vibrating with symmetric vertical motion. However, if the concept of inextensibility is adhered to, it must be concluded from the previous analyses that the classical first symmetric vertical mode does not exist if even the slightest sag is present. This is at odds with reality and the matter is resolved in the following paragraphs.

2. The Linear Theory

Consider a uniform cable, which hangs in static equilibrium in a vertical plane through supports located at the same level, the profile of which is given by

$$y = \frac{w\ell^2}{2H}\left\{\frac{x}{\ell} - \left(\frac{x}{\ell}\right)^2\right\}$$

The cable is then given a small, arbitrary displacement from its position of static equilibrium. In general, the resulting small, free vibrations have three components (see Fig. 9):

(i) longitudinal motion u,

(ii) transverse vertical motion v,

(iii) transverse horizontal motion w.

Subsequently, the equilibrium of an element of the cable requires that

$$\text{(i)}\quad \frac{\partial}{\partial s}\left\{(T + \tau)\left(\frac{dx}{ds} + \frac{\partial u}{\partial s}\right)\right\} = m\frac{\partial^2 u}{\partial t^2}$$

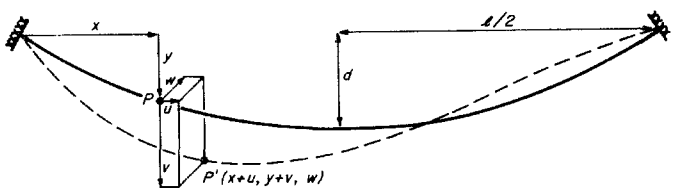

Figure 9 Definition diagram for cable vibrations.

$$\text{(ii)}\quad \frac{\partial}{\partial s}\left\{(T+\tau)\left(\frac{dy}{ds}+\frac{\partial v}{\partial s}\right)\right\} = m\frac{\partial^2 v}{\partial t^2} - mg$$

$$\text{(iii)}\quad \frac{\partial}{\partial s}\left\{(T+\tau)\frac{\partial w}{\partial s}\right\} = m\frac{\partial^2 w}{\partial t^2}$$

where u and v are the in-plane components of the motion, w is the component of motion perpendicular to the vertical plane through the supports, m is the mass per unit length of the cable, g is the acceleration due to gravity and τ is the additional cable tension caused by the motion. The components of motion u, v and w and the additional tension τ are functions of both position and time.

These equations may be simplified for the problem at hand. Each equation is expanded, the equations of static equilibrium are substituted for, and terms of the second order are neglected. In

addition, since the analyses are to be valid only for cables with ratios of sag to span of about 1:8, or less, the longitudinal component of the equations of motion is unimportant and may be ignored. Consequently, the equations of motion reduce to

$$H \frac{\partial^2 v}{\partial x^2} + h \frac{d^2 y}{dx^2} = m \frac{\partial^2 v}{\partial t^2} \tag{1.65}$$

$$H \frac{\partial^2 w}{\partial x^2} = m \frac{\partial^2 w}{\partial t^2} \tag{1.66}$$

where h is defined as the additional horizontal component of cable tension and is a function of time alone.

The linearized cable equation, which provides for the elastic and geometric compatibility of the cable element (Appendix II), reads

$$\frac{h\left(\frac{ds}{dx}\right)^3}{E_c A_c} = \frac{\partial u}{\partial x} + \frac{dy}{dx}\frac{\partial v}{\partial x} \tag{1.67}$$

The cable equation gives the closure condition for the symmetric vertical motion. It also allows for the calculation of the longitudinal motion. Thus, Eqs. 1.65, 1.66 and 1.67 are the linearized equations which govern the problem.

It will be noted that the transverse horizontal motion has uncoupled from the in-plane motion because, to first order, the transverse horizontal motion involves no additional cable tension. This is consistent with experience since, for a chain hanging across a driveway, the only mode of vibration easily excited is its first, swinging mode. Therefore, to first order, a disturbance which has no in-plane

components will induce only transverse horizontal motion, and vice-versa.

Under the restrictions placed here on cable geometry, it is the vertical component of the motion which is most apparent when the cable vibrates in an in-plane mode. The amplitude of the corresponding longitudinal modal component is always substantially less than the amplitude of the vertical motion. Consequently, a symmetric in-plane mode is defined as one in which the vertical component of the mode is symmetric, and vice-versa. In many situations the longitudinal modal components are of no importance and, as a result, the vertical modal components could be called the in-plane modes. However, for completeness, and in order to emphasize that an in-plane mode consists of two components, the more accurate nomenclature will be used.

Because the transverse horizontal motion is the easiest to analyze it will be considered first.

a. The transverse horizontal motion

By writing $w(x, t) = \tilde{w}(x)e^{i\omega t}$, where ω is the natural circular frequency of vibration, Eq. 1.66 is reduced to

$$H \frac{d^2\tilde{w}}{dx^2} + m\omega^2\tilde{w} = 0 \qquad (1.68)$$

The general solution of Eq. 1.68 is

$$\tilde{w} = A \sin \beta x + B \cos \beta x$$

where $\beta^2 = \frac{m\omega^2}{H}$ and A, B are constants. The boundary conditions are

$$\tilde{w}(0) = \tilde{w}(\ell) = 0$$

from which it is found that the natural frequencies of the vibration are given by

$$\omega_n = \frac{n\pi}{\ell}\sqrt{\left(\frac{H}{m}\right)} \qquad n = 1, 2, 3... \tag{1.69}$$

The modes are given by

$$\tilde{w}_n(x) = A_n \sin\left(\frac{n\pi x}{\ell}\right) \qquad n = 1, 2, 3... \tag{1.70}$$

where $n = 1, 2, 3...$ signifies the first, second, third, etc. modes, respectively.

The frequency of the first transverse horizontal mode (i. e. $n = 1$) is the lowest natural frequency of any given parabolic cable.

b. The in-plane motion

As defined previously, antisymmetric in-plane modes consist of antisymmetric vertical components and (as will be shown) symmetric longitudinal components, while symmetric in-plane modes consist of symmetric vertical components and antisymmetric longitudinal components. In the former case, to first order, no additional cable tension is induced by the motion, however, additional cable tension is induced by the motion in the latter case.

(i) Antisymmetric in-plane modes

Since, to first order, the additional horizontal component of cable tension is zero, Eq. 1.65 becomes

$$H \frac{d^2\tilde{v}}{dx^2} + m\omega^2\tilde{v} = 0 \qquad (1.71)$$

where the substitution, $v(x, t) = \tilde{v}(x)e^{i\omega t}$, has been made. The cable equation (Eq. 1.67) becomes just a statement of geometric compatibility

$$\frac{d\tilde{u}}{dx} + \frac{dy}{dx}\frac{d\tilde{v}}{dx} = 0 \qquad (1.72)$$

where the substitution, $u(x,t) = \tilde{u}(x)e^{i\omega t}$, has also been made. Together with the boundary conditions

$$\tilde{v}(0) = \tilde{v}\left(\frac{\ell}{2}\right) = 0$$

Eqs. 1.71 and 1.72 are sufficient to obtain the natural frequencies and modal components of the antisymmetric in-plane modes.

It is easily shown that the natural frequencies are given by

$$\omega_n = \frac{2n\pi}{\ell}\sqrt{\left(\frac{H}{m}\right)} \qquad n = 1, 2, 3\ldots \qquad (1.73)$$

where ω_1, ω_2, ω_3 ... are the natural frequencies of the first, second, third, etc. antisymmetric in-plane modes, respectively.

The antisymmetric vertical modal components are given by

$$\tilde{v}_n(x) = A_n \sin\left(\frac{2n\pi x}{\ell}\right) \qquad n = 1, 2, 3... \tag{1.74}$$

The longitudinal components of motion in these modes are found from Eq. 1.72, and it is seen that these components are symmetric, since $\left(\frac{dy}{dx}\right)$ is zero at mid-span. The symmetric longitudinal modal components are thus given by

$$\tilde{u}_n(x) = -\frac{dy}{dx}\tilde{v}_n(x) - \frac{w}{H}\int_0^x \tilde{v}_n(x)\,dx \tag{1.75}$$

After substitution of Eq. 1.74, integration and rearrangement it is found that

$$\tilde{u}_n(x) = -\frac{1}{2}\left(\frac{w\ell}{H}\right) A_n \left\{\left(1 - 2\left(\frac{x}{\ell}\right)\right)\sin\left(\frac{2n\pi x}{\ell}\right) + \frac{1}{n\pi}\left(1 - \cos\left(\frac{2n\pi x}{\ell}\right)\right)\right\}$$

$$n = 1, 2, 3... \tag{1.76}$$

where, as before, A_n is the amplitude of the n^{th} antisymmetric vertical component of the mode.

It is clear that the amplitudes of the longitudinal components become very small as the cable becomes flatter. However, these longitudinal components have some peculiar properties. The maximum displacement of the first component occurs at the quarter-span points and not at mid-span. The displacement is a local minimum at mid-span (see Fig. 10 (a)). Also, both the slope and displacement are zero at mid-span for the second component (see Fig. 10 (b)). This pattern repeats itself for the higher longitudinal components.

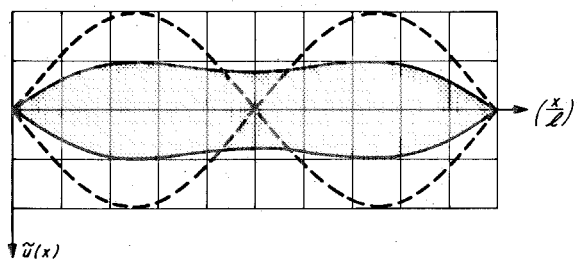

(a) First symmetric longitudinal modal component

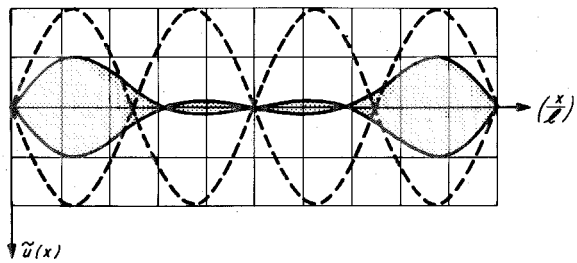

(b) Second symmetric longitudinal modal component

Figure 10 Longitudinal components and associated vertical components of first two antisymmetric in-plane modes (vertical scale arbitrary).

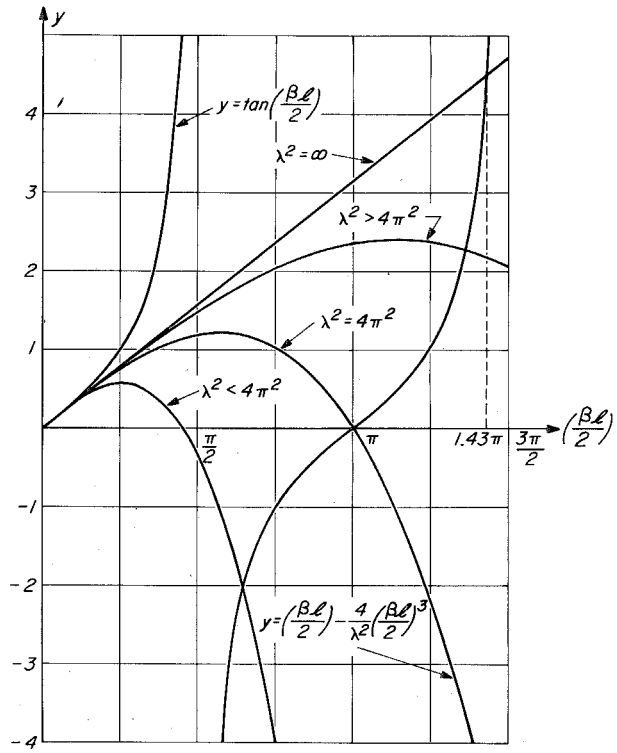

Figure 11 Graphical solution for first non-zero root of Eq. 1.81.

Equations 1.73, 1.74 and 1.76 are similar to those given by Routh[16], which he deduced from an exact analysis of the inextensible, cycloidal cable by allowing the ratio of sag to span to become small.

A more exact analysis of the antisymmetric in-plane modes of a parabolic cable, done concurrently by Caughey[2], has shown that the assumption, $h = 0$, is a very good one. For a cable with a ratio of sag to span of 1:8, this assumption results in an error of less than 4% in the determination of the natural frequencies and modal components. The error may be attributed to the longitudinal component of the equations of motion which has been neglected. When this is accounted for small, second order changes in cable tension do occur.

(ii) Symmetric in-plane modes

Here, additional cable tension is induced by the motion and Eq. 1.65 becomes

$$H \frac{d^2 \tilde{v}}{dx^2} + m\omega^2 \tilde{v} = w \frac{\tilde{h}}{H} \qquad (1.77)$$

where the substitutions, $v(x, t) = \tilde{v}(x)e^{i\omega t}$, $h(t) = \tilde{h}e^{i\omega t}$ and $\frac{d^2y}{dx^2} = -\frac{w}{H}$, have been made. The cable equation (Eq. 1.67) becomes

$$\frac{\tilde{h}\left(\frac{ds}{dx}\right)^3}{E_c A_c} = \frac{d\tilde{u}}{dx} + \frac{dy}{dx}\frac{d\tilde{v}}{dx} \qquad (1.78)$$

where, again, the substitution, $u(x, t) = \tilde{u}(x)e^{i\omega t}$, has been made. Together with the boundary conditions

$$\tilde{u}(0) = \tilde{u}(\ell) = 0 \quad , \quad \tilde{v}(0) = \tilde{v}(\ell) = 0$$

Eqs. 1.77 and 1.78 are sufficient to obtain the natural frequencies and modal components of the symmetric in-plane modes.

It proves convenient to proceed with a detailed discussion of the natural frequencies and the vertical components. A discussion of the longitudinal components will be given later.

The solution of Eq. 1.77, with the given boundary conditions, is

$$\frac{\tilde{v}(x)}{\left(\frac{w\ell^2}{H}\right)} = \frac{\tilde{h}}{H} \frac{1}{(\beta\ell)^2} \left\{1 - \tan\left(\frac{\beta\ell}{2}\right) \sin \beta x - \cos \beta x\right\} \qquad (1.79)$$

where the value of $(\beta\ell)$ specifies the particular (symmetric) vertical modal component.

Use is now made of the cable equation (Eq. 1.78), which becomes

$$\frac{\tilde{h} L_e}{E_c A_c} = \frac{w}{H} \int_0^{\ell} \tilde{v}(x)\, dx \qquad (1.80)$$

to eliminate $\tilde{h}$ and obtain the following transcendental equation from which the natural frequencies of the symmetric in-plane modes may be found

$$\tan\left(\frac{\beta\ell}{2}\right) = \left(\frac{\beta\ell}{2}\right) - \frac{4}{\lambda^2} \left(\frac{\beta\ell}{2}\right)^3 \qquad (1.81)$$

where, as before

$$\lambda^2 = \left(\frac{w\ell}{H}\right)^2 \frac{\ell}{\left(\frac{HL_e}{E_c A_c}\right)}$$

This equation is of fundamental importance in the theory of cable vibrations. It is seen that λ^2, the parameter involving cable geometry and elasticity, governs the nature of the roots of the equation. The eigenvalue problem specified by Eq. 1.81 is strongly non-linear with respect to this parameter.

In order to illustrate the following discussion, reference should be made to Fig. 11 where a graphical solution of Eq. 1.81 is presented.

When λ^2 is very large, the cable may be assumed inextensible and Eq. 1.81 is reduced to

$$\tan\left(\frac{\beta\ell}{2}\right) = \left(\frac{\beta\ell}{2}\right) \qquad (1.82)$$

This is the transcendental equation first given by Rohrs[14], and later by Routh[16]. The equation appears in other branches of mechanics; for example, it arises in the flexural buckling of a strut pinned at one end and fixed at the other, and it also arises in the torsional buckling of a strut fully fixed at each end.

Using a more exact analysis, Caughey[2] has shown that Eq. 1.82 is in error by less than 0.2% for an inextensible cable with a ratio of sag to span of 1:8.

The first two roots of Eq. 1.82 are

$$(\beta\ell)_{1,2} \simeq 2.86\pi,\ 4.92\pi \qquad (1.83)$$

and higher roots are quite accurately given by

$$(\beta\ell)_n \simeq (2n + 1)\,\pi \qquad n = 3, 4, 5\ldots \qquad (1.84)$$

where $(\beta\ell)_n$ contains the frequency of the n^{th} symmetric in-plane mode of an inextensible cable.

The other limiting value of λ^2 occurs when the ratio of sag to span becomes very small. The cable approaches a taut string and λ^2 is very small. The general transcendental equation is then reduced to

$$\tan\left(\frac{\beta\ell}{2}\right) = -\infty \qquad (1.85)$$

and the roots of this equation correspond to those of the symmetric modes of the taut string, namely

$$(\beta\ell)_n = (2n - 1)\,\pi \qquad n = 1, 2, 3\ldots \quad (1.86)$$

A comparison of Eqs. 1.86 and 1.84 shows that the condition of inextensibility causes a shift of almost 2π in the roots obtained from the transcendental equation governing the symmetric modes of the taut string.

Therefore, for a general parabolic cable, the natural frequency of the first symmetric in-plane mode is contained in the first non-zero root of Eq. 1.81, and this root lies between

$$\pi < (\beta\ell)_1 < 2.86\,\pi$$

The second symmetric natural frequency is contained in the second non-zero root which lies between

$$3\pi < (\beta\ell)_2 < 4.92\,\pi$$

and so on. The actual values of the roots depend on the value of λ^2.

Three important cases are now considered:

(i) If $\lambda^2 < 4\pi^2$,

then the frequency of the first symmetric in-plane mode is less than the frequency of the first antisymmetric in-plane mode. The first symmetric vertical modal component has no internal nodes along the span (see Fig. 12(a)).

(ii) If $\lambda^2 = 4\pi^2$,

then the frequency of the first symmetric in-plane mode is equal to the frequency of the first antisymmetric in-plane mode. This value of λ^2 gives the first "cross-over" point. The first symmetric vertical modal component is tangential to the static cable profile at each support (see Fig. 12(b)).

(iii) If $\lambda^2 > 4\pi^2$,

then the frequency of the first symmetric in-plane mode is greater than the frequency of the first antisymmetric in-plane mode. The first symmetric vertical modal component has two internal nodes along the span (see Fig. 12(c)).

It may also be noted that if

$$4\pi^2 < \lambda^2 < 16\pi^2$$

both the first and second symmetric vertical modal components have two internal nodes along the span. If

$$\lambda^2 = 16\pi^2$$

then the frequency of the second symmetric in-plane mode is equal to the frequency of the second antisymmetric in-plane mode. This value of λ^2 gives the second "cross-over" point. And so on.

It is obvious from the above discussion that solutions of Eq. 1.81 are strongly influenced by the value of the characteristic parameter, λ^2. This parameter can appear in the analysis only if the full first order cable equation is used. If the cable is assumed inextensible from the outset, the correct solution cannot be found. In most practical problems it is the cable geometry term, $\left(\frac{w\ell}{H}\right)^2$, rather than the cable elasticity term

$$\frac{\ell}{\left(\frac{HL_e}{E_cA_c}\right)}$$

which dictates the size of λ^2. By assuming the cable to be inextensible Saxon and Cahn[17], and others, were led to the wrong conclusion regarding the symmetric in-plane modes as the ratio of sag to span becomes small.

The longitudinal modal components are found from Eq. 1.78, namely

$$\frac{d\tilde{u}}{dx} + \frac{dy}{dx}\frac{d\tilde{v}}{dx} = \frac{\tilde{h}\left(\frac{ds}{dx}\right)^3}{E_cA_c}$$

and therefore

$$\tilde{u}(x) = \frac{\tilde{h}}{E_cA_c}\int_0^x \left(\frac{ds}{dx}\right)^3 dx - \frac{dy}{dx}\tilde{v}(x) - \frac{w}{H}\int_0^x \tilde{v}(x)\,dx \qquad (1.87)$$

These longitudinal components are antisymmetric since the two above equations show that the longitudinal displacement and slope are always zero and non-zero at mid-span, respectively. After Eq. 1.79 is substituted into Eq. 1.87 and the integration is performed, the following equation is obtained

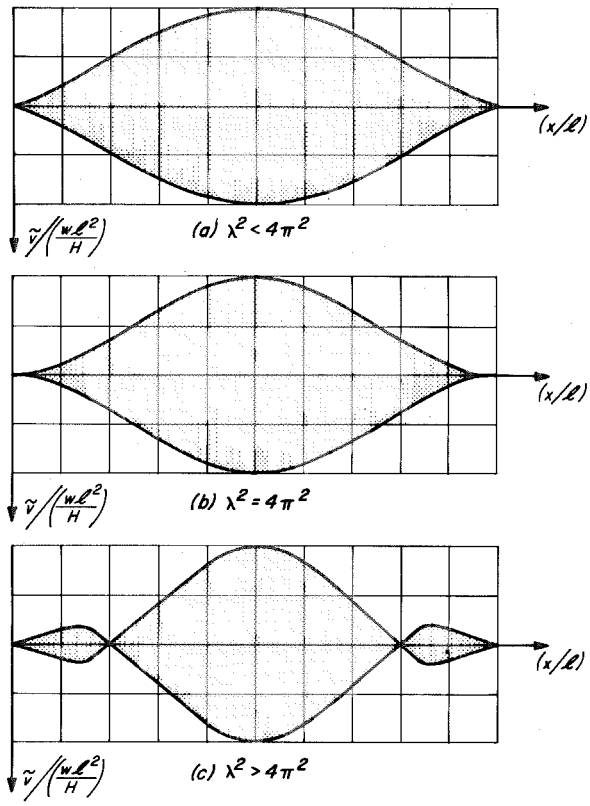

Figure 12 Possible forms of the first symmetric vertical modal component.

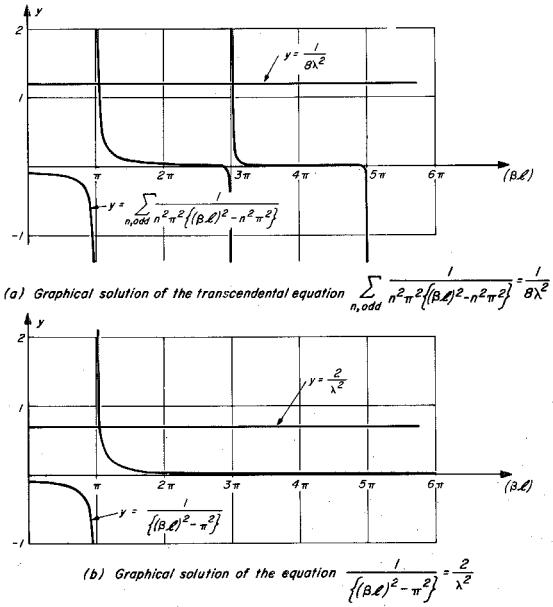

Figure 13

$$\frac{\tilde{u}(x)}{\left(\frac{w\ell^2}{H}\right)} = \left(\frac{w\ell}{H}\right)\frac{\tilde{h}}{H}\frac{1}{(\beta\ell)^2}\left\{\frac{(\beta\ell)^2}{\lambda^2}\frac{L_x}{L_e} - \frac{1}{2}\left(1 - 2\left(\frac{x}{\ell}\right)\right)\left(1 - \tan\left(\frac{\beta\ell}{2}\right)\sin\beta x - \cos\beta x\right)\right.$$

$$\left. - \frac{1}{(\beta\ell)}\left((\beta x) - \tan\left(\frac{\beta\ell}{2}\right)\left(1 - \cos\beta x\right) - \sin\beta x\right)\right\} \qquad (1.88)$$

where L_x is as defined by Eq. 1.28. Like the symmetric vertical modal components, the nature of the antisymmetric longitudinal modal components depends on the value of the characteristic parameter, λ^2.

c. Examples

Several examples are now given in order to illustrate and augment the theories which have been developed. The examples generally relate to the vertical components of vibration since these are encountered most often in practice.

Example 6.

The use of Fourier series permits the analysis of the vertical components of the symmetric modes of vibration of a suspended parabolic cable to be approached from a different viewpoint. The differential equation governing the motion is

$$\frac{d^2\tilde{v}}{dx^2} + \beta^2\tilde{v} = \frac{w\tilde{h}}{H^2}$$

The non-homogeneous term is expanded in a Fourier series as

$$\frac{w\tilde{h}}{H^2} = \frac{w\tilde{h}}{H^2}\sum_{n,\text{odd}}\frac{4}{n\pi}\sin\left(\frac{n\pi x}{\ell}\right)$$

and $\tilde{v}(x)$ is expanded in a Fourier series as

$$\tilde{v}(x) = \sum_{n,\text{odd}} A_n \sin\left(\frac{n\pi x}{\ell}\right)$$

After the required substitutions are made in the differential equation, it is found that

$$A_n = \left(\frac{w\ell^2}{H}\right)\frac{\tilde{h}}{H}\frac{4}{n\pi}\frac{1}{\{(\beta\ell)^2 - n^2\pi^2\}}$$

Hence

$$\frac{\tilde{v}(x)}{\left(\frac{w\ell^2}{H}\right)} = \frac{\tilde{h}}{H}\sum_{n,\text{odd}} \frac{4}{n\pi\{(\beta\ell)^2 - n^2\pi^2\}} \sin\left(\frac{n\pi x}{\ell}\right)$$

and the vertical component of each mode is specified by a value of $(\beta\ell)$.

The cable equation is

$$\frac{\tilde{h}L_e}{E_cA_c} = \frac{w}{H}\int_0^{\ell} \tilde{v}(x)\,dx$$

and after the substitution is made and the integration is performed, the following transcendental equation is obtained

$$\sum_{n,\text{odd}} \frac{1}{n^2\pi^2\{(\beta\ell)^2 - n^2\pi^2\}} = \frac{1}{8\lambda^2}$$

where

$$\lambda^2 = \left(\frac{w\ell}{H}\right)^2 \frac{\ell}{\left(\frac{HL_e}{E_cA_c}\right)}$$

When λ^2 is very small, the right hand side of the above equation becomes very large and the solutions of the transcendental equation tend to those of the taut string, namely

$$\beta\ell = n\pi \qquad n = 1, 3, 5\ldots$$

On the other hand, when λ^2 is very large, the cable may be assumed inextensible, and the transcendental equation reduces to

$$\sum_{n,\text{odd}} \frac{1}{n^2\pi^2\left\{(\beta\ell)^2 - n^2\pi^2\right\}} = 0$$

This infinite series for the inextensible cable was given by Rohrs[14], although his method of solution was less direct than that given here. A very good approximation to the first root may be had by setting the sum of the first two terms equal to zero. For example,

$$10(\beta\ell)_1^2 \simeq 82\,\pi^2$$

$$(\beta\ell)_1 \simeq 2.86\,\pi$$

For intermediate values of λ^2, reference may be made to Fig. 13(a) where a graphical solution is presented. As expected, the "cross-over" points occur at $\lambda^2 = 4\pi^2$, $16\pi^2$, $36\pi^2$, etc. If λ^2 is large it will be difficult to obtain accurate values of the roots from Fig. 13(a). The graphical solution presented in Fig. 11 should always be used in practical cases.

A final point concerns the construction of an infinite series for the tangent function. Since two different transcendental equations have been obtained for the same problem, it follows that

$$\tan x = x + 2x \sum_{n,\text{odd}} \frac{x^2}{\frac{n^2\pi^2}{4}\left\{\frac{n^2\pi^2}{4} - x^2\right\}}$$

By expanding the right hand side into partial fractions and noting that

$$\sum_{n,\text{odd}} \frac{1}{n^2} = \frac{\pi^2}{8}$$

the above series for tan x may be reduced to the standard form

$$\tan x = 2x \sum_{n,\text{odd}} \frac{1}{\left\{\frac{n^2\pi^2}{4} - x^2\right\}}$$

The former series for $\tan x$ is more rapidly convergent than is the latter series.

Example 7

Suppose a steady, non-inertial loading (e. g. pressure) is applied to a uniform cable so that the static deflection is given by

$$y(x) = d \sin\left(\frac{\pi x}{\ell}\right) \qquad \text{where} \quad \frac{d}{\ell} \leq \frac{1}{8}$$

The free, symmetric vertical vibrations of this cable are to be investigated.

The governing differential equation is

$$\frac{d^2\tilde{v}}{dx^2} + \beta^2\tilde{v} = \frac{\tilde{h}}{H}\frac{\pi^2 d}{\ell^2} \sin\left(\frac{\pi x}{\ell}\right)$$

The solution is, directly

$$\frac{\tilde{v}(x)}{d} = \frac{\tilde{h}}{H}\frac{\pi^2}{\{(\beta\ell)^2 - \pi^2\}} \sin\left(\frac{\pi x}{\ell}\right)$$

and from the cable equation it is found that

$$\frac{1}{\{(\beta\ell)^2 - \pi^2\}} = \frac{2}{\lambda^2}$$

or

$$(\beta\ell)^2 = \pi^2 + \frac{\lambda^2}{2}$$

where, here

$$\lambda^2 = \pi^4 \left(\frac{d}{\ell}\right)^2 \frac{\ell}{\left(\frac{HL_e}{E_c A_c}\right)}$$

Under this particular non-inertial static loading, only the first symmetric mode involves additional cable tension. Also, if $\lambda^2 \to \infty$,

$(\beta\ell)_1 \to \infty$; if $\lambda^2 \to 0$, $(\beta\ell)_1 \to \pi$ (see Fig. 13(b).

All other symmetric modes do not involve additional cable tension and the frequencies at which these higher modes occur are contained in the classical formula

$$(\beta\ell)_n = (2n - 1)\,\pi \qquad n = 2, 3, 4\ldots$$

and the modal components are given by

$$\tilde{v}_n(x) = A_n \sin\left\{(2n - 1)\,\frac{\pi x}{\ell}\right\} \qquad n = 2, 3, 4\ldots$$

It is obvious that the general form of the solution for the antisymmetric modes is unaffected by this choice of static loading.

Example 8

A proof of orthogonality

The linearized equations governing the vibrations of a parabolic cable have been shown to be

$$\frac{d^2\tilde{v}}{dx^2} + \beta^2\tilde{v} = \frac{w}{H}\frac{\tilde{h}}{H}$$

$$\frac{d^2\tilde{w}}{dx^2} + \beta^2\tilde{w} = 0$$

and

$$\frac{\tilde{h}\left(\frac{ds}{dx}\right)^3}{E_c A_c} = \frac{d\tilde{u}}{dx} + \frac{dy}{dx}\frac{d\tilde{v}}{dx}$$

The transverse horizontal motion, $\tilde{w}$, separates out from the in-plane motion (i.e. $\tilde{u}$, $\tilde{v}$), and so it is a trivial matter to prove orthogonality for the transverse horizontal modes.

Consider, therefore, the vertical motion (i.e. $\tilde{v}$).

Since

$$\frac{\tilde{h}\, L_e}{E_c A_c} = \frac{w}{H}\int_0^{\ell} \tilde{v}\, dx$$

the equation of motion for the i^{th} mode may be written in the dimensionless form

$$\frac{d^2\tilde{v}_{*i}}{dx_*^2} + (\beta\ell)_i^2\ \tilde{v}_{*i} = \lambda^2 q_i$$

where

$$\tilde{v}_* = \frac{\tilde{v}}{\left(\frac{w\ell^2}{H}\right)}\ ,\quad x_* = \frac{x}{\ell}\ ,\quad q_i = \int_0^1 \tilde{v}_{*i}\, dx_*$$

This is a general representation since, if $\tilde{v}_{*i}$ is an antisymmetric modal component, q_i is zero.

Similarly, the dimensionless equation of motion for the j^{th} component reads

$$\frac{d^2\tilde{v}_{*j}}{dx_*^2} + (\beta\ell)_j^2\ \tilde{v}_{*j} = \lambda^2 q_j$$

Premultiply this equation by $\tilde{v}_{*i}$, integrate the result term by term, and premultiply the previous equation by $\tilde{v}_{*j}$ and integrate the result term by term. This gives

$$-\int_0^1 \frac{d\tilde{v}_{*i}}{dx_*}\frac{d\tilde{v}_{*j}}{dx_*}\, dx_* + (\beta\ell)_j^2 \int_0^1 \tilde{v}_{*i}\,\tilde{v}_{*j}\, dx_* = \lambda^2 q_i q_j$$

$$-\int_0^1 \frac{d\tilde{v}_{*j}}{dx_*}\frac{d\tilde{v}_{*i}}{dx_*}\, dx_* + (\beta\ell)_i^2 \int_0^1 \tilde{v}_{*j}\,\tilde{v}_{*i}\, dx_* = \lambda^2 q_j q_i$$

Since the order of integration is immaterial, the desired result is obtained by subtracting one equation from the other, namely

$$\left\{(\beta\ell)_i^2 - (\beta\ell)_j^2\right\} \int_0^1 \tilde{v}_{*i}\, \tilde{v}_{*j}\, dx_* = 0$$

When $\lambda^2 = 4\pi^2$, $16\pi^2$, $36\pi^2$ ... the frequency of the first symmetric in-plane mode is the same as the frequency of the first antisymmetric in-plane mode, etc. That is

$$(\beta\ell)_i = (\beta\ell)_j$$

It is easily shown that, in this situation

$$\int_0^1 \tilde{v}_{*i}\, \tilde{v}_{*j}\, dx_* = 0$$

This is a property which all self-adjoint systems possess.

Orthogonality of the longitudinal components (i. e., $\tilde{u}$) follows from the orthogonality of the vertical components.

It is worth noting that orthogonality could also have been proved directly from the general equations of motion.

The way is now clear to obtain solutions, in terms of the eigenfunctions of the problem, for the dynamic response of parabolic cables under the influence of various forcing functions which may be of interest.

Example 9

It is required to find the periods of the first two symmetric in-plane modes of vibration of the long-span suspension bridge (span, 915 m) given in Example 2 (p. 34). Two cases are to be considered:

(1) cables in free-hanging position,

(2) when construction of deck is complete.

(1) Cables in free-hanging position

Here, $\lambda^2 >> 4\pi^2 = 2 \times 10^3$ (see Example 2), and the transcendental equation to be solved becomes

$$\tan\left(\frac{\beta\ell}{2}\right) = \left(\frac{\beta\ell}{2}\right) - \frac{1}{500}\left(\frac{\beta\ell}{2}\right)^3$$

The first two roots are found to differ only by an infinitesimal amount from those obtaining for the inextensible cable. Hence

$$(\beta\ell)_{1,2} = 2.86\pi,\ 4.92\pi$$

The periods of the first two symmetric in-plane modes are

$$T_{1,2} = 5.5 \text{ secs},\ 3.2 \text{ secs}.$$

The first in-plane mode is the first antisymmetric mode, with period 7.9 secs.

(2) When construction of the deck is complete

Here, $\lambda^2 > 4\pi^2 = 187$ (see end of Example 4), and the transcendental equation to be solved becomes

$$\tan\left(\frac{\beta\ell}{2}\right) = \left(\frac{\beta\ell}{2}\right) - \frac{1}{47}\left(\frac{\beta\ell}{2}\right)^3$$

from which

$$(\beta\ell)_{1,2} = 2.86\pi,\ 4.24\pi$$

The first root has changed hardly at all from that given by the inextensible theory, but the second and higher roots are changed appreciably. The periods of the first two symmetric modes are now

$$T_{1,2} = 5.7 \text{ secs},\ 3.85 \text{ secs}.$$

The period of the first mode has risen slightly because, with the deck in place, the sag has increased by 5.43 m. Again, the first in-plane mode is the first antisymmetric mode with period 8.16 secs.

The flexural stiffness of the deck has been ignored, which is a good assumption at this stage of construction, since full flexural continuity is rarely provided until after the whole deck is in position.

At present the decks of long-span suspension bridges are often made from streamlined boxgirder sections. These boxgirders usually have relatively little flexural stiffness although their torsional stiffness is often high. A reasonable approximation to the first few flexural modes of vibration can be found using the theory presented here, however, the analysis of the torsional modes requires more refined techniques[4].

Once again, the possible influence of the towers has been ignored in the analysis. Where necessary, an allowance for these effects may be made by adapting a procedure given by Irvine[5].

Example 10

It is required to find the period of the first symmetric in-plane mode of vibration of the "flying-fox" (span, 91.5 m) given in Example 3. The cable, which has a ratio of sag to span of 1:50, is in the free-hanging position.

Here, $\lambda^2 > 4\pi^2 = 60.2$ and the transcendental equation becomes

$$\tan\left(\frac{\beta\ell}{2}\right) = \left(\frac{\beta\ell}{2}\right) - \frac{1}{15.05}\left(\frac{\beta\ell}{2}\right)^3$$

from which the first non-zero root is found to be

$$(\beta\ell)_1 = 2.34\pi$$

This is substantially different from that which the inextensible theory

would give. The period of this mode is

$$T_1 = 1.04 \text{ secs}$$

The first in-plane mode of the "flying-fox" is the first antisymmetric mode, with period 1.22 secs.

Example 11

It is desired to calculate the period of the first symmetric in-plane mode of vibration of the 91.5 m by 30.5 m cable roof structure given in Example 5 (p. 54). Only vibrations in which the nodal lines are parallel to the longer side are to be considered.

Since the cables span only the shorter side, the strip of roof structure associated with one cable is representative of the whole roof structure. As was shown in Example 5, the equilibrium position, after the roof is in position, is specified by

$$d = 0.905 \text{ m}, \quad H = 386 \text{ kN}$$

and so

$$\lambda^2 = 17.2 < 4\pi^2$$

The transcendental equation to be solved is

$$\tan\left(\frac{\beta\ell}{2}\right) = \left(\frac{\beta\ell}{2}\right) - \frac{1}{4.3}\left(\frac{\beta\ell}{2}\right)^3$$

and the first root is found to be

$$(\beta\ell)_1 = 1.54\pi$$

The period of this mode is

$$T_1 = 1.12 \text{ secs}$$

The first in-plane mode of this roof structure is the first symmetric mode; the period of the first antisymmetric mode is 0.86 secs.

These last three examples show how important it is to include the effects of cable geometry and elasticity in the dynamic analysis.

3. Cable Vibration Experiments

Vibration experiments were conducted on a model cable in order to test the linear theory presented in the preceding sections. The experiments were made very simple because only a qualitative verfication of the theory seemed necessary. It was felt that, if the first "cross-over"point of the in-plane modes of vibration could be shown to exist, the validity of the theory would be established.

a. Experimental procedure

A fine copper wire was fastened between two supports which were at the same level, and about 2 m apart. One support was a burette stand which was bolted to the table, the other support was a vice, by means of which the sag of the cable could be adjusted.

The cable was placed between the poles of a magnetron magnet, and an amplifier, connected to an oscillator, was used to pass a small alternating current along the cable. The interaction of the alternating current and the magnetic field caused a small, alternating (substantially) vertical force to be exerted on the cable. In this way, (substantially) in-plane vibrations were excited in the cable (see Fig. 14(a)).

Modes of vibration were found by tuning the oscillator so that the frequency of the alternating current coincided with the natural frequency of the required mode. By ensuring that the gain of

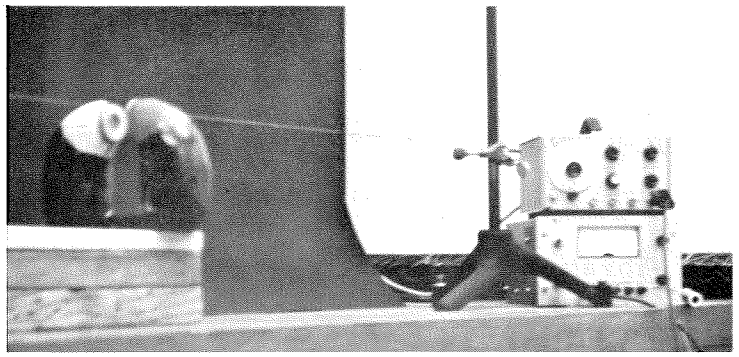

Figure 14(a) Experimental set up.

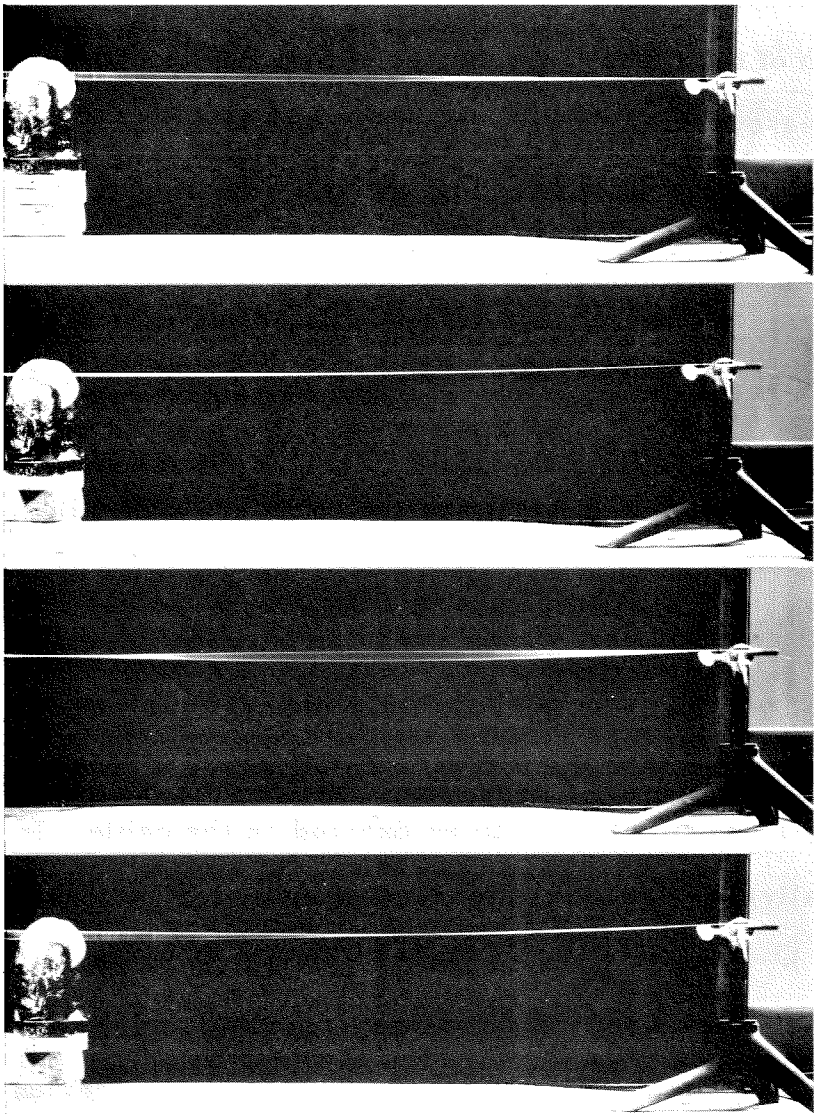

Figure 14(b) Possible forms of the first in-plane mode (left-hand edge is at mid-span).

the amplifier was kept low, a steady-state situation was achieved in which the small damping forces in the cable were sufficient to prevent the occurrence of large amplitudes of vibration. The magnet was placed at a quarter-span point to excite an antisymmetric mode, and it was placed at mid-span to excite a symmetric mode.

When a mode had been isolated, a long-exposure photograph was taken to capture the envelope of the vibration. The cable was painted white, strong overhead lighting was used, and the photographs were taken against a black background to ensure that high contrast was achieved. Photographs were taken (at f16 and 16 seconds exposure) on High Contrast Copy Film, using an ordinary 35 mm camera supported by a tripod (see Fig. 14(b)).

b. Experimental results

The experimental results are shown in Fig. 14(b), and enlarged versions (in the same order) are shown in Fig. 15. Only the first in-plane modes of the suspended cable appear. Since the form of the first antisymmetric in-plane mode was found to be constant for the parabolic cable (as predicted by the theory), only one such mode has been shown. The other modes are various forms of the first symmetric in-plane mode.

It is clear that changes in the value of the characteristic parameter, λ^2, caused substantial changes in the first symmetric in-plane mode. Changes in λ^2 were brought about by varying the sag of the cable. With the cable pulled taut, λ^2 was very small, and the first mode was that of the classical taut string (see Fig. 15(a)). In order to search for

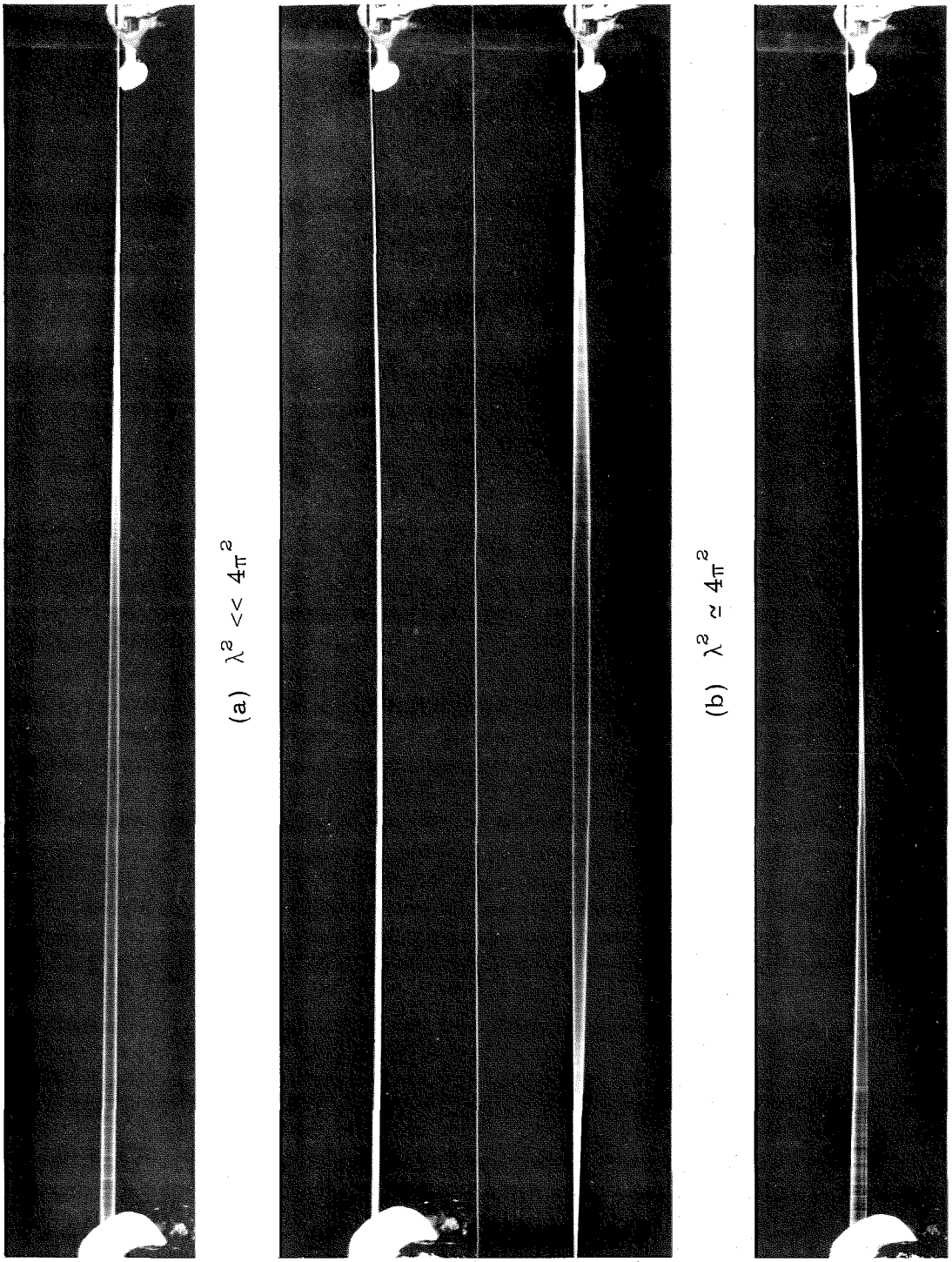

Figure 15 Enlarged versions of Fig. 14(b).

the first "cross-over" point (i. e. $\lambda^2 = 4\pi^2$), the cable was gradually slackened off until a point was reached where the natural frequencies of the first symmetric and first antisymmetric in-plane modes were substantially equal (see Fig. 15(b)). With a further increase in sag, the frequencies of the first symmetric and first antisymmetric in-plane modes diverged again. However, here the frequency of the first symmetric mode was greater than the frequency of the first anti-symmetric mode. Only a very small increase in sag was necessary before the ratio of the natural frequencies settled down to a value of about 1.4:1, as required by the inextensible theory (see Fig. 15(c)).

It will be noticed from the photographs in Figs. 14(b) and 15 that the first "cross-over" point occurred at a very small value of the sag to span ratio; the ratio was about 1:50. It should not be inferred from this that such a value of the ratio of sag to span is typical of parabolic cables in general. It is not. For example, if the same copper wire had spanned 200 m instead of 2 m then, provided that it did not break under its own weight, it can easily be shown that the first "cross-over" point would occur at a ratio of sag to span of about 1:11.

It would have been ideal to be able to experiment on a cable of appreciable span. In that situation the determination of the first "cross-over" point would have been easier in many respects. However, the desire to photograph the envelopes of the modes necessitated the use of a cable of small span. As a result, the determination of the "cross-over" point was a tedious and time-consuming exercise. It proved very difficult to adjust the length of the cable so that the sag

of the cable was just right. As it was, equality of the frequencies of the first symmetric and first antisymmetric in-plane modes was achieved to within 5%.

Another problem which arose was the tendency for the cable to vibrate in a transverse horizontal mode as well as in the in-plane mode. This behavior was an unavoidable result of small imperfections in the cable and in the direction of the electromagnetic exciting force.

When the cable was taut, whirling modes were observed. This was of no importance since the whirling frequency was the same as the frequencies of the two planar components. At the first "cross-over" point there were three modes of vibration which had the same natural frequency. These were the first antisymmetric transverse horizontal mode, the first antisymmetric in-plane mode and the first symmetric in-plane mode. Only by very careful tuning could the required in-plane mode be isolated. Even then, the isolated mode was observed to jump to one of the other two modes and then to jump back again. Such behavior gave striking visual proof of the existence of the "cross-over" point. For larger values of the sag the influence of the transverse horizontal motion was minimized by carefully tuning the oscillator.

Conclusion

In view of the excellent agreement observed between experiment and theory, the validity of the linear theory of vibration of a parabolic cable, presented here, has been established.

Chapter II

THE CABLE TRUSS

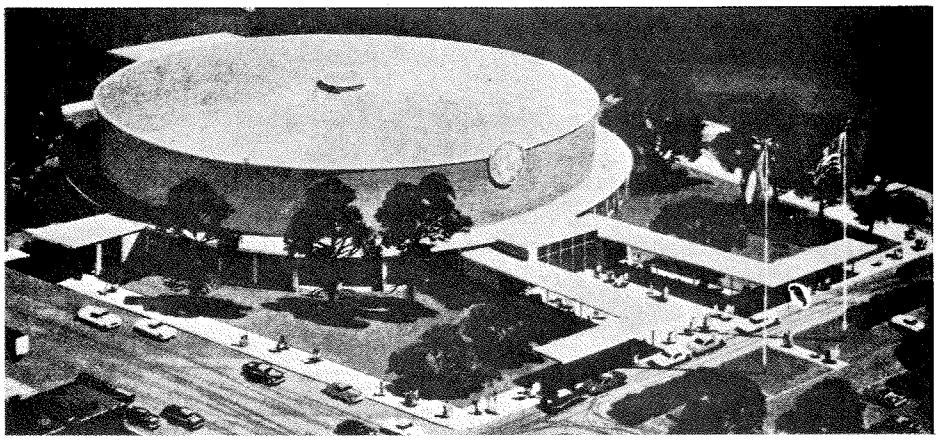

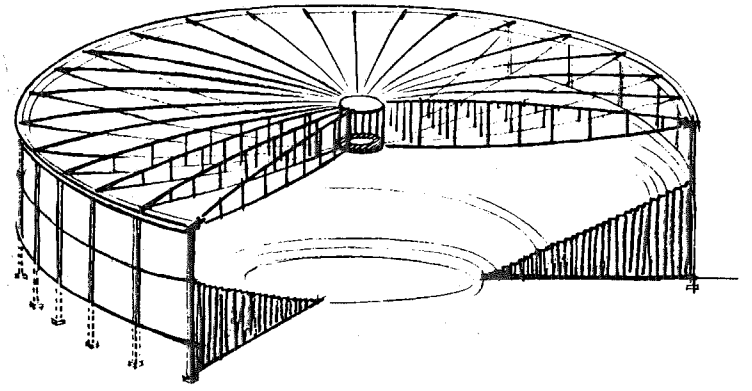

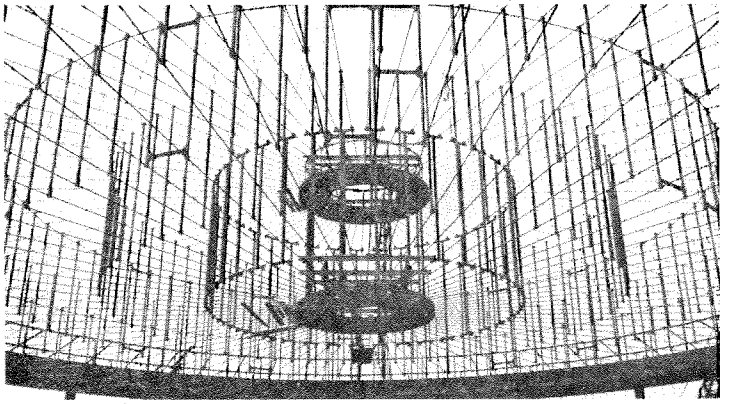

The Municipal Auditorium,
Utica, New York (span 76m) opened 1959.

The last part of this study of simple cable systems is concerned with the static and dynamic analyses of cable trusses, where the top and bottom chords consist of continuous prestressed cables, which are anchored at each end, and between which numerous vertical light, rigid spacers are placed. Since the initial cable prestress is usually high, the geometry of the truss is determined, in large part, by the span and by the lengths of the spacers. A few possible geometries are shown in Fig. 16.

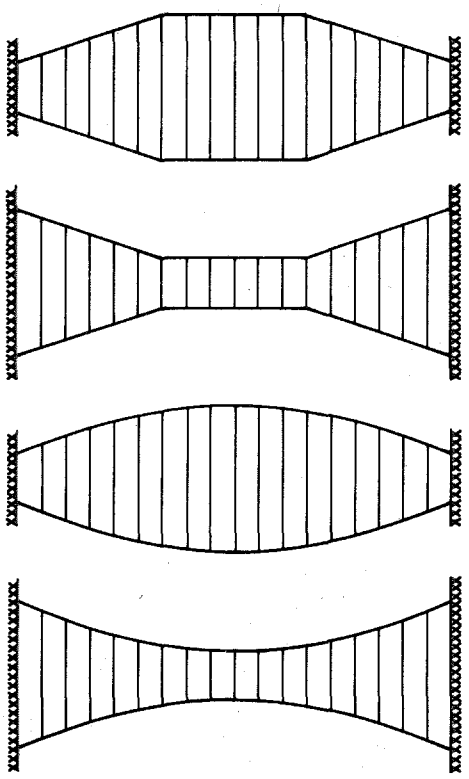

Figure 16

As a means of supporting the roofs of buildings of large span, the cable truss has many advantages. Because of the structural efficiency of the truss, the roof is light yet it possesses considerable

rigidity. For this reason, the problem posed by the possible aerodynamic instability of the roof is often rendered insignificant.

Although it appears to be a relatively recent invention, there is a growing body of technical literature on the subject. A recent report[19], by the Subcommittee on Cable-Suspended Structures of the American Society of Civil Engineers, includes a section on the cable truss. The report also cites references to recent work on the analysis, design and construction of cable trusses.

One of the first structures where cable trusses were utilized was the Municipal Auditorium in Utica, New York[25]. This structure, which was completed in 1959, is circular in plan and the roof is supported by radial cable trusses which span a distance of 76 m (250 ft). Since then, many other structures have been built which incorporate the cable truss.

As occasionally happens in engineering practice, it appears that the art of construction of cable truss roofs is more advanced than is the knowledge of the way in which these structures behave. A review of the literature, cited by the Subcommittee on Cable-Suspended Structures, reveals a lack of adequate theories on which design can be based. A discussion of the engineering principles upon which design is based has been given by Zetlin[25], who was one of the first to develop the cable truss. The most comprehensive analytical treatment is that given by Schleyer[18].

In the analysis of the cable truss presented here, heavy reliance will be placed on the principles outlined in the first chapter

of this study, which relate to the analysis of the single, suspended cable. The behavior of certain forms of the cable truss differs from the behavior of the single cable and, as a consequence, useful simplifications may be made.

The cable truss will be analysed as a single entity and its structural uses, which are primarily to support vertical loads, will be illustrated by examples. The static analyses will include the response to various vertical loadings including a point load, a uniformly distributed load and a triangular loading block. In the dynamic analyses an investigation will be made of the natural frequencies and modes of vibration. Also, a detailed discussion will be given of the possible lateral instability of such truss systems under the effects of applied load.

A. RESPONSE TO TRANSVERSE STATIC LOADING

1. General Theory

The analysis will proceed on the assumption that the top and bottom chords of the truss are either bi-convex or bi-concave (see Fig. 16). Of course, other geometrical possibilities exist, although some of these will not be structurally useful. In the case where both top and bottom chords are initially straight and parallel, the analyses presented in Chapter I, for the taut cable, may be readily adapted.

The relatively small weight of the spacers and the cables will be ignored so that the initial, free-hanging geometry of the truss will be specified by the initial cable pretensions, the lengths of the spacers and the span. In the analysis, the spacers will be replaced by a continuous diaphragm in which adjacent vertical elements may slide freely with respect to each other. Each vertical element of the diaphragm is considered inextensible.

The analyses to be presented will be accurate provided that the slopes of the chords are, and remain, small. As a rule of thumb, the maximum difference between spacer length and the vertical spacing of the chords at a support should be less than one quarter of the span. In practical situations this requirement will almost always be met.

The small longitudinal movements of the chords, associated with the vertical movements of the truss under load, must be allowed to occur freely. The analyses will not hold for bi-concave systems (under loads which are not symmetrical about mid-span) if, for

example, the chords are clamped together at mid-span.

Finally, only trusses in which the spacers are vertical will be considered. The use of inclined spacers leads to analyses which are exceedingly complicated. Inclined spacers may stiffen the truss considerably, but there are sometimes problems associated with connecting spacers of this type to the chords.

Consider a bi-convex cable truss, anchored on rigid supports, as shown in Fig. 17(a). Suppose that, under applied vertical loading, the shear force at some cross section x, along the span, is S. Then, from vertical equilibrium at this cross section, it is clear that (see Fig. 17(b))

$$(H_1 + h_1)\frac{d}{dx}(y_1 + v) - (H_2 - h_2)\frac{d}{dx}(y_2 - v) = S \qquad (2.1)$$

where H_1 and H_2 are the horizontal components of the pretensions in the cables, h_1 and h_2 are the additional horizontal components of cable tension owing to applied load, y_1 and y_2 are the initial shapes of the bottom and top chords, respectively, and v is the vertical deflection of the cross section.

The internal equilibrium of the unloaded truss is given by

$$H_1 \frac{dy_1}{dx} = H_2 \frac{dy_2}{dx} \qquad (2.2)$$

This allows for the calculation of the axial forces which the spacers must resist in the initial geometry.

Therefore, Eq. 2.1 may be reduced to

$$(H_1 + H_2)\frac{dv}{dx} + (h_1 - h_2)\frac{dv}{dx} + h_1 \frac{dy_1}{dx} + h_2 \frac{dy_2}{dx} = S \qquad (2.3)$$

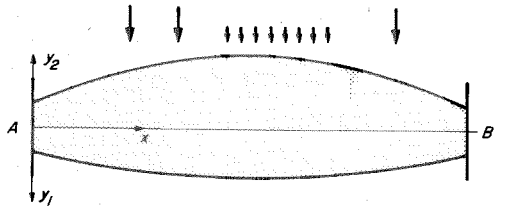

(a) Definition diagram

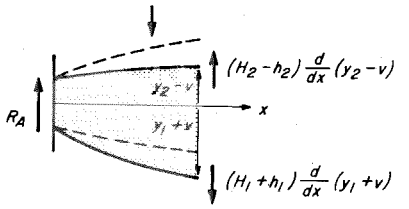

(b) Vertical equilibrium at a cross-section

Figure 17

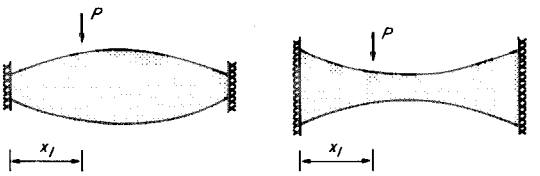

(a) Point load

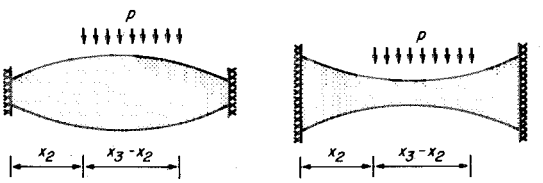

(b) Uniformly distributed load

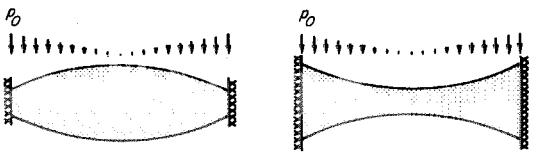

(c) Triangular load block

Figure 18 Definition diagrams for loading on the parabolic cable truss.

The cable equations for the bottom and top chords read

$$\left.\begin{aligned} \frac{h_1 L_{e1}}{E_c A_{c_1}} &= \int_0^{\ell} \frac{dy_1}{dx}\,\frac{dv}{dx}\,dx + \frac{1}{2}\int_0^{\ell}\left(\frac{dv}{dx}\right)^2 dx \\ \frac{h_2 L_{e2}}{E_c A_{c2}} &= \int_0^{\ell} \frac{dy_2}{dx}\,\frac{dv}{dx}\,dx + \frac{1}{2}\int_0^{\ell}\left(\frac{dv}{dx}\right)^2 dx \end{aligned}\right\} \qquad (2.4)$$

where A_{c_1} and A_{c2} are the areas of the bottom and top chords, respectively, and L_{e1} and L_{e2} are virtual lengths of these chords specified by

$$L_{e1,2} = \int_0^{\ell}\left(\frac{ds_{1,2}}{dx}\right)^3 dx$$

These equations are sufficient to obtain closed form solutions for the dependent variables v, h_1, h_2. Within reason, numerous different truss geometries could be chosen to yield a variety of architecturally pleasing, structural solutions. In general, to each of these, a separate solution is required.

Here, however, attention will be confined to those bi-convex or bi-concave trusses in which

$$\left.\begin{aligned} H_1 &= H_2 = H_0 \\ A_{c_1} &= A_{c2} = A_c \end{aligned}\right\} \qquad (2.5)$$

The first of these implies that

$$y_1 = y_2 = y$$

so that the truss is initially symmetrical about the longitudinal axis. Both together imply that

$$h_1 = h_2 = h$$

With these conditions, the non-linear, second order term in Eq. 2.3, $(h_1 - h_2)\frac{dv}{dx}$, is identically zero and, therefore, Eq. 2.3 now reads

$$2H_0 \frac{dv}{dx} + 2h \frac{dy}{dx} = S \tag{2.6}$$

The cable equation may be written as

$$\frac{hL_e}{E_c A_c} = \int_0^{\ell} \frac{dy}{dx} \frac{dv}{dx}\, dx \tag{2.7}$$

and the non-linear, second order term $\frac{1}{2}\int_0^{\ell}\left(\frac{dv}{dx}\right)^2 dx$ is unnecessary since owing to the form of Eq. 2.6, its effects will now be too small to materially affect the results. It is reiterated that Eqs. 2.6 and 2.7 hold true only if the truss is either bi-convex or bi-concave and is symmetrical about the longitudinal axis.

Equations 2.6 and 2.7 are linear, but they accurately describe the response of a structure the components of which behave in a strongly non-linear manner. This facet of cable behavior does not appear to have been recognized before. Irvine[5] has shown that the same phenomenon arises in the torsional analysis of suspension bridges where, as with the cable truss, the geometry of the cables changes by equal and opposite amounts.

The phenomenon is well known in other branches of mechanics and physics. For example, the linear range of an amplifier can be extended considerably if two amplifiers are used, which are connected in a "push-pull" arrangement.

In order to develop the analysis further, it will now be

assumed that the shape of each chord is given by the parabola

$$y = b\left\{1 + 4\left(\frac{d-b}{b}\right)\left(\left(\frac{x}{\ell}\right) - \left(\frac{x}{\ell}\right)^2\right)\right\} \qquad (2.8)$$

where $2b$ is the spacing of the chords at the supports and $2d$ is the spacing of the chords at mid-span. It will be assumed that

$$\left|\frac{d-b}{\ell}\right| \leq \frac{1}{8}$$

and it is clear that Eq. 2.8 holds whether the truss is bi-convex or bi-concave. The following loading conditions are now investigated.

2. Point Load on a Parabolic Cable Truss

Consider a point load, P, acting on the top chord of the truss, at a distance x_1 from the left-hand support (see Fig. 18(a)). Only the results of the analysis will be given; the details are similar to those presented in the corresponding section of Chapter I (p. 27).

The dimensionless expressions for the additional vertical deflection of the truss are:

(i) for $0 \leq \frac{x}{\ell} \leq \frac{x_1}{\ell}$,

$$v_* = \left[\left(1 - \frac{x_1}{\ell}\right)\frac{x}{\ell} - \frac{h_*}{P_*}\left(\frac{1}{2}\left(\frac{x}{\ell}\right) - \frac{1}{2}\left(\frac{x}{\ell}\right)^2\right)\right] \qquad (2.9)$$

(ii) for $\frac{x_1}{\ell} \leq \frac{x}{\ell} \leq 1$,

$$v_* = \left[\frac{x_1}{\ell}\left(1 - \frac{x}{\ell}\right) - \frac{h_*}{P_*}\left(\frac{1}{2}\left(\frac{x}{\ell}\right) - \frac{1}{2}\left(\frac{x}{\ell}\right)^2\right)\right] \qquad (2.10)$$

where

$$v_* = \frac{v}{\left(\frac{P\ell}{2H_0}\right)} \quad , \quad h_* = \frac{h}{H_0} \quad , \quad P_* = \frac{1}{2}\,\frac{P\ell}{8(d-b)H_0} \; .$$

Notice that P_* is negative if the truss is bi-concave (i. e., if $b > d$).

The horizontal component of cable tension reads

$$h_* = \frac{1}{\left(1 + \frac{12}{\lambda^2}\right)} \, 6 P_* \left\{ \left(\frac{x_1}{\ell}\right) - \left(\frac{x_1}{\ell}\right)^2 \right\} \qquad (2.11)$$

where

$$\lambda^2 = \left(\frac{8(d - b)}{\ell}\right)^2 \frac{\ell}{\left(\frac{H_0 L_e}{E_c A_c}\right)}$$

When P_* is negative, h_* is negative, which means that the bottom chord of the bi-concave truss suffers a reduction in cable tension. This is as expected.

It is clear that for given P_* and λ^2, the maximum value of h_* occurs when the point load is placed at mid-span.

The position of the point load which causes the overall maximum additional deflection can be found using the same principles as were obtained in Chapter I (p. 29). In particular:

(i) If $\lambda^2 \geq 24$,

then v_* has an overall maximum when

$$\left(\frac{x_1}{\ell}\right) = \frac{1}{2}\left(1 \mp \sqrt{1 - \frac{2}{3}\left(1 + \frac{12}{\lambda^2}\right)}\right) \qquad (2.12)$$

When $\lambda^2 >> 24$ (i.e. the chords are "inextensible")

$$\left(\frac{x_1}{\ell}\right) \to \frac{1}{2}\left(1 \mp \frac{1}{\sqrt{3}}\right) = 0.211, \; 0.789$$

The overall maximum value of v_* is

$$v_* = \frac{1}{12}\left(1 + \frac{12}{\lambda^2}\right) \qquad (2.13)$$

and when $\lambda^2 \gg 24$

$$v_* \to \frac{1}{12}$$

(ii) If $\lambda^2 \leq 24$,

then v_* has an overall maximum when

$$\left(\frac{x_1}{\ell}\right) = \frac{1}{2} \tag{2.14}$$

and the value of v_* is

$$v_* = \frac{1}{4}\left(1 - \frac{3}{4\left(1 + \frac{12}{\lambda^2}\right)}\right) \tag{2.15}$$

When $\lambda^2 << 24$ (i.e. as the chords become flat)

$$v_* \rightarrow \frac{1}{4}$$

It is reiterated that, when the chords are initially straight and parallel, the response of the truss is non-linear since the additional tension is positive in both chords. This restricts the applicability of the result given above.

3. Uniformly Distributed Load on a Parabolic Cable Truss

Consider a uniformly distributed load, of intensity p per unit length, acting on the top chord of the truss from $x = x_2$ to $x = x_3$ (see Fig. 18(b)).

The dimensionless expressions for the additional vertical deflection of the truss are:

(i) for $0 \leq \frac{x}{\ell} \leq \frac{x_2}{\ell}$,

$$v_* = \left[\left\{\left(\frac{x_3}{\ell} - \frac{x_2}{\ell}\right) - \frac{1}{2}\left(\left(\frac{x_3}{\ell}\right)^2 - \left(\frac{x_2}{\ell}\right)^2\right)\right\}\left(\frac{x}{\ell}\right) - \frac{h_*}{p_*}\left(\frac{1}{2}\left(\frac{x}{\ell}\right) - \frac{1}{2}\left(\frac{x}{\ell}\right)^2\right)\right] \tag{2.16}$$

(ii) for $\frac{x_2}{\ell} \leq \frac{x}{\ell} \leq \frac{x_3}{\ell}$,

$$v_* = \left[\left\{ -\frac{1}{2}\left(\frac{x_2}{\ell}\right)^2 + \left(\frac{x_3}{\ell}\right)\left(\frac{x}{\ell}\right) - \frac{1}{2}\left(\frac{x}{\ell}\right)^2 - \frac{1}{2}\left(\left(\frac{x_3}{\ell}\right)^2 - \left(\frac{x_2}{\ell}\right)^2\right)\left(\frac{x}{\ell}\right)\right\} - \frac{h_*}{p_*}\left(\frac{1}{2}\left(\frac{x}{\ell}\right) - \frac{1}{2}\left(\frac{x}{\ell}\right)^2\right)\right] \qquad (2.17)$$

(iii) for $\frac{x_3}{\ell} \le \frac{x}{\ell} \le 1$,

$$v_* = \left[\left\{\frac{1}{2}\left(\left(\frac{x_3}{\ell}\right)^2 - \left(\frac{x_2}{\ell}\right)^2\right)\left(1 - \frac{x}{\ell}\right)\right\} - \frac{h_*}{p_*}\left(\frac{1}{2}\left(\frac{x}{\ell}\right) - \frac{1}{2}\left(\frac{x}{\ell}\right)^2\right)\right] \qquad (2.18)$$

where

$$v_* = \frac{v}{\left(\frac{p\ell^2}{2H_0}\right)} \quad , \quad h_* = \frac{h}{H_0} \quad , \quad p_* = \frac{1}{2}\,\frac{p\ell^2}{8(d-b)H_0} \, .$$

The additional horizontal component of cable tension is

$$h_* = \frac{1}{\left(1 + \frac{12}{\lambda^2}\right)}\, 6\, p_* \left\{\frac{1}{2}\left(\left(\frac{x_3}{\ell}\right)^2 - \left(\frac{x_2}{\ell}\right)^2\right) - \frac{1}{3}\left(\left(\frac{x_3}{\ell}\right)^3 - \left(\frac{x_2}{\ell}\right)^3\right)\right\} \qquad (2.19)$$

A case of some practical importance arises when a parallel array of parabolic cable trusses are used to support the roof of a rectangular building and the roof load, p, is uniformly distributed across the span. Then

$$v_* = \frac{1}{2}\left(1 - \frac{h_*}{p_*}\right)\left(\left(\frac{x}{\ell}\right) - \left(\frac{x}{\ell}\right)^2\right) \qquad (2.20)$$

$$h_* = \frac{p_*}{\left(1 + \frac{12}{\lambda^2}\right)} \qquad (2.21)$$

From these two equations the additional deflections and tensions, which

the cable truss undergoes in resisting the roof load, can be estimated. The flexural stiffness associated with the roof material has been neglected, which is often a valid approximation.

4. Triangular Load Block on a Parabolic Cable Truss

Consider a triangular load block, of maximum intensity p_0 per unit length, acting on the top chord of the truss (see Fig. 18(c)).

From the symmetry of the problem, the dimensionless expression for the additional vertical deflection of the truss is, for $0 \le \frac{x}{\ell} \le \frac{1}{2}$,

$$v_* = \left[\frac{1}{3}\left(\frac{1}{8} - \left(\frac{1}{2} - \frac{x}{\ell}\right)^3\right) - \frac{h_*}{p_*}\left(\frac{1}{2}\left(\frac{x}{\ell}\right) - \frac{1}{2}\left(\frac{x}{\ell}\right)^2\right)\right] \qquad (2.22)$$

where

$$v_* = \frac{v}{\left(\frac{p_0 \ell^2}{2H_0}\right)} \quad , \quad h_* = \frac{h}{H_0} \quad , \quad p_* = \frac{1}{2}\,\frac{p_0 \ell^2}{8(d-b)H_0} \; .$$

The additional horizontal component of cable tension is

$$h_* = \frac{\frac{3}{8}\,p_*}{\left(1 + \frac{12}{\lambda^2}\right)} \qquad (2.23)$$

It is easily shown that if $\lambda^2 > 96$, the mid-span of the truss will rise under this loading.

These results will be useful for buildings which are circular in plan, where the roof is supported by parabolic cable trusses which are oriented along radii.

5. The Response of the Parabolic Cable Truss to Live Loading

In the previous three loading cases consideration was given to the truss's response under dead loading. When the cable truss is to be used as a structural member supporting a roof, it is clear that the dead load configuration is the one in which the roof load is supported. It is therefore necessary to extend this theory of the parabolic cable truss to cover situations in which the response of the truss to live loadings, such as rain, snow or the static effects of the wind, is required.

For these purposes, suppose that vertical equilibrium under dead load is specified by

$$2H_0 \frac{dv_0}{dx} + 2h_0 \frac{dy}{dx} = S_0 \qquad (2.24)$$

where v_0 is the deflection from the initial free-hanging geometry, h_0 is the additional horizontal component of cable tension owing to the dead load, and S_0 is the shear force at the cross section.

Under liveloading an additional shear force, S, is developed. The corresponding additional deflection is v, and the additional horizontal component of cable tension is h. Vertical equilibrium at the cross section in the new displaced configuration requires that

$$(H_0+h_0+h) \frac{d}{dx} (y+v_0+v) - (H_0-h_0-h) \frac{d}{dx} (y-v_0-v) = S_0+S \qquad (2.25)$$

Upon expanding Eq. 2.25 and substituting for Eq. 2.24 the following equation is obtained

$$2H_0 \frac{dv}{dx} + 2h \frac{dy}{dx} = S \qquad (2.26)$$

and it can be shown that, to first order, the cable equation becomes

$$\frac{hL_e}{E_c A_c} = \int_0^{\ell} \frac{dy}{dx} \frac{dv}{dx} dx \qquad (2.27)$$

These equations will be useful in practical problems, although they do nothing more than embody the principle of superposition. Finally, it is seen that, for the parabolic cable truss, the total horizontal reaction at a support is always $2H_0$. The addition of vertical loading causes a rearrangement in the distribution of this reaction between the top and the bottom chords, but the sum remains constant.

Later, it will be shown that Eqs. 2.26 and 2.27 have their counterparts in the theory of vertical vibration of the cable truss. First, however, two numerical examples are given to illustrate the results obtained so far.

6. Examples

Example 12

A sports area, of plan dimensions 61 m × 122 m, is to have its roof supported by a series of bi-concave parabolic cable trusses which span the shorter side (see Fig. 19). As one possible structural solution the following data are specified: ℓ = 61 m, b = 3.05 m, d = 0.61 m, $E_c = 104 \times 10^6$ kN/m^2, $A_c = 3.22 \times 10^{-3}$ m^2, H_0 = 1110 kN. It is required to find the changes in the horizontal component of cable tension and the additional vertical deflection at

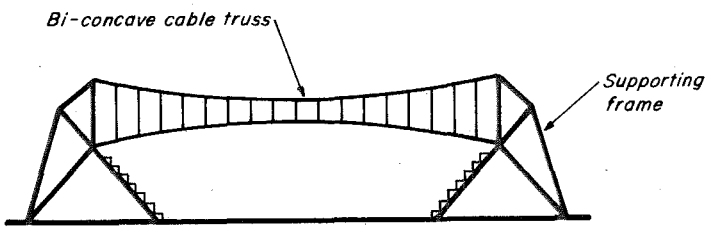

Figure 19 Schematic of rectangular sports arena.

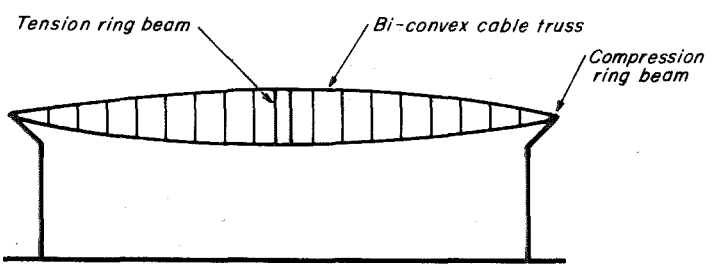

Figure 20 Schematic of circular auditorium.

mid-span under two loading conditions:

(i) After roof load of 5.83 kN/m has been placed,

(ii) Under snow loading of 5.83 kN/m which covers the first half of the span.

(i) Roof load

$\lambda^2 = 30.4$ $\quad p_* = -0.5$ (negative because the trusses are bi-concave)

Hence, from Eq. 2.21

$$h_* = -0.358$$

Thus, the horizontal component of cable tension in the bottom chord reduces to 710 kN, and the horizontal component of cable tension in the top chord increases to 1510 kN.

From Eq. 2.20

$$v = 0.348 \text{ m}$$

That is, the sag of the top chord increases from 2.44 m to 2.79 m , while the "sag" of the bottom chord reduces from 2.44 m to 2.09 m .

(ii) Snow load

Because of Eqs. 2.26 and 2.27, the principle of superposition applies to this problem

$$\lambda^2 = 30.4 \qquad p_* = -0.5$$

From Eq. 2.19

$$h_* = -0.179$$

Hence, under this liveloading, the horizontal component of cable tension in the top chord becomes 1710 kN, and the horizontal component of cable tension in the bottom chord becomes 510 kN.

From Eq. 2.17

$$v = 0.174 \text{ m}$$

The sag of the top chord increases from 2.79 m to 2.96 m and the "sag" of the bottom chord reduces from 2.09 m to 1.92 m .

This analysis neglects the stiffness associated with the roof material and it also assumes that the supporting frames are rigid. The addition of the roof load causes a substantial alteration to the distribution of the horizontal components of the cable forces, and it is obvious that the pretension must be high so that (for the bi-concave system) the tension in the bottom chord does not become too low. The alteration of the cable forces may cause a significant redistribution of the resisting stresses in the supporting frames.

Changes in temperature may cause effects which are important. However, the calculation of these effects is not straightforward since it is clear that uniform temperature increments, in both the top and bottom chords, are most unlikely to occur in practice. Equations 2.3 and 2.4 can be used in such situations, provided that the cable equations are modified as outlined in Appendix II.

Example 13

A circular auditorium, of diameter 61 m, is to have its roof supported by sixteen radial, bi-convex parabolic cable trusses (see Fig. 20). As one possible structural solution the following data are specified: $\ell = 61$ m, $b = 0$, $d = 3.05$ m, $E_c = 104 \times 10^6$ kN/m^2, $A_c = 3.22 \times 10^{-3}$ m^2, $H_0 = 890$ kN. It is required to investigate the structural behavior of the roof under two loading conditions:

(i) After roof load, of maximum intensity $p_0 = 11.4$ kN/m, has been placed,

(ii) When account is taken of the weight of the tension ring beam (of weight 44.5 kN).

(i) Roof load

$$\lambda^2 = 60 \qquad p_* = 0.982$$

Hence, from Eq. 2.23

$$h_* = 0.307$$

Consequently, the horizontal component of cable tension in the bottom chord increases to 1160 kN, while the horizontal component of cable tension in the top chord reduces to 620 kN.

From Eq. 2.22

$$v = 0.061 \text{ m}$$

The "sag" of the top chord reduces from 3.05 m to 2.99 m and the sag of the bottom chord increases from 3.05 m to 3.11 m. The small increase in deflection may be attributed to the triangular nature of the load block which each truss resists.

(ii) Load owing to tension ring beam

It is probably inadvisable to ignore the effect of the weight of the ring beam in the analysis. Each truss therefore sustains a point load at mid-span, of magnitude

$$P = 2.78 \text{ kN}$$

from which

$$P_* = 3.92 \times 10^{-3}$$

$$\lambda^2 = 60$$

From Eq. 2.11

$$h_* = 4.9 \times 10^{-3}$$

which is negligibly small.

However, from Eq. 2.10

$$v = 0.024 \text{ m}$$

Consequently, a more accurate description of the truss geometry under full dead load is that the "sag" of the top chord is 2.965 m and the sag of the bottom chord is 3.135 m.

One of the advantages of the cable truss system is that service machinery, such as air conditioning equipment, may be placed in the roof. Such roof systems may be readily insulated and their shape reduces the volume of air required to be conditioned; factors which may lead to substantial savings in the operating expenses of a building.

Viewed from the outside, a roof consisting of a system of bi-convex cable trusses will appear to be resisting the applied loads as a shell. In fact, of course, the principal structural resistance will be provided by tension members.

B. THE LINEAR THEORY OF FREE VIBRATIONS OF THE PARABOLIC CABLE TRUSS

As has been stated, cable trusses will find applications principally as structural members supporting the roofs of buildings. A knowledge of the dynamic characteristics of such roof systems, in which the trusses often span large distances, is essential if the possible dynamic effects of wind or earthquakes are to be assessed.

Two different situations will be investigated. In the first, which relates to buildings rectangular in plan, the weight of roof associated with each truss is assumed to be uniformly distributed along the span. In the second, which relates to buildings circular in plan, the weight of the roof associated with each truss is assumed to be distributed as a triangular load block.

Only the vertical components of the vibrations of the parabolic cable truss will be considered since they are of most importance. For simplicity, the word "mode" will be applied to the vertical components, although it is recognized that an in-plane mode must consist of two components.

1. Uniformly Distributed Roof Load

The theory to be presented here has marked similarities with the theory of vertical vibrations of the parabolic cable given in Chapter I. If the truss is given a small vertical disturbance the subsequent vertical equilibrium of an element of the truss requires that

$$(H_0 + h_0 + h)\frac{\partial^2}{\partial x^2}(y + v_0 + v) - (H_0 - h_0 - h)\frac{\partial^2}{\partial x^2}(y - v_0 - v) = -p + m\frac{\partial^2 v}{\partial t^2} \qquad (2.28)$$

where H_0 is the horizontal component of the initial pretension in each chord, h_0 is the additional horizontal component of cable tension owing to the roof load p, h is the additional horizontal component of cable tension owing to the free vertical vibrations of the truss, $y+v_0$ and $y-v_0$ are the shapes of the chords under prestress and roof load, v is the vertical deflection of the element owing to the vibrations and m is the mass of the roof associated with each truss per unit length.

The equation of static equilibrium of the truss under roof load is

$$2H_0 \frac{d^2v_0}{dx^2} + 2h_0 \frac{d^2y}{dx^2} = -p \qquad (2.29)$$

After expanding Eq. 2.28 and substituting for Eq. 2.29, the following linear partial differential equation is obtained

$$2H_0 \frac{\partial^2 v}{\partial x^2} + 2h \frac{d^2y}{dx^2} = m \frac{\partial^2 v}{\partial t^2} \qquad (2.30)$$

The important feature of this equation (and in this it differs from the parabolic cable) is that h_0 and v_0 are absent as a result of the symmetry.

If the following substitutions are made, namely

$$v(x,t) = \tilde{v}(x)e^{i\omega t} \quad , \quad h(t) = \tilde{h}e^{i\omega t} \quad , \quad \frac{d^2y}{dx^2} = -\frac{8(d-b)}{\ell^2}$$

where ω is the natural circular frequency of vibration, then Eq. 2.30 becomes the ordinary differential equation

$$2H_0 \frac{d^2\tilde{v}}{dx^2} + m\omega^2\tilde{v} = 2\tilde{h}\frac{8(d-b)}{\ell^2} \qquad (2.31)$$

and the linearized cable equation is

$$\frac{\tilde{h}L_e}{E_c A_c} = \frac{8(d-b)}{\ell^2} \int_0^{\ell} \tilde{v}\, dx \qquad (2.32)$$

As with the parabolic cable, there are two cases to consider:

a. The antisymmetric modes of vibration which result in an odd number of internal nodes along the span. Here $\tilde{h}$ is zero.

b. The symmetric modes of vibration in which there are an even number of internal nodes along the span. Here $\tilde{h}$ is not zero.

a. Antisymmetric modes

Since, to first order $\tilde{h}$ is zero Eq. 2.31 reads

$$2H_0 \frac{d^2\tilde{v}}{dx^2} + m\omega^2 \tilde{v} = 0 \qquad (2.33)$$

and the boundary conditions which each antisymmetric mode must satisfy are

$$\tilde{v}(0) = \tilde{v}\left(\frac{\ell}{2}\right) = 0$$

It is then found, upon solving Eq. 2.33, that the natural circular frequencies of the antisymmetric vertical modes of vibration are

$$\omega_n = \frac{2n\pi}{\ell} \sqrt{\left(\frac{2H_0}{m}\right)} \qquad n = 1, 2, 3... \qquad (2.34)$$

and the antisymmetric modes are

$$\tilde{v}_n(x) = A_n \sin\left(\frac{2n\pi x}{\ell}\right) \qquad n = 1, 2, 3... \qquad (2.35)$$

where $n = 1, 2, 3...$ signify the first, second, third, etc. antisymmetric vertical modes. The analogy with the parabolic cable is obvious.

b. Symmetric modes

When the truss vibrates in a symmetric vertical mode, stretching and contraction of the chords take place and, as a consequence, $\tilde{h} \neq 0$. The full non-homogeneous differential equation must be solved

$$2H_0 \frac{d^2\tilde{v}}{dx^2} + m\omega^2 \tilde{v} = 2\tilde{h} \frac{8(d-b)}{\ell^2}$$

The boundary conditions are

$$\tilde{v}(0) = \tilde{v}(\ell) = 0$$

and the solution for the symmetric vertical modes is

$$\frac{\tilde{v}(x)}{8(d-b)} = \frac{\tilde{h}}{H_0} \frac{1}{(\beta\ell)^2} \left\{ 1 - \tan\left(\frac{\beta\ell}{2}\right) \sin\beta x - \cos\beta x \right\} \qquad (2.36)$$

where

$$\beta^2 = \frac{m\omega^2}{2H_0}$$

Use is now made of the cable equation (Eq. 2.32) to eliminate $\tilde{h}$ and obtain the following transcendental equation from which the frequencies of the symmetric vertical modes of vibration may be found

$$\tan\left(\frac{\beta\ell}{2}\right) = \left(\frac{\beta\ell}{2}\right) - \frac{4}{\lambda^2}\left(\frac{\beta\ell}{2}\right)^3 \qquad (2.37)$$

where

$$\lambda^2 = \left(\frac{8(d-b)}{\ell}\right)^2 \frac{\ell}{\left(\frac{H_0 L_e}{E_c A_c}\right)}$$

This is of the same form as the corresponding equation for the parabolic cable, although here β^2 and λ^2 are defined differently (see p. 71).

Because of this, it is unnecessary to give a detailed discussion of the properties of the above equation. Suffice it to say that:

(i) If $\lambda^2 < 4\pi^2$,

then the first mode of vertical vibration is the first symmetric mode.

(ii) If $\lambda^2 > 4\pi^2$,

then the first mode of vertical vibration is the first antisymmetric mode.

For parabolic cable truss systems, where this latter inequality holds, good use may be made of a structural device which is common in long-span suspension bridges. The device consists of either clamping the chords of the truss together at mid-span (if d = 0), or fixing a rigid cross-brace frame, in the plane of the truss, between the chords at mid-span. In this way the symmetric longitudinal chord movements, associated with the antisymmetric vertical movements, are supressed at mid-span. The structure is stiffened considerably. By analogy with another similar problem[4], it may be shown that the lowest frequency of vibration will be raised if this device is employed for truss systems in which $\lambda^2 > 4\pi^2$.

2. Roof Load Distributed as a Triangular Load Block

The vibration theory to be developed here will be of use for determining the dynamic characteristics of roofs which are circular in plan and which are supported by radial cable trusses.

Only axially symmetric vertical vibrations will be considered. The antisymmetric modes are not considered since they depend

on both polar coordinates (r, θ). The assumption of zero stiffness in the θ-direction precludes their discussion. This is not to imply that antisymmetric vertical vibrations will not occur in practice. However, the presence of the rigid tension ring at mid-span will modify their form considerably and it is virtually certain that the lowest frequency will always be that of the first symmetric mode.

The basic partial differential equation of the symmetric vertical motion is

$$2 H_0 \frac{\partial^2 v}{\partial r^2} + 2 h \frac{d^2 y}{dr^2} = m_0 \frac{r}{R} \frac{\partial^2 v}{\partial t^2} \tag{2.38}$$

where m_0 is the maximum mass per unit length of the triangular load block associated with each truss and R is the radius of the roof.

If the substitutions

$$v(r, t) = \tilde{v}(r) e^{i\omega t} \quad , \quad h(t) = \tilde{h} e^{i\omega t}$$

are made, then Eq. 2.38 reduces to

$$\frac{d^2 \tilde{v}}{dr^2} + r\beta^2 \tilde{v} = - \frac{\tilde{h}}{H_0} \frac{d^2 y}{dr^2} \tag{2.39}$$

where

$$\beta^2 = \frac{m_0 \omega^2}{2RH_0}$$

and the cable equation reads

$$\frac{\tilde{h} R_e}{E_c A_c} = \int_0^R \frac{dy}{dr} \frac{d\tilde{v}}{dr} \, dr \tag{2.40}$$

where R_e is a virtual length of the chord defined by

$$R_e = \int_0^R \left(\frac{ds}{dr}\right)^3 dr$$

It is noted in passing that, if the cable truss were a single entity supporting a triangular load block (a most unlikely situation), the frequencies of the antisymmetric modes could be found from the roots of [21]

$$J_{\frac{1}{3}}\left(\frac{2}{3}\beta R^{\frac{3}{2}}\right) = 0 \qquad (2.41)$$

and the antisymmetric modes would be

$$\tilde{v}(r) = A\sqrt{\beta^{\frac{2}{3}} r}\; J_{\frac{1}{3}}\left(\frac{2}{3}\beta r^{\frac{3}{2}}\right) \qquad (2.42)$$

where $J_{\frac{1}{3}}$ is the Bessel function of the first kind and one-third order. These equations do not apply, however, to this circular roof.

Returning to Eq. 2.39, it is obvious from the form of this equation that, if parabolic cable trusses are used, the solution is not straightforward. A particular integral could be found using the method of variation of parameters but this would cause the analysis to be unnecessarily complicated. Therefore, it will be assumed, for convenience, that the initial shape of the chords is given by the cubic

$$y(r) = d\left\{1 - \left(\frac{d-b}{d}\right)\left(\frac{r}{R}\right)^3\right\} \qquad (2.43)$$

Since this shape differs little from the parabola

$$y(r) = d\left\{1 - \left(\frac{d-b}{d}\right)\left(\frac{r}{R}\right)^2\right\} \qquad (2.44)$$

the analysis which follows can,for practical purposes, be assumed to describe the parabolic cable truss.

Consequently, Eq. 2.39 becomes

$$\frac{d^2\tilde{v}}{dr^2} + r\beta^2\tilde{v} = \frac{\tilde{h}}{H_0}\, 6(d-b)\,\frac{r}{R^3} \tag{2.45}$$

and the cable equation becomes

$$\frac{\tilde{h}R_e}{E_cA_c} = \frac{6(d-b)}{R^3}\int_0^R r\,\tilde{v}\,dr \tag{2.46}$$

The boundary conditions which the symmetric modes must satisfy are

$$\frac{d\tilde{v}(0)}{dr} = 0 \quad , \quad \tilde{v}(R) = 0$$

and so the symmetric vertical modes are given by

$$\frac{\tilde{v}(r)}{6(d-b)} = \frac{\tilde{h}}{H_0}\,\frac{1}{(\beta^2R^3)}\left\{1 - \frac{r^{\frac{1}{2}}J_{-\frac{1}{3}}\left(\frac{2}{3}\beta r^{\frac{3}{2}}\right)}{R^{\frac{1}{2}}J_{-\frac{1}{3}}\left(\frac{2}{3}\beta R^{\frac{3}{2}}\right)}\right\} \tag{2.47}$$

where $J_{-\frac{1}{3}}$ is the Bessel function of the first kind and minus one-third order and each mode is specified by a value of $\left(\beta R^{\frac{3}{2}}\right)$.

By use of Eqs. 2.46 and 2.47, the transcendental equation from which the frequencies of the symmetric modes can be found is

$$\frac{J_{\frac{2}{3}}(X)}{J_{-\frac{1}{3}}(X)} = \frac{3}{4}X - \frac{27}{8\lambda^2}X^3 \tag{2.48}$$

where

$$X = \frac{2}{3}\beta R^{\frac{3}{2}} \quad , \quad \lambda^2 = \left(\frac{6(d-b)}{R}\right)^2 \frac{R}{\left(\frac{H_0R_e}{E_cA_c}\right)}$$

and $J_{\frac{2}{3}}$ is the Bessel function of the first kind and two-thirds order.

It may readily be shown[22] that

$$\lim_{X \to 0} \frac{J_{\frac{2}{3}}(X)}{J_{-\frac{1}{3}}(X)} = \frac{3}{4}X$$

which means that the first root of the above transcendental equation is the trivial result $X = 0$. In this respect, and in many others, Eq. 2.48 is analogous to Eq. 2.37.

As has been found repeatedly throughout this study, the solution of Eq. 2.48 is heavily dependent on the value of the characteristic parameter λ^2. When λ^2 is very small (that is, when the chords of the truss are only very slightly bi-concave or bi-convex), the transcendental equation reduces to

$$J_{-\frac{1}{3}}(X) = 0 \tag{2.49}$$

the first root of which is

$$X = 1.87$$

This is the equation which would obtain for the determination of the symmetric modes of vibration of a taut string (tension $2H_0$), in which the string's mass is distributed as a triangular block. However, when λ^2 is very large (indicating that the chords of the truss are substantially inextensible), the transcendental equation reduces to

$$\frac{J_{\frac{2}{3}}(X)}{J_{-\frac{1}{3}}(X)} = \frac{3}{4}X \tag{2.50}$$

the first non-zero root of which is

$$X = 4.72$$

By referring to Fig. 21 the following conclusions may be made, which hold strictly only for the cubic cable truss. The curves

were plottted with the aid of tables[6].

(i) If $\lambda^2 < 51.7$, then the first symmetric mode has no internal nodes along a diameter.

(ii) If $\lambda^2 = 51.7$, then the first symmetric mode has no internal nodes along a diameter, but the slope is zero at each support.

(iii) If $\lambda^2 > 51.7$, then the first symmetric mode has two internal nodes along a diameter.

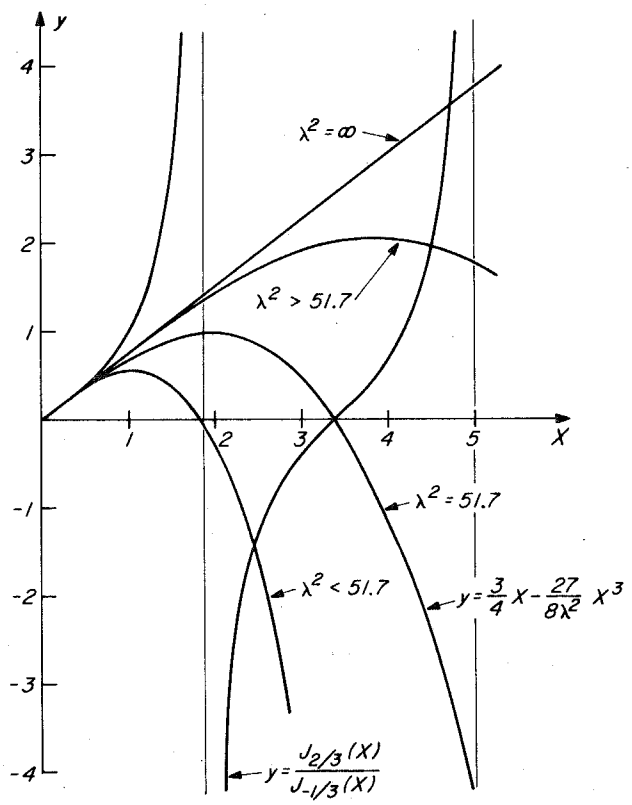

Figure 21 Graphical solution for the first non-zero root of Eq. 2.48.

3. Examples

Example 14

It is required to find the period of the first symmetric mode of vibration of the cable truss roof of the sports arena, the details of which were given in Example 12 (p. 108).

Here

$$\lambda^2 = 30.4 < 4\pi^2$$

From Eq. 2.37 it is found that

$$(\beta\ell)_1 = 1.84\pi$$

and the period of the first symmetric mode is

$$T_1 = 1.08 \text{ secs}$$

This is the fundamental period of the system since the period of the first antisymmetric mode is

$$T_1 = 1.0 \text{ secs} \quad .$$

Example 15

Calculate the period of the first symmetric mode of vibration of the circular roof of the auditorium, the details of which were given in Example 13 (p. 111). From Eq. 2.48

$$\lambda^2 = 135 > 51.7$$

and it is then found that the first non-zero root of Eq. 2.48 is

$$X_1 = 4.3$$

The period of the first symmetric mode is

$$T_1 = 0.76 \text{ secs}$$

In both these examples the fundamental periods are quite low which indicates the rigidity inherent in this type of structural support system.

C. THE LATERAL STABILITY OF THE CABLE TRUSS

In this final section attention is turned to the lateral stability of the cable truss. A single cable truss may be laterally unstable under the influence of applied vertical loading, although this aspect does not appear to have received attention in the literature[19].

The problem is probably of limited practical importance because, in a well designed roof system, the presence of the roofing material and cross-bracing members between adjacent trusses will make lateral instability an unlikely possibility. Nonetheless, the theory is of some interest and it appears to open up a new field of buckling problems.

The lateral stability of the cable truss is not directly analogous to any of the well-known classes of buckling problems. The nearest analogy is with the lateral buckling of a thin, deep beam, but even here it will become apparent that there are substantial differences between the two systems.

Attention will be confined to those cable trusses which are symmetrical about the longitudinal axis. Variational methods are used to set up the fundamental differential equation and then solutions are given for trusses of different geometries under different vertical loading conditions.

1. The Fundamental Differential Equation

Consider a cable truss, the chords of which are either bi-convex or bi-concave, under the action of some vertical loading, p (see Fig. 22(a)). As has been shown in the previous sections, the

geometry ofthe chords changes (to y ± v) under the vertical load, but the spacing of the chords does not change because the spacers are assumed inextensible. Likewise, in resisting this vertical load, the horizontal component of cable tension in the chords increases and decreases by the same amount (to $H_0 \pm h$), when the truss is symmetrical about the longitudinal axis.

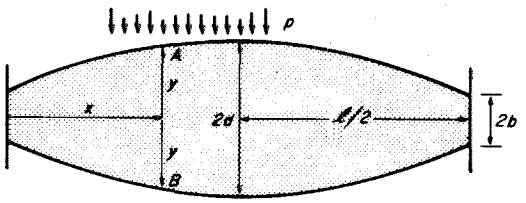

(a) Typical bi-convex system

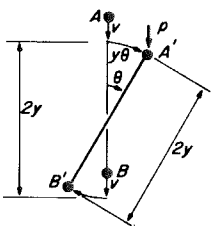

(b) View in elevation of displaced geometry of AB

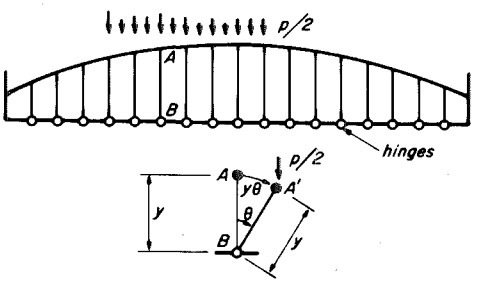

(c) Equivalent system for bi-convex truss

Figure 22

With the truss in this vertically displaced position, any small torsional disturbance which is applied to the truss will be resisted at each cross section by a torque, which depends on the horizontal components of tension $(H_0 + h)$ and $(H_0 - h)$ in the chords, and the moment arm 2y. Under these conditions, the vertical movement v does not enter the problem. Also, the components of the resisting

torque, owing to the additional horizontal components of cable tension, cancel and, therefore, Fig. 22(c) is the equivalent system by which the lateral stability of these bi-convex or bi-concave cable trusses may be studied.

The small torsional disturbance causes a small rotation, $\theta(x)$, of the spacers in a direction perpendicular to the plane of truss (see Fig. 22(b)). The chords move by equal and opposite amounts, although the line connecting the centers of the spacers does not move. The vertical load is assumed to be applied at the top chord; if it is applied anywhere from mid-way down the spacers to the bottom chord, no problem of lateral stability can exist. In these basic respects (and, of course, in the nature of the structural resistance), the cable truss differs from the thin, deep beam. Finally, it is assumed that $\theta(x)$ is so small that negligible additional tension is induced by the lateral movements of the chords.

If, in the original network (see Fig. 22(c)), the length of an element of the chord is ds, and its length in the laterally displaced position is ds', then

$$ds^2 = dx^2 + dy^2$$

and

$$ds'^2 = dx^2 + \{(y+dy)\cos(\theta+d\theta) - y\cos\theta\}^2 + \{(y+dy)\sin(\theta+d\theta) - y\sin\theta\}^2$$

Because $\theta(x)$ is small

$$ds'^2 \simeq ds^2 + y^2(d\theta)^2$$

from which

$$ds' - ds \simeq \frac{1}{2} y^2 \left(\frac{d\theta}{ds}\right)^2 ds \qquad (2.51)$$

The pretension in the chord is T_0 and, therefore, the additional energy stored in the element is

$$dV = \frac{1}{2} T_0 y^2 \left(\frac{d\theta}{ds}\right)^2 ds$$

But

$$T_0 = H_0 \frac{ds}{dx}$$

where H_0 is the horizontal component of the pretension.

Therefore

$$dV = \frac{1}{2} H_0 y^2 \left(\frac{d\theta}{dx}\right)^2 dx \qquad (2.52)$$

and the additional energy stored in both chords is

$$V = \int_0^{\ell} H_0 y^2 \left(\frac{d\theta}{dx}\right)^2 dx \qquad (2.53)$$

The work done by the load, p, is

$$W = \int_0^{\ell} p\, y\, (1 - \cos\theta)\, dx$$

that is

$$W \simeq \int_0^{\ell} \frac{1}{2} py\theta^2\, dx \qquad (2.54)$$

The difference between W and V is E, where

$$E = \int_0^{\ell} \left\{ -H_0 y^2 \left(\frac{d\theta}{dx}\right)^2 + \frac{1}{2} py\theta^2 \right\} dx \qquad (2.55)$$

Performing the variation with respect to θ yields

$$\delta E = \int_0^{\ell} \left\{ -2H_0 y^2 \frac{d\theta}{dx} \frac{d(\delta\theta)}{dx} + py\theta\delta\theta \right\} dx = 0$$

and upon integration (by parts, where necessary) the following equation is obtained

$$-2H_0\, y^2 \frac{d\theta}{dx}\,\delta\theta\Big|_0^{\ell} + \int_0^{\ell} \left\{ 2H_0 \frac{d}{dx}\left(y^2 \frac{d\theta}{dx}\right) + py\theta \right\} \delta\theta\, dx = 0$$

If the boundary conditions are such that

$$2H_0\, y^2 \frac{d\theta}{dx}\,\delta\theta\Big|_0^{\ell} = 0 \qquad (2.56)$$

then, since $\delta\theta$ is arbitrary, it follows that the differential equation governing the lateral stability of the cable truss is

$$2H_0 \frac{d}{dx}\left(y^2 \frac{d\theta}{dx}\right) + py\theta = 0 \qquad (2.57)$$

This equation is correct to the first order of small quantities, provided that the truss is symmetrical about the longitudinal axis and either bi-convex or bi-concave.

Equation 2.57 may equally well be written in terms of the lateral displacement ϵ, where $\epsilon = y\theta$, and, therefore

$$2H_0 \frac{d}{dx}\left(y \frac{d\epsilon}{dx} - \epsilon \frac{dy}{dx}\right) + p\epsilon = 0 \qquad (2.58)$$

This equation, which is no longer in self-adjoint form, could also have been obtained from considerations of the torsional equilibrium of an element of the truss.

For some of the solutions given later it proves convenient to use Eq. 2.58 rather than Eq. 2.57. This is not essential, of course, but it allows the physical nature of the problem to be more clearly portrayed.

Cable trusses in which the chords are initially straight and parallel are the easiest to analyse and, therefore, are considered first.

2. Parallel Chord Cable Truss

a. Effect of a point load

As is shown in Fig. 23(a), (b), a truss of this type may buckle laterally under the effect of a point load P, applied at some distance x_1 from the left-hand support. Because the chords of the truss are initially straight and parallel, the additional tensions induced in the chords, owing to the application of the vertical load, must be accounted for. The additional tensions are now both positive and the effects do not cancel as is the case when the truss is either bi-convex or bi-concave. It is easily shown that the governing differential equation is then

$$2d\,(H_0 + h)\,\frac{d^2\epsilon}{dx^2} + p\epsilon = 0 \qquad (2.59)$$

where h is the additional horizontal component of cable tension. Integrating this equation yields

$$2d\,(H_0 + h)\,\frac{d\epsilon}{dx}\Bigg|_{x_1^-}^{x_1^+} + P\epsilon_1 = 0 \qquad (2.60)$$

where ϵ_1 is the lateral displacement at x_1. From Fig. 23(b)

$$\frac{d\epsilon}{dx}\Bigg|_{x_1^-}^{x_1^+} = -\frac{\epsilon_1}{x_1\left(1 - \frac{x_1}{\ell}\right)} \qquad (2.61)$$

and the critical load is thus given by

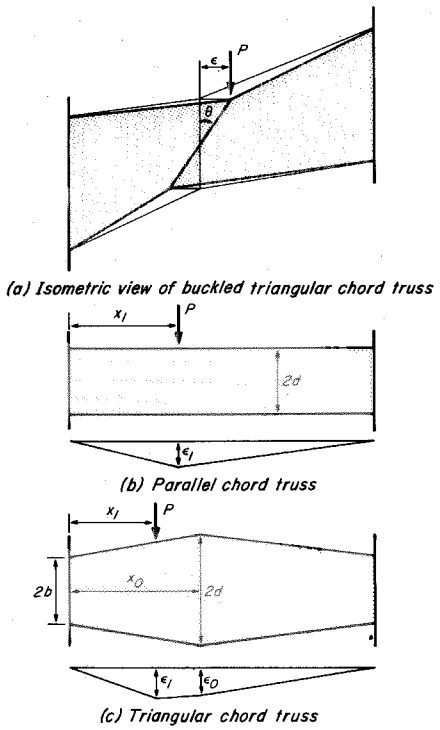

Figure 23

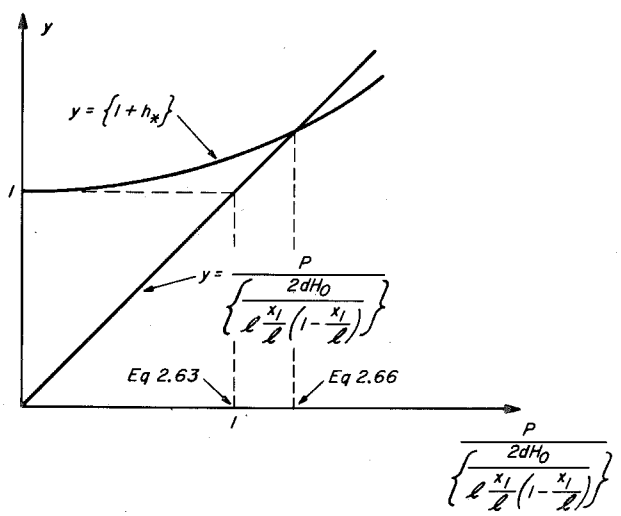

Figure 24 Graphical solution for non-linear stiffening effect in the lateral buckling of a parallel chord truss.

$$P_{crit} = \frac{2d\,(H_0 + h)}{x_1\left(1 - \frac{x_1}{\ell}\right)} \tag{2.62}$$

If the additional horizontal component of cable tension is ignored for the present, then Eq. 2.62 becomes

$$P_{crit} = \frac{2dH_0}{x_1\left(1 - \frac{x_1}{\ell}\right)} \tag{2.63}$$

the minimum value of which occurs at $x_1 = \frac{\ell}{2}$, and is

$$P_{crit} = \frac{8dH_0}{\ell} \tag{2.64}$$

However, in most situations the additional horizontal component of cable tension will cause a significant increase in the critical load, above that given by Eq. 2.63. The methods of Chapter I may be employed to evaluate h and, in particular, Eq. 1.43 may be adapted to give

$$h_* = \frac{1}{\sqrt[3]{C}}\left(\sqrt[3]{C} - \frac{1}{3}\right)^2 \tag{2.65}$$

where

$$h_* = \frac{h}{H_0} \quad , \quad C = -\frac{q}{2} + \sqrt{\frac{q^2}{4} + \frac{p^3}{27}}$$

and

$$p = -\frac{1}{3} \quad , \quad q = -\frac{2}{27} - \frac{E_c A_c}{8H_0}\left(\left(\frac{x_1}{\ell}\right) - \left(\frac{x_1}{\ell}\right)^2\right)\left(\frac{P_{crit}}{H_0}\right)^2$$

Equation 2.62 then becomes

$$P_{crit} = (1 + h_*)\frac{2dH_0}{x_1\left(1 - \frac{x_1}{\ell}\right)} \tag{2.66}$$

where $h_* = fn\left(\frac{x_1}{\ell}, P_{crit}\right)$, as given by Eq. 2.65. It appears that no explicit form for P_{crit} exists and, therefore, a graphical solution is best. The form that a graphical solution would take is shown in Fig. 24, from which it is seen that P_{crit} may be very high, in fact, buckling may not occur. At present it does not seem possible to determine, in simple form, the properties of the parallel chord truss in which the non-linear stiffening effect is such that lateral buckling will not occur under a point load.

b. Effect of a uniformly distributed load

When p is constant along the span, the general solution to Eq. 2.59 is

$$\epsilon(x) = A \sin \alpha x + B \cos \alpha x \qquad (2.67)$$

where

$$\alpha^2 = \frac{p}{2d(H_0 + h)}$$

The boundary conditions are

$$\epsilon(0) = \epsilon(\ell) = 0$$

The first requires that $B = 0$, the second requires that

$$\alpha\ell = n\pi \qquad n = 1, 2, 3\ldots \qquad (2.68)$$

Since the first eigenvalue is the only one of interest for the problem at hand

$$p_{crit} = (1 + h_*) \frac{2\pi^2 d H_0}{\ell^2} \qquad (2.69)$$

and

$$\epsilon(x) = A \sin\left(\frac{\pi x}{\ell}\right) \qquad (2.70)$$

Again, if h_* is ignored for the present, Eq. 2.69 becomes

$$p_{crit} = \frac{2\pi^2 dH_0}{\ell^2} \tag{2.71}$$

which suggests that if P_{crit} is the critical point load, applied at $x_1 = \frac{\ell}{2}$ (see Eq. 2.64), then a load of $\frac{\pi^2}{4} P_{crit}$ may be distributed uniformly along the truss before buckling will occur.

As before, however, it is inadvisable to ignore h_*. Equation 1.64 can be adapted to read

$$h_* = \frac{1}{\sqrt[3]{D}} \left(\sqrt[3]{D} - \frac{1}{3} \right)^2 \tag{2.72}$$

where

$$h_* = \frac{h}{H_0} \quad , \quad D = -\frac{s}{2} + \sqrt{\frac{s^2}{4} + \frac{r^3}{27}}$$

and

$$r = -\frac{1}{3} \quad , \quad s = -\frac{2}{27} - \frac{E_c A_c}{96 H_0} \left(\frac{p_{crit} \ell}{H_0} \right)^2$$

Equations 2.69 and 2.72 provide the basis for obtaining a graphical solution to the problem. It is noted again that p_{crit} may be very large, even infinite, for some parallel chord trusses.

Clearly, the most conservative results for the buckling loads of a parallel chord truss are given by Eqs. 2.63 and 2.71.

c. Effect of a triangular load block

The theory presented here will find an application when radial, parallel chord trusses are used to support the roofs of circular buildings. In such cases the roof load may be approximated by a triangular load block. It is convenient to take coordinates about mid-span (span 2R). To obtain the most conservative result, h will be ignored, and then Eq. 2.59 becomes

$$2dH_0 \frac{d^2\epsilon}{dr^2} + \frac{r}{R} p_0 \epsilon = 0 \qquad (2.73)$$

where p_0 is the intensity of the load on the perimeter.

The general solution of Eq. 2.73 is[21]

$$\epsilon(r) = \left(\alpha^{\frac{2}{3}} r\right)^{\frac{1}{2}} \left\{ AJ_{\frac{1}{3}}\left(\frac{2}{3}\alpha r^{\frac{3}{2}}\right) + BJ_{-\frac{1}{3}}\left(\frac{2}{3}\alpha r^{\frac{3}{2}}\right)\right\} \qquad (2.74)$$

where

$$\alpha^2 = \frac{p_0}{2dH_0R}$$

and $J_{\pm\frac{1}{3}}$ are Bessel functions of the first kind and $\pm\frac{1}{3}$ order.

Since the component trusses are arranged radially, there will almost always be a rigid tension ring beam at the center and, therefore, the boundary conditions are

$$\epsilon(0) = \epsilon(R) = 0$$

From which it is found that the critical load is contained in the first non-zero root of

$$J_{\frac{1}{3}}\left(\frac{2}{3}\alpha R^{\frac{3}{2}}\right) = 0 \qquad (2.75)$$

That is

$$\left(\frac{2}{3}\alpha R^{\frac{3}{2}}\right) = 2.90$$

and therefore

$$\frac{p_{0\,crit}}{\left(\frac{2\pi^2 dH_0}{(2R)^2}\right)} = 7.68 \qquad (2.76)$$

The deflected shape is given by

$$\epsilon(r) = A\left(\alpha^{\frac{2}{3}} r\right)^{\frac{1}{2}} J_{\frac{1}{3}}\left(\frac{2}{3}\alpha r^{\frac{3}{2}}\right) \qquad (2.77)$$

It is noted that if no lateral restraint is provided at the center, the boundary conditions are

$$\frac{d\epsilon}{dr}(0) = \epsilon(R) = 0$$

and the critical load is contained in the first root of

$$J_{-\frac{1}{3}}\left(\frac{2}{3}\alpha R^{\frac{3}{2}}\right) = 0 \qquad (2.78)$$

from which

$$\frac{p_{0\,crit}}{\left(\frac{2\pi^2 dH_0}{(2R)^2}\right)} = 3.19 \qquad (2.79)$$

and the deflected shape is then

$$\epsilon(r) = B\left(\alpha^{\frac{2}{3}} r\right)^{\frac{1}{2}} J_{-\frac{1}{3}}\left(\frac{2}{3}\alpha r^{\frac{3}{2}}\right) \qquad (2.80)$$

This latter situation is unlikely to be of practical importance.

3. Triangular Chord Cable Truss

a. Effect of a point load

Consider a point load P which acts on the top chord of a triangular chord truss at a distance x_1 from the left-hand support. The geometry of the truss is such that its apex occurs at x_0, where $x_1 \leq x_0$ (see Fig. 23(a), (c)).

When the truss is displaced laterally the out-of-plane rotations of the apex and the point of load application are θ_0 and θ_1, respectively. The relationship between θ_0 and θ_1 must be found first.

The initial lengths of the components of a chord are

a, c and e, where

$$a^2 = x_1^2 + (y_1 - b)^2 \quad , \quad c^2 = (x_0 - x_1)^2 + (d - y_1)^2 \quad , \quad e^2 = (\ell - x_0)^2 + (d - b)^2$$

and y_1 is half the spacing of the chords at the point of load application. Owing to the lateral displacements, the lengths of the components increase to

$$(a + \Delta a)^2 = x_1^2 + (y_1 \cos\theta_1 - b)^2 + y_1^2 \sin^2\theta_1$$

from which

$$\Delta a \simeq \frac{1}{2} \frac{b y_1 \theta_1^2}{a} \tag{2.81}$$

$$(c + \Delta c)^2 = (x_0 - x_1)^2 + (d\cos\theta_0 - y_1\cos\theta_1)^2 + (d\sin\theta_0 - y_1\sin\theta_1)^2$$

from which

$$\Delta c \simeq \frac{1}{2} \frac{d y_1 (\theta_0 - \theta_1)^2}{c} \tag{2.82}$$

$$(e + \Delta e)^2 = (\ell - x_0)^2 + (d\cos\theta_0 - b)^2 + d^2 \sin^2\theta_0$$

from which

$$\Delta e \simeq \frac{1}{2} \frac{b d \theta_0^2}{e} \tag{2.83}$$

The additional potential energy stored in the chords as a result of these displacements is

$$V = H_0 \left\{ \frac{b y_1 \theta_1^2}{x_1} + \frac{d y_1 (\theta_0 - \theta_1)^2}{(x_0 - x_1)} + \frac{b d \theta_0^2}{(\ell - x_0)} \right\} \tag{2.84}$$

For a given θ_1, the correct θ_0 is that which minimizes V. Hence

$$\frac{\partial V}{\partial \theta_0} = 0$$

which implies that

$$\frac{\theta_0}{\theta_1} = \frac{y_1(\ell - x_0)}{\{y_1(\ell - x_0) + b(x_0 - x_1)\}} \leq 1 \qquad (2.85)$$

and the lateral displacements are in the ratio

$$\frac{\epsilon_0}{\epsilon_1} = \frac{d(\ell - x_0)}{\{y_1(\ell - x_0) + b(x_0 - x_1)\}} \qquad (2.86)$$

These relationships could also have been found from integration of the differential equations, Eqs. 2.57 and 2.58, respectively. However, the geometrical arguments advanced here are more convenient for this relatively simple discrete system.

Equation 2.58 may be integrated to give

$$2H_0 \left(y \frac{d\epsilon}{dx} - \epsilon \frac{dy}{dx}\right)\Bigg|_{x_0^-}^{x_0^+} + 2H_0 \left(y \frac{d\epsilon}{dx}\right)\Bigg|_{x_1^-}^{x_1^+} + P\epsilon_1 = 0 \qquad (2.87)$$

After substitution and rearrangement it is found that

$$P_{crit} = 2bH_0 \left\{ \frac{1}{x_1} + \frac{\left(\frac{\epsilon_0}{\epsilon_1}\right)}{(\ell - x_0)} \right\}$$

Substituting for Eq. 2.86, and noting that

$$y_1 = b \left\{ 1 + \left(\frac{d - b}{b}\right) \frac{x_1}{x_0} \right\}$$

yields, finally

$$P_{crit} = \frac{2bH_0}{x_1} \left\{ \frac{\left(1 - \frac{x_1}{x_0}\right) b + \frac{x_1}{x_0} d}{\left(1 - \frac{x_1}{x_0}\right) b + \frac{x_1}{x_0} \left(1 - \frac{x_0}{\ell}\right) d} \right\} \qquad (2.88)$$

Equation 2.88 holds regardless of whether the truss is bi-convex or bi-concave. Several cases of interest are contained in this general result:

(i) When $b = 0$, $P_{crit} = 0$ and the truss will rotate as a rigid body if any load is applied (see Eq. 2.85).

(ii) When $d = 0$,

$$P_{crit} = \frac{2bH_0}{x_1} \tag{2.89a}$$

but here the situation where the load is applied at the apex (i.e. when $x_1 = x_0$) must be excluded, since no work can be done by the load, and therefore, no energy can be stored in the chords.

(iii) When $b = d$, the result for the parallel chord truss is obtained (see Eq. 2.63).

(iv) When $b \to \infty$, $P_{crit} \to \infty$ and the truss becomes a vertical member which is obviously stable under applied load.

(v) Finally, when the load is applied at the apex (i.e. when $x_1 = x_0$), and $d \neq 0$,

$$P_{crit} = \frac{2bH_0}{x_1\left(1 - \frac{x_1}{\ell}\right)} \tag{2.89b}$$

In this last case, P_{crit} is independent of d and has a minimum when $x_1 = \frac{\ell}{2}$.

In order to illustrate the application of Eqs. 2.88 and 2.89(b), consider a triangular chord truss with apex at $x_0 = \frac{\ell}{2}$ and $d \neq 0$. If the load is placed at the apex

$$P_{crit} = \frac{8bH_0}{\ell}$$

and, if the load is placed at $x_1 = \frac{\ell}{4}$

$$P_{crit} = \frac{8bH_0}{\ell} \frac{(b + d)}{\left(b + \frac{d}{2}\right)} > \frac{8bH_0}{\ell}$$

As a final remark, it is of interest to consider the lateral stability of the sloping chord truss. Here, the chords are straight lines of opposite slope, initially, and $2d$ is to be interpreted as the spacing of the chords at the right-hand support. Now, from Eq. 2.58

$$2H_0 y \frac{d\epsilon}{dx}\Big|_{x_1^-}^{x_1^+} + P\epsilon_1 = 0 \qquad (2.90)$$

and since here, $y = b\left\{1 + \left(\frac{d - b}{b}\right)\frac{x}{\ell}\right\}$, it is easily shown that

$$P_{crit} = \frac{2bH_0}{x_1\left(1 - \frac{x_1}{\ell}\right)} \left\{1 + \frac{x_1}{\ell}\left(\frac{d - b}{b}\right)\right\} \qquad (2.91)$$

When either b or d is zero, the resisting torque is zero to the left and to the right of the load, respectively. The situation is similar to that described by Eq. 2.89(a).

b. Effect of a uniformly distributed load

Suppose now that a uniformly distributed load, of intensity p per unit length, extends from one end of the span to the other. For convenience, the coordinate axes are shifted to mid-span and it is assumed that the apex of the triangular chord cable truss occurs at mid-span.

Equation 2.57 is

$$2H_0 \frac{d}{dx}\left(y^2 \frac{d\theta}{dx}\right) + py\theta = 0 \qquad (2.92)$$

where

$$y = d\left\{1 - \left(\frac{d-b}{d}\right)\left(\frac{2x}{\ell}\right)\right\}$$

and the boundary conditions are given by

$$2H_0\, y^2 \frac{d\theta}{dx}\,\delta\theta\Big|_0^{\frac{\ell}{2}} = 0 \qquad (2.93)$$

For the lowest critical load, the eigenfunction is even about the mid-span point. Therefore, the boundary conditions are

$$\frac{d\theta(0)}{dx} = 0 \quad , \quad \theta\left(\frac{\ell}{2}\right) = 0$$

If,

$$z = \left\{1 - \left(\frac{d-b}{d}\right)\left(\frac{2x}{\ell}\right)\right\} \qquad (2.94)$$

then Eq. 2.92 is transformed to

$$\frac{d}{dz}\left(z^2 \frac{d\theta}{dz}\right) + \alpha^2 z\theta = 0 \qquad (2.95$$

where

$$\alpha^2 = \frac{p\ell^2}{8\left(\frac{d-b}{d}\right)^2 d\, H_0}$$

and the boundary conditions become

$$\frac{d\theta(1)}{dz} = 0 \quad , \quad \theta\left(\frac{b}{d}\right) = 0 \qquad (2.96)$$

The general solution of Eq. 2.95 is[21]

$$\theta(z) = z^{-\frac{1}{2}} \left\{ AJ_1\left(2\alpha z^{\frac{1}{2}}\right) + BY_1\left(2\alpha z^{\frac{1}{2}}\right) \right\} \qquad (2.97)$$

and when account is taken of the boundary conditions, the following matrix equation is obtained

$$\begin{bmatrix} J_1\left(2\alpha\sqrt{\frac{b}{d}}\right) & Y_1\left(2\alpha\sqrt{\frac{b}{d}}\right) \\ J_2(2\alpha) & Y_2(2\alpha) \end{bmatrix} \begin{Bmatrix} A \\ B \end{Bmatrix} = \begin{Bmatrix} 0 \\ 0 \end{Bmatrix} \qquad (2.98)$$

For non-trivial solutions the determinant must be zero, and when this operation is carried out the following transcendental equation is obtained

$$\frac{J_1\left(2\alpha\sqrt{\frac{b}{d}}\right)}{Y_1\left(2\alpha\sqrt{\frac{b}{d}}\right)} = \frac{J_2(2\alpha)}{Y_2(2\alpha)} \qquad (2.99)$$

where J_i and Y_i are Bessel functions of the i^{th} order and first and second kinds, respectively.

For the problem under consideration the buckling load is contained in the first non-zero root of Eq. 2.99, that is, α_1. The value of this root depends upon the value of the characteristic geometric parameter, $\sqrt{\frac{b}{d}}$. The eigenfunctions are given by

$$\theta(z) = Az^{-\frac{1}{2}} J_1\left(2\alpha\sqrt{\frac{b}{d}}\right) \left\{ \frac{J_1\left(2\alpha z^{\frac{1}{2}}\right)}{J_1\left(2\alpha\sqrt{\frac{b}{d}}\right)} - \frac{Y_1\left(2\alpha z^{\frac{1}{2}}\right)}{Y_1\left(2\alpha\sqrt{\frac{b}{d}}\right)} \right\} \qquad (2.100)$$

It is not convenient to solve Eq. 2.99 when the difference between b and d is small. Instead, the Rayleigh-Ritz technique may

be applied to give an approximate solution (upper bound) for the buckling load. The general, first-term approximation to the buckling load is

$$p_{crit} \leq \frac{2H_0 \int_0^{\ell} y^2 \left(\frac{d\theta}{dx}\right)^2 dx}{\int_0^{\ell} y\,\theta^2\, dx} \tag{2.101}$$

If θ is chosen as

$$\theta = A \sin\left(\frac{\pi x}{\ell}\right)$$

then, for the triangular chord cable truss, Eq. 2.101 yields

$$\frac{p_{crit}}{\left(\frac{2\pi^2 d H_0}{\ell^2}\right)} = \frac{\frac{b}{d}\left\{1 + \left(1 - \frac{4}{\pi^2}\right)\left(\frac{d-b}{b}\right) + \left(\frac{1}{3} - \frac{2}{\pi^2}\right)\left(\frac{d-b}{b}\right)^2\right\}}{\left\{1 + \left(\frac{1}{2} + \frac{2}{\pi^2}\right)\left(\frac{d-b}{b}\right)\right\}} \tag{2.102}$$

which will be accurate provided that

$$\frac{3}{4} < \frac{d}{b} < \frac{5}{4}$$

There is no difficulty in showing that if the chords of the truss are restrained against lateral movement at the apex, the critical load is contained in the first non-zero root of the transcendental equation

$$\frac{J_1\left(2\alpha\sqrt{\frac{b}{d}}\right)}{Y_1\left(2\alpha\sqrt{\frac{b}{d}}\right)} = \frac{J_1(2\alpha)}{Y_1(2\alpha)} \tag{2.103}$$

For example:

(i) If $b = 4d$,

then the first non-zero root of Eq. 2.99 is found to be

$$\alpha_1 = 1.135$$

from which the critical load is

$$\frac{p_{crit}}{\left(\frac{2\pi^2 dH_0}{\ell^2}\right)} = 4.7$$

If the chords of the truss are restrained at the apex then the first non-zero root of Eq. 2.103 is

$$\alpha_1 = 1.598$$

from which the critical load is

$$\frac{p_{crit}}{\left(\frac{2\pi^2 dH_0}{\ell^2}\right)} = 9.35$$

(ii) If $d = 4b$,

then the first non-zero root of Eq. 2.99 is found to be

$$\alpha_1 = 0.983$$

from which the critical load is

$$\frac{p_{crit}}{\left(\frac{2\pi^2 dH_0}{\ell^2}\right)} = 0.22$$

If the chords are restrained at the apex then the first non-zero root of Eq. 2.103 is

$$\alpha_1 = 3.196$$

from which the critical load is

$$\frac{P_{crit}}{\left(\frac{2\pi^2 d H_0}{\ell^2}\right)} = 2.33$$

In the case of the bi-convex truss a very substantial stiffening effect is provided by the placing of lateral restraints at mid-span.

4. General Results

Some time has been spent in considering the lateral stability of the parallel chord truss and the triangular chord truss. These cases appear to be the most straightforward. For other trusses, in which the chord profiles are given by higher order curves and/or the vertical loading is other than that considered already, the problem of finding an analytical solution to the fundamental differential equation (Eq. 2.57) becomes more difficult.

One simple, general result which can be given concerns the buckling of a truss under a point load. If the point of load application and the apex of the truss are both at mid-span then, from Eq. 2.57, it can be shown that

$$P_{crit} = H_0 F(b, d, \ell) \qquad (2.104)$$

where

$$F(b, d, \ell) = \frac{4}{d \int_0^{\frac{\ell}{2}} y^{-2}\, dx}$$

Results for the parallel chord truss and the triangular chord truss are easily shown to be the same as those given previously. If the truss is parabolic, that is

$$y = d\left\{1 - \left(\frac{d-b}{d}\right)\left(\frac{2x}{\ell}\right)^2\right\}$$

where the coordinates are taken about mid-span, then:

(i) For bi-convex trusses[7],

$$P_{crit} = \frac{8bH_0}{\ell} \frac{2}{\left\{1 + \left(\frac{b}{d}\right)\left(\frac{d}{d-b}\right)^{\frac{1}{2}} \tanh^{-1}\left(\frac{d-b}{d}\right)^{\frac{1}{2}}\right\}} \tag{2.105}$$

(ii) For bi-concave trusses,

$$P_{crit} = \frac{8bH_0}{\ell} \frac{2}{\left\{1 + \left(\frac{b}{d}\right)\left(\frac{d}{b-d}\right)^{\frac{1}{2}} \tan^{-1}\left(\frac{b-d}{d}\right)^{\frac{1}{2}}\right\}} \tag{2.106}$$

The ease with which analytical solutions can be found for more complicated cases will depend on whether the integral contained in $F(b, d, \ell)$ can be evaluated. Numerical methods are particularly well suited for this purpose.

For bi-convex or bi-concave trusses under the action of a uniformly distributed load, the Sturm comparison theorem may be applied to Eq. 2.57 in order to obtain an idea of the range which may be expected in the critical load. This theorem reveals that the critical load must satisfy the following requirements:

(i) For bi-convex trusses,

$$\left(\frac{b}{d}\right)^2 < \frac{P_{crit}}{\left(\frac{2\pi^2 dH_0}{\ell^2}\right)} < \frac{d}{b} \tag{2.107}$$

(ii) For bi-concave trusses,

$$\frac{d}{b} < \frac{P_{crit}}{\left(\frac{2\pi^2 dH_0}{\ell^2}\right)} < \left(\frac{b}{d}\right)^2 \tag{2.108}$$

Of course, solutions may be found to Eq. 2.57 when the shape of the

truss and/or the loading is complicated. However, a power series solution will often be necessary and the labor involved will be excessive. Approximate solutions, based on the Rayleigh-Ritz technique or on numerical methods, will provide adequate results in many situations.

SUMMARY AND CONCLUSIONS

A detailed presentation has been made for the response of simple, suspended cable systems to static and dynamic loadings. It is believed that many of the results are new.

The analyses presented are accurate provided that the slope of the cable remains small. For example, this requires that the ratio of sag to span of a suspended cable be about 1:8, or less. In most practical situations this restriction is not of concern since structural efficiency necessitates the use of flat-sag cable systems.

Particular attention has been given to the method and presentation of solutions. Where necessary, the solutions of the governing differential and integral equations have been given accurate to the second order of small quantities. Only in this way can an assessment be made of the importance of the non-linearities inherent in the response of the cable. For the most part, solutions have been presented in dimensionless form so that the mechanics of the problem are more readily portrayed. It has been shown that a characteristic parameter λ^2, which accounts for the effects of cable geometry and elasticity, is of fundamental importance.

The two simple cable systems chosen were the single, suspended cable and the counterstressed, double cable system, the cable truss. These two systems were chosen because they illustrate a fundamental difference in response which is common to cable structures in general. The single cable responds in a non-linear manner while a bi-convex or bi-concave cable truss, which is initially symmetrical about the

longitudinal axis, is essentially linear in its response to applied loading.

The suspended parabolic cable was considered in the first chapter. After a preliminary derivation of the properties of an inextensible parabolic cable, solutions were given which allow for the elastic stretching which such a cable must, in reality, undergo when it is placed in the free-hanging position. It was shown that the solution of the elastic parabola is valid provided that the additional deflections are small. Limiting cases, as when λ^2 is large (e.g., a suspension bridge cable) or when λ^2 is small (e.g., a taut, flat cable), were discussed. It was concluded that the only case of practical importance arises in the construction of the cables of suspension bridges.

General theories, accurate to the second order of small quantities, were developed for the response of a parabolic cable to applied load. Simplifications which can be made to the general theory were presented. One simplification is to linearize the equations by removing all second order terms. Another is valid for cables which are initially taut and flat. A short experimental program was conducted which confirmed the second order theory of the taut, flat cable under a point load. Since this theory is derived from the general theory in a consistent manner, the experimental results lend credence to the validity of the general theory. Several realistic numerical examples were presented which demonstrate that the general theory is usually indispensible if accurate solutions are to be obtained.

The second section of the first chapter dealt with the linear theory of free vibrations of a suspended parabolic cable. Both in-plane and out-of-plane modes were considered.

The theory of cable vibrations is an old mechanical problem, the foundations of which can be traced back to the beginning of the eighteenth century. As was pointed out in the introduction, there is a discrepancy which arises in the theory of the symmetric in-plane modes of flat-sag cables which has not been reconciled by previous investigators. If the cable is assumed inextensible it is easily shown that the theory of the symmetric in-plane modes does not reduce to the theory of the symmetric modes of a taut string, as the ratio of sag to span becomes very small. In fact, the natural frequencies of the first symmetric in-plane mode differ by almost 300%. Only by allowing for cable elasticity, and thereby introducing the characteristic geometric and elastic parameter λ^2, can the matter be resolved. Then, when λ^2 is very small the theory of the taut string is obtained and when λ^2 is very large the inextensible theory is obtained.

The theory shows that "cross-over" points exist. For example, at the first "cross-over" point (i.e. at $\lambda^2 = 4\pi^2$), the frequencies of the first symmetric and first antisymmetric in-plane modes are equal. Simple qualitative experiments were performed which proved the existence of these "cross-over" points.

The behavior of the cable truss was investigated in the second chapter. A general theory of the response to static loading was developed and this theory was simplified to apply to cable trusses which are either bi-convex or bi-concave, and initially symmetrical about the longitudinal axis. Because of the opposite curvature of the chords of the truss, the second order terms in the deflection equations

are zero and it was found that the response of such a truss is strongly linear. Because of the linearity of the response, the total horizontal reaction at a support remains at twice the value of the horizontal component of pretension in a chord. Detailed results were presented for trusses in which the chords are given by parabolic profiles. Numerical examples illustrated the ease with which the theory can be applied to the analyses of roof structures which are supported either by parallel arrays of trusses, as in rectangular roofs, or by radial arrays of trusses, as in circular roofs. The flexural stiffness of the roof was neglected which is usually a valid assumption for such forms of construction.

A brief treatment was given for the vertical vibrations of the parabolic cable truss. As with the static analyses, the results were very similar to the suspended parabolic cable.

In the final section of the thesis, an investigation was made of the possible lateral instability which the cable truss may exhibit in resisting applied loading. Variational methods were used to set up the governing differential equation and a few solutions were given. It was found that, for trusses in which the chords are initially straight and parallel, the non-linear stiffening effect of the applied load may sometimes be sufficient to avoid the possibility of lateral buckling. In other situations, where the trusses are either bi-convex or bi-concave and symmetrical about the longitudinal axis, no non-linear stiffening effect can exist. The additional tensions owing to the vertical load are then of opposite sign and do not contribute to the resisting torque.

Solutions were given for the parallel chord truss under a point load, a uniformly distributed load and a triangular load block. The lateral stability of the triangular chord truss under a point load and a uniformly distributed load was examined. Analytical solutions appear difficult to obtain in more complicated situations. However, a simple general result was found for the buckling of a truss under a point load, where the position of load application and the apex both occur at mid-span. From this, specific results were given for the parabolic cable truss.

A concluding remark concerns the practical applications of the theories presented in this thesis. Although the solutions given here were found using analytical techniques, the method of real-time computation on the digital computer, using some of the results, would be invaluable in the analysis and design of these simple cable systems.

APPENDIX I

The Influence of Flexural Rigidity in a Cable

When the flexural stiffness of the cable is accounted for, the statement of shear force equilibrium at a cross section requires that

$$H \frac{dy}{dx} - E_c I_c \frac{d^3y}{dx^3} = \frac{w\ell}{2} - wx$$

where I_c is the second moment of area of the cable and the other symbols are as defined previously. The equation is accurate provided that $\frac{dy}{dx}$ is everywhere small[8], and, in another form, is recognized as the differential equation governing the deflection of a beam under a uniform axial tension.

The general solution is

$$y = \frac{w\ell^2}{2H}\left(\left(\frac{x}{\ell}\right) - \left(\frac{x}{\ell}\right)^2\right) + A \sinh(\gamma x) + B \cosh(\gamma x) + C$$

where A, B, C are constants of integration and

$$\gamma^2 = \frac{H}{E_c I_c}$$

Specific solutions may be had depending on the boundary conditions chosen.

(i) Cable slope zero at supports

Here the boundary conditions are

$$\frac{dy}{dx}(0) = \frac{dy}{dx}(\ell) = 0$$

and one of

$$y(0) = y(\ell) = 0$$

The solution is then

$$y = \frac{w\ell^2}{2H}\left\{\left(\left(\frac{x}{\ell}\right) - \left(\frac{x}{\ell}\right)^2\right) - \frac{\sinh(\gamma x)}{(\gamma\ell)} + \frac{\coth\left(\frac{\gamma\ell}{2}\right)}{(\gamma\ell)}\left(\cosh(\gamma x) - 1\right)\right\}$$

and when $x = \frac{\ell}{2}$, $y = d$ where

$$d = \frac{w\ell^2}{8H}\left\{1 - \frac{\tanh\left(\frac{\gamma\ell}{4}\right)}{\left(\frac{\gamma\ell}{4}\right)}\right\} < \frac{w\ell^2}{8H}$$

The size of the dimensionless characteristic parameter, $(\gamma\ell)$, determines the influence which flexural rigidity has on the response of the cable.

When $(\gamma\ell)$ is very small (i.e., E_cI_c is very large)

$$\left\{1 - \frac{\tanh\left(\frac{\gamma\ell}{4}\right)}{\left(\frac{\gamma\ell}{4}\right)}\right\} = \frac{1}{3}\left(\frac{\gamma\ell}{4}\right)^2 + \text{higher order terms}$$

Therefore

$$d \to \frac{w\ell^4}{384\ E_cI_c}$$

which is the result for the central deflection of a uniform beam, fully restrained at each end.

When $(\gamma\ell)$ is very large (i.e., E_cI_c is very small)

$$\left\{1 - \frac{\tanh\left(\frac{\gamma\ell}{4}\right)}{\left(\frac{\gamma\ell}{4}\right)}\right\} \to 1$$

and

$$d \to \frac{w\ell^2}{8H}$$

This is the result which obtains for the perfectly flexible, parabolic cable.

(ii) Bending moment zero at supports

The boundary conditions here are

$$\frac{d^2y}{dx^2}(0) = \frac{d^2y}{dx^2}(\ell) = 0$$

and one of

$$y(0) = y(\ell) = 0$$

The solution is then

$$y = \frac{w\ell^2}{2H}\left\{\left(\left(\frac{x}{\ell}\right) - \left(\frac{x}{\ell}\right)^2\right) - \frac{2}{(\gamma\ell)^2}\left(1 + \tanh\left(\frac{\gamma\ell}{2}\right)\sinh(\gamma x) - \cosh(\gamma x)\right)\right\}$$

and when $x = \frac{\ell}{2}$, $y = d$ where

$$d = \frac{w\ell^2}{8H}\left\{1 - \frac{8}{(\gamma\ell)^2}\left(1 - \operatorname{sech}\left(\frac{\gamma\ell}{2}\right)\right)\right\} < \frac{w\ell^2}{8H}$$

When $(\gamma\ell)$ is very small

$$\left\{1 - \frac{8}{(\gamma\ell)^2}\left(1 - \operatorname{sech}\left(\frac{\gamma\ell}{2}\right)\right)\right\} = \frac{5}{12}\left(\frac{\gamma\ell}{2}\right)^2 + \text{higher order terms}$$

Therefore

$$d \to \frac{5}{384}\frac{w\ell^4}{E_c I_c}$$

which is the result for the central deflection of a uniform beam, simply supported at each end.

When $(\gamma\ell)$ is very large

$$\left\{1 - \frac{8}{(\gamma\ell)^2}\left(1 - \operatorname{sech}\left(\frac{\gamma\ell}{2}\right)\right)\right\} \to 1$$

and

$$d \rightarrow \frac{w\ell^2}{8H}$$

In the vast majority of practical cable problems the parameter $(\gamma\ell)$ is very large, often of order 10^3, or more. The effects of flexural rigidity are then quite unimportant and can be ignored. However, if small scale models of cable systems are constructed, some care is required to ensure that model cable properties reflect prototype cable properties. In the case of the relative flexural rigidity, it would be ideal to have $(\gamma\ell)$ the same in both model and prototype. This is usually unnecessary if $(\gamma\ell)$ is large and it suffices to ensure that $(\gamma\ell)$ is also large in the model. In this regard the use of piano wire as the model material will sometimes cause problems.

APPENDIX II

The Cable Equation

The cable equation provides a compatibility or closure condition relating the changes which occur in the cable tension to the changes in cable geometry when the cable is displaced (in-plane) from its original equilibrium position. Consider an element PQ in the original configuration which, because of some applied load, moves to a new position P'Q'. From the geometry of the displacement (see Fig. 25), it is seen that, if ds is the length of PQ and ds' is the length of P'Q'

$$ds^2 = dx^2 + dy^2$$

$$ds'^2 = (dx + du)^2 + (dy + dv)^2$$

where u and v are the longitudinal and vertical components of the displacement from P to P'.

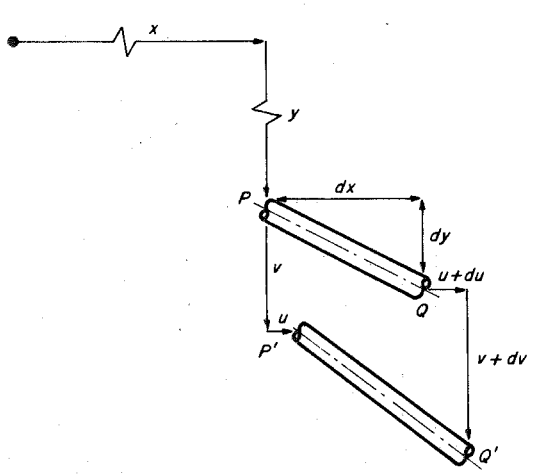

Figure 25

For flat-sag cables the fractional increment in the length of the cable element, correct to the second order of small quantities, is

$$\frac{ds'-ds}{ds} = \frac{du}{ds}\frac{dx}{ds} + \frac{dy}{ds}\frac{dv}{ds} + \frac{1}{2}\left(\frac{dv}{ds}\right)^2$$

Hooke's Law, applied to the element, requires that

$$\frac{\tau}{E_c A_c} = \frac{ds'-ds}{ds}$$

where τ is the increment in tension exerted on the element. Now, to second order

$$\tau = h\frac{ds}{dx}$$

where h is the increment in the horizontal component of cable tension. Consequently, the cable equation for the element reads

$$\frac{h\left(\frac{ds}{dx}\right)^3}{E_c A_c} = \frac{du}{dx} + \frac{dy}{dx}\frac{dv}{dx} + \frac{1}{2}\left(\frac{dv}{dx}\right)^2$$

The effects of increments in temperature can readily be accommodated, and the elemental equation then is

$$\frac{h\left(\frac{ds}{dx}\right)^3}{E_c A_c} = \frac{du}{dx} + \frac{dy}{dx}\frac{dv}{dx} + \frac{1}{2}\left(\frac{dv}{dx}\right)^2 - \epsilon_t \Delta T\left(\frac{ds}{dx}\right)^2$$

where ϵ_t is the coefficient of expansion, ΔT is the incremental rise in temperature.

In the case of a suspended cable, hanging between rigid supports, the above equation may be integrated to give

$$\frac{hL_e}{E_c A_c} = \int_0^{\ell} \frac{dy}{dx}\frac{dv}{dx}\,dx + \frac{1}{2}\int_0^{\ell} \left(\frac{dv}{dx}\right)^2 dx - \epsilon_t \Delta T L_t$$

where

$$L_e = \int_0^{\ell} \left(\frac{ds}{dx}\right)^3 dx \quad , \quad L_t = \int_0^{\ell} \left(\frac{ds}{dx}\right)^2 dx$$

and it has been assumed that ΔT is uniform along the span. If the increment in the horizontal component of cable tension causes some longitudinal movement of the supports, then the integrated equation is

$$\frac{hL_e}{E_c A_c} = u(\ell) - u(0) + \int_0^{\ell} \frac{dy}{dx}\frac{dv}{dx}\,dx + \frac{1}{2}\int_0^{\ell} \left(\frac{dv}{dx}\right)^2 dx - \epsilon_t \Delta T L_t$$

where $u(\ell)$, $u(0)$ are the longitudinal movements at the supports.

REFERENCES

1. Buchanan, G. R., "Two Dimensional Cable Analysis", Journal of the Structural Division, American Society of Civil Engineers, ST 7, Vol. 96, July 1970, pp. 1581-1587.

2. Caughey, T. K., Personal communication.

3. Inglis, C., "Applied Mechanics for Engineers", Dover, 1963, Chapter III, p. 60.

4. Irvine, H. M., "Torsional Vibrations in Boxgirder Suspension Bridges", submitted for publication, International Journal of Earthquake Engineering and Structural Dynamics, December 1973.

5. Irvine, H. M., "Torsional Analysis of Boxgirder Suspension Bridges", to be published, Journal of the Structural Division, American Society of Civil Engineers.

6. Janke, E., Emde, F., Lösch, F., "Tables of Higher Functions", Sixth Edition, McGraw-Hill, 1960.

7. Klerer, M., Grossman, F., "A New Table of Indefinite Integrals", Dover, 1971, pp. 7, 8, 44.

8. Love, A. E. H., "A Treatise on the Mathematical Theory of Elasticity", Fourth Edition, Dover, 1944, pp. 422-423.

9. O'Brien, T., "General Solution of Suspended Cable Problems", Journal of the Structural Division, American Society of Civil Engineers, ST 1, Vol. 93, February 1967, pp. 1-26.

10. Pugsley, A. G., "The Theory of Suspension Bridges", Edward Arnold, London, 1957, Chapters I, II, III.

11. Pugsley, A. G., "On the Natural Frequencies of Suspension Chains", Quarterly Journal of Mechanics and Applied Mathematics, Vol. II, Part 4, 1949, pp. 412-418.

12. Rannie, W. D., "The Failure of the Tacoma Narrows Bridge", Board of Engineers, Amman, O. H., von Kármán, T., Woodruff, G., Federal Works Agency, March 28, 1941, Appendix VI.

13. Rannie, W. D., Personal communication.

14. Rohrs, J. H., "On the Oscillations of a Suspension Chain", Transactions Cambridge Philosophical Society, Vol. IX, Part III, December 1851, pp. 379-398.

15. Routh, E. J., "Analytical Statics", Cambridge, 1891, Vol. 1, Chapter X.

16. Routh, E. J., "Advanced Dynamics of Rigid Bodies", Sixth Edition, Dover, 1955, p. 278, Chapter XIII, and, in particular, pp. 410-412.

17. Saxon, D. S., Cahn, A. S., "Modes of Vibration of a Suspended Cable", Quarterly Journal of Mechanics and Applied Mathematics, Vol. VI, Part 3, 1953, pp. 273-285.

18. Schleyer, F.-K., "Tensile Structures", Edited by Otto, F., MIT Press, 1969, Vol. II, Chapter 4, pp. 153-163.

19. Subcommittee on Cable-Suspended Structures, "Cable-Suspended Roof Construction State-of-the-Art, Journal of the Structural Division, American Society of Civil Engineers, ST 6, Vol. 97, June 1971, pp. 1715-1761, (this paper contains a comprehensive bibliography).

20. Uspensky, J. V., "Theory of Equations", McGraw-Hill, 1948, Chapter V.

21. von Kármán, T., Biot, M. A., "Mathematical Methods in Engineering", McGraw-Hill, 1940, p. 66.

22. Watson, G. N., "Theory of Bessel Functions", Second Edition, Cambridge, 1966, pp. 3-5, 153.

23. Whittaker, E. T., "Analytical Dynamics", Fourth Edition, Dover, 1944, pp. 34, 177.

24. Vincent, G. S., "A Summary of Laboratory and Field Studies in the United States on Wind Effects on Suspension Bridges", Proceedings of Conference on Wind Effects on Buildings and Structures, Teddington, England, H. M. S. O., 1965, Vol II, pp. 488-515. (Also see a discussion, Transactions A. S. C. E., 1945, Vol. 110, pp. 512-522.)

25. Zetlin, Lev, "Steel Cable Creates Novel Structural Space Systems", American Institute of Steel Construction Engineering Journal, reprint, January 1964.